MODERN PATHOLOGY

ABSTRACTS

LIVER PATHOLOGY

(1591-1661)

USCAP 109TH ANNUAL MEETING
2020
EYES ON YOU

FEBRUARY 29-MARCH 5, 2020

LOS ANGELES CONVENTION CENTER
LOS ANGELES, CALIFORNIA

1591 Granulomatous Inflammation is a Characteristic Feature of Liver Injury Induced by Immune Checkpoint Inhibitors (ICIs)

Jun-Ichi Akahira[1], Yasuteru Kondo[2], Mareyuki Endo[2]
[1]Sendai, Miyagi, Japan, [2]Sendai Kousei Hospital, Sendai, Miyagi, Japan

Disclosures: Jun-Ichi Akahira: None

Background: Immune checkpoint inhibitors (ICIs) have dramatically improved the survival of advanced non-small cell lung carcinoma. These drugs stimulate the immune system and lead to anti-tumoral response. Recently, various kinds of immune-related adverse events (irAEs) after treatment with ICIs have been reported including our institution (JAMA oncol 2018). However, the detailed pathological characteristics of liver injury induced by ICIs have remained to be cleared. In this report, we evaluated liver injury mainly regarding with lymphoplasmacytic infiltration and degree of granulomatous change.

Design: In the medical record, 162 advanced non-small cell lung cancer patients, who received nivolumab (118 patients) or pembrolizumab (44 patients), were identified at our institution between January 2016 and April 2018. After analyzing serum liver enzymes (G1 to G4), liver biopsy was performed for 18 patients at the onset of liver damage. Histopathological features (portal and lobular inflammation, necrosis, fibrosis and granulomatous change) as well as immunohistochemical features such as T-cell markers (CD3, CD4, CD8), B-cell marker (CD20), and plasma cell marker (CD138) were analyzed in all of the patients, and compared to those in patients with typical auto-immune hepatitis (AIH) and drug induced liver injury (DILI).

Results: Ten and 8 patients received liver biopsy after or during Nivolumab and Pembrolizumab treatment, respectively. The degree of portal and lobular inflammation, fibrosis, and necrotic change were significantly increased in patients with Grade3/4 patients compared to Grade1/2 patients ($p<0.05$). The ratios of inflammatory cells CD4/CD8, and CD138/CD3 in ICIs (0.63 and 0.044) were significantly lower than AIH (1.89 and 0.21) or DILI (1.08 and 0.39) patients ($p<0.05$, respectively). Granulomatous change, especially large granulomatous change with necrosis (Fig.1), was significantly increased in patients with ICIs patients compared with DILI and AIH patients ($p<0.05$). Steatosis, ballooning, Mallory's body was rarely identified in these patients.

Figure 1 - 1591
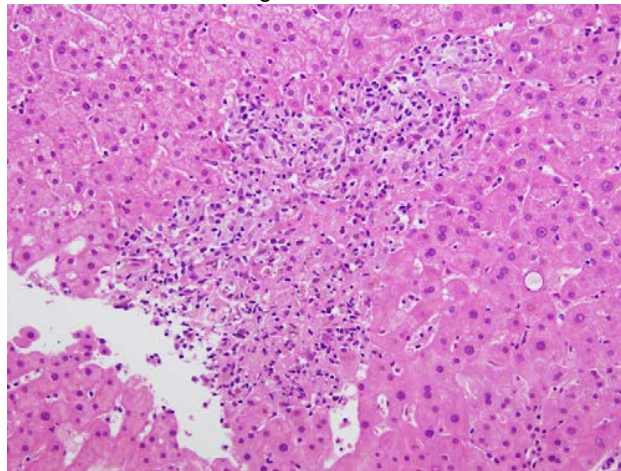
Conclusions: Granulomatous change, especially large granulomatous inflammation with necrosis, seemed to be a characteristic feature of severe liver damage due to ICIs. Also, the population of lymphoplasmacytic cells in patients with ICIs were different from those with AIH or DILI. We consider that ICIs should be added to one of the drugs that cause granulomatous inflammation of the liver.

1592 Macrotrabecular Growth Pattern is Associated with Poor Prognosis in Patients with Hepatocellular Carcinoma

Suhair Al Salihi[1], Amit Singal[1], Yujin Hoshida[1], Nicole Rich[1], Purva Gopal[1]
[1]University of Texas Southwestern Medical Center, Dallas, TX

Disclosures: Suhair Al Salihi: None; Amit Singal: None; Yujin Hoshida: None; Nicole Rich: None; Purva Gopal: None

Background: Recent studies have shown hepatocellular carcinoma (HCC) with macrotrabecular (MT) pattern may be a distinct aggressive HCC subtype. The aim of this study is to evaluate the clinicopathologic significance of MT growth pattern in HCC patients.

Design: We included HCC patients who underwent surgical resection at 2 large health systems between Jan 2008 - Dec 2017. Pathology slides were reviewed and HCC histologic features recorded including tumor focality, size, grade, necrosis, macro and micro-lymphovascular invasion, and inflammatory cell infiltrates. Presence and percentage of HCC histologic patterns were assessed including conventional/trabecular, steatohepatitic, pseudoglandular, compact/solid, clear cell, pleomorphic/giant cell and MT (defined as trabeculae > 6 cells thick; **Figure 1**). We used Fisher exact test to compare demographics, clinical and tumor characteristics between patients with and without MT. We used univariable and multivariable Cox regression analysis to compare survival between the two groups.

Results: We identified 97 eligible patients. Median age was 62 (27-90 years), and 70 (72.2%) patients were male. The most common liver disease etiologies were hepatitis C (63.9%), non-alcoholic steatohepatitis (16.5%), and hepatitis B (11.3%). Most lesions (93.8%) were unifocal, and median tumor size was 3 (range 1.2 – 16.7) cm. Overall MT was identified in 41 (42.2%) patients. MT appeared more common in hepatitis B patients (8 of 10), although the proportion with MT did not significantly differ by liver disease etiology (p=0.15) or presence vs. absence of cirrhosis on surgical specimen (p=0.22). MT was significantly associated with larger tumor size (3.5 vs. 2.7 cm; p=0.03), increased microvascular invasion (MVI; 80.5% vs. 30.4%; p<0.001), higher grade (53.7% vs. 14.3%;p<0.001), and less infiltrating lymphocytes (41.5% vs. 63.5%, p=0.06). MT patients had higher AFP (median 41 vs. 11 ng/mL) but this did not reach statistical significance (p=0.21). MT patients had increased residual disease or early recurrence after surgical resection (33.5% vs. 4.0%, p=0.001). In multivariable Cox regression, MT pattern was independently associated with increased mortality risk (HR 2.47, 95%CI 1.04-5.86) after adjusting for tumor focality, size, grade, and MVI (Table 1).

Table 1: Factors associated with survival among patients with HCC undergoing surgical resection

Variable	Adjusted HR	95% CI
MT pattern	2.47	1.04 – 5.86
Unifocal lesion	0.57	0.24 – 1.38
Tumor size	1.03	0.95 – 1.13
Tumor grade	1.25	0.68 – 2.30
Microvascular invasion	1.53	0.64 – 3.65

Figure 1 - 1592
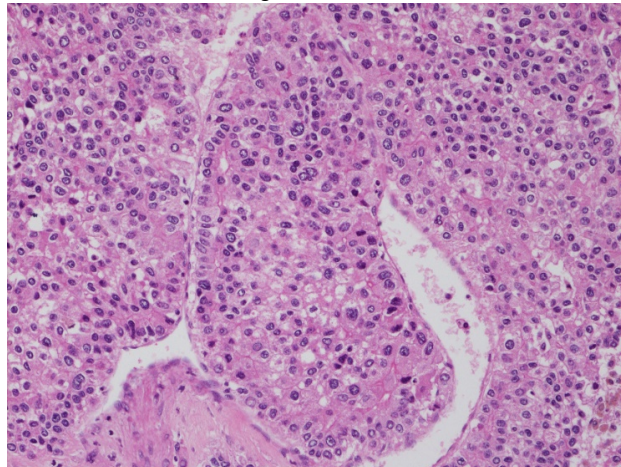
Conclusions: The presence of MT growth pattern is independently associated with poor prognosis in HCC patients including increased high-risk pathologic features, decreased response to treatment, and worse overall survival.

1593 Fibrohistiocytic-Type Inflammatory Pseudotumor of the Liver: A Distinct Clinicopathological Entity

Kshitij Arora[1], Vikram Deshpande[2], Jonathan England[3]
[1]Jackson Memorial Hospital/University of Miami Hospital, Miami, FL, [2]Massachusetts General Hospital, Boston, MA, [3]University of Miami Miller School of Medicine/Jackson Health System, Miami, FL

Disclosures: Kshitij Arora: None; Vikram Deshpande: *Grant or Research Support*, Advanced Cell Diagnostics; *Advisory Board Member*, Viela; *Grant or Research Support*, Agios Pharmaceuticals; Jonathan England: None

Background: Hepatic pseudotumor (HPT) is a generic term used to designate hepatic inflammatory mass-forming lesions, one that includes a range of inflammatory and neoplastic lesions. Our goal was to retrospectively analyze the clinical, imaging, and pathological features of inflammatory non-neoplastic HPT.

Design: Clinical and pathology databases were used to identify cases of inflammatory HPT diagnosed at the Massachusetts General Hospital (MGH), University of Miami Hospital, and Jackson Memorial Hospital, Miami. The clinical, radiologic and pathologic features were recorded. Neoplastic diseases previously classified as HPT, including inflammatory myofibroblastic tumors and dendritic cell sarcomas, were excluded. Immunohistochemistry for IgG4 and IgG was performed.

Results: We identified 10 patients with inflammatory HPT. We classified six cases as fibrohistiocytic variants of inflammatory HPT (Group 1) and four cases as mass-forming IgG4-related disease (Group 2). Clinically, Group 1 patients presented with abdominal pain (100%), fever (50%), and elevated liver function tests (LFTs) (67%). Group 2 patients presented with elevated LFTs (67%) and jaundice (100%). On imaging, these lesions were solitary (50%) or multiple (50%), and favored to represent a neoplasm (5 cases) or abscess (2 cases). In three cases, no diagnosis was offered. Histologically, two distinct patterns were recognized: Group 1 was characterized by fibrohistiocytic inflammation with scattered eosinophils and neutrophils, and virtually absent IgG4 positive cells (<50 per high power field (HPF) and the IgG4 to IgG ratio was < 40%.) Group 2 showed dense lymphoplasmacytic inflammation, eosinophils, storiform fibrosis and increased numbers of IgG4 (>50 per HPF) and IgG4 to IgG ratio (>40%) positive cells. A partial hepatectomy was performed in one of six patients in Group 1, and two of four cases in Group 2. Within the conservatively managed group, the patients in Group 1 resolved on antibiotic therapy while Group 2's patients responded favorably with steroids.

Conclusions: The fibrohistiocytic variant of inflammatory HPT is a histologically distinct lesion that is responsive to antibiotic therapy.

1594 Segmental Atrophy (Pseudotumor) of the Liver: A Marker of Cardiovascular Disease That Mimics Neoplasia

Naziheh Assarzadegan[1], Rafael Estevez-Castro[2], Danielle Hutchings[3], Annika Windon[4], Kevan Salimian[5], Elizabeth Montgomery[6], Robert A. Anders[5], Kiyoko Oshima[4]
[1]Department of Pathology, The Johns Hopkins Medical Institutions, Baltimore, MD, [2]Laboratorio de Patologia Dra. Rosario Castro, Santiago, Dominican Republic, [3]Johns Hopkins Medicine, Baltimore, MD, [4]Johns Hopkins Hospital, Baltimore, MD, [5]Johns Hopkins, Baltimore, MD, [6]Johns Hopkins Medical Institutions, Baltimore, MD

Disclosures: Naziheh Assarzadegan: None; Rafael Estevez-Castro: None; Danielle Hutchings: None; Annika Windon: None; Kevan Salimian: None; Elizabeth Montgomery: None; Robert A. Anders: None; Kiyoko Oshima: None

Background: Segmental atrophy (SA) of the liver can present radiographically as a mass, and can be a diagnostic challenge for radiologists and pathologists alike. SA is a rare and under-recognized entity with only a few reported series in the literature.

Design: A search of our pathology data system from 1984 to 2019 identified 27 cases. Clinical information was collected. H&E stained slides were reviewed. The tumor location, size, percentage of elastosis, entrapped hepatocytes, presence of thickened, prominent or thrombosed vessels, arterial vs venous proliferation, presence of biliary cysts or dilated bile ducts were analyzed.

Results: Lesions predominantly arose in middle-aged adults with a mean age of 60 (range 3 to 83) years and a slight female predominance (N = 16, 59%). Specimens included 8 partial hepatectomies (N=8, 30%), 6 needle biopsies (N=6, 22%), 8 explants (N=8, 30%), 2 segmental resections (N=2, 7%), 2 excisions (N=2, 7%) and 1 wedge biopsy (N=1, 3%). Clinically, 10 patients presented with a mass (N=10, 37%). The remaining 17 cases were identified incidentally during procedures performed for other reasons or during biopsies (N=17, 62%). 15 patients had a history of cardiovascular disease (55%) such as hypertension, diabetes-associated vascular disease, coronary artery disease, and heart failure. Two patients (7%) had connective tissue disorders (Behçet disease and undifferentiated connective tissue disease). The slides were available for review in 7 cases that presented as mass lesions. All lesions were subcapsular (N=7, 100%) and ranged in size from 1.7 to 4.4 cm (mean 3.3 cm) radiologically. All cases showed thickened and prominent vessels (N=7, 100%). Arterial proliferation was the predominant component in the majority of the cases (N=5, 71%) and only 2 cases demonstrated marked venous proliferation (N=2, 29%). Thrombosed vessels were present in 1 case (N=1, 14%). Bile ducts were dilated in 2 cases (N=2, 29%). No biliary cysts were identified. Elastic stain was available in 3 cases and revealed the extent of elastosis to range from < 5 to 20%. The percentage of entrapped hepatocytes varied from 5-60%. Additional pathological findings were present in 3 cases and included steatohepatitis, granulomatous and xanthomatous inflammation.

Conclusions: SA often arises in patients with a longstanding cardiovascular disease and may be associated with connective tissue disorders. It can present as a tumor clinically and recognition of this entity is important to arrive at the correct diagnosis.

1595 Delayed Liver Graft Injury: An Analysis of Process, Pattern, and Clinical Implications

Justin Bateman[1], Oyedele Adeyi[2]
[1]University of Minnesota, Minneapolis, MN, [2]University of Minnesota Medical School, Minneapolis, MN

Disclosures: Justin Bateman: None; Oyedele Adeyi: None

Background: Delayed graft injury (i.e. liver injury occurring > 6 months post-transplant, [post-TXP]) represents a challenge for pathologists and clinicians. This is partly due to atypical patterns of alloimmune injury that need accurate diagnosis for appropriate treatment. To our knowledge the spectrum of these late injuries has not been described. In this study we review a single institution's experience to define the spectrum of liver allograft injuries occurring late, including alloimmune and non-alloimmune, as well as highlight their relative prevalence and clinical implications.

Design: Liver allograft biopsies performed >6 months post-TXP over a period of 5 years (2014-19) at an academic transplant center were reviewed. Clinical information was extracted from the patient's electronic medical records. Histologic parameters were assessed and correlated with clinical data including timing of onset and intervention outcomes. Cases classified as alloimmune were further sub-classified into variants.

Results: 282 liver biopsies from 180 patients were reviewed (Table 1). Alloimmune rejection occurred in 146 (52%) biopsies. The commonest non-alloimmune injury was recurrent disease in 44 cases (16%), including 13 from HCV, and de-novo parenchymal disease of which 19 cases (7%) were steatosis/steatohepatitis. 36 (13%) of biopsies showed advanced fibrosis. Rejection pattern was "typical"/portal-based in 55/146 (38%) cases. Other variants of alloimmune injury were ductopenic rejection (DR) in 35/146 (24%) and "atypical"/hepatitic in 43/146 (29%); the latter comprising plasma cell rich (PCR) and "idiopathic" post-TXP hepatitis. Cases with "non-specific portal inflammation" were classified based on recent understanding as alloimmune injury (12/146, 8%). PCR was the most likely cause of repeat biopsies (median=4) as a result of transient response to treatment but with recurrence at treatment completion, with 4 of 20 patients experiencing graft loss. Other direct causes of graft loss include DR, in which 60% of cases were associated with graft loss and death or re-transplantation.

Table 1: Demographics and Diagnoses in Delayed Graft Injury Liver Biopsies (2014-19)	
Total # of biopsies	282 (180 individual patients)
Age (years)	Mean=42 (Range:1-77)
Sex	M= 63% F=37%
Graft age (months)	Mean=52; Median=116 (range: 6-358)
Biopsy Diagnosis	
No significant abnormality	20 (7%)
Advanced fibrosis of uncertain etiology	8 (3%)
De novo steatohepatitis	19 (7%)
De novo HCV	1 (0.4%)
Vascular abnormality	25 (9%)
Large duct obstruction	8 (3%)
Recurrent Disease	44 (16%)
Typical/lobular acute cellular rejection	55 (20%)
Chronic ductopenic rejection	35 (12%)
Atypical/hepatitic pattern of acute cellular rejection	43 (15%)
Antibody-mediated rejection	1 (0.4%)
Minimal portal inflammation (alloimmune)	12 (4%)
CMV infection	2 (0.7%)
EBV infection	2 (0.7%)
Medication reaction	4 (1.4%)
Other	8 (3%)

Conclusions: As expected, atypical forms of rejection are a major cause of late dysfunction, with PCR showing relative resistance to usual rejection treatment of steroid bolus. Although alloimmune rejection accounted for more than half of diseases, this report highlights several other entities including recurrent disease and new-onset steatohepatitis. Furthermore, the presence of advanced fibrosis was not uncommon in our series.

1596   Early Liver Transplantation for Severe Alcoholic Hepatitis: Clinical and Pathologic Features in a Controversial Therapeutic Setting

Sepideh Besharati[1], Feriyl Bhaijee[2], Atoosa Rabiee[3], Ahmet Gurakar[1], Andrew Cameron[1], Amy Kim[1], Kiyoko Oshima[4], Robert A. Anders[5], Lydia Wu[6], Qingfeng Zhu[5]
[1]Johns Hopkins University, Baltimore, MD, [2]AmeriPath Indiana, Indianapolis, IN, [3]Washington DC VA Medical Center, Washington, DC, [4]Johns Hopkins Hospital, Baltimore, MD, [5]Johns Hopkins, Baltimore, MD, [6]Columbia University, New York, NY

Disclosures: Sepideh Besharati: None; Feriyl Bhaijee: None; Atoosa Rabiee: None; Ahmet Gurakar: None; Andrew Cameron: None; Amy Kim: None; Kiyoko Oshima: None; Robert A. Anders: None; Lydia Wu: None; Qingfeng Zhu: None

Background: Severe alcoholic hepatitis (SAH) has a high mortality, comorbidities, and complications. Liver transplantation (LT) for SAH has remained controversial due to concerns about the limited organ supply and the risk of recidivism. However, with recent studies showing good outcome with high survival rate and sobriety, more transplant centers are adapting to strict protocols to transplant patients with SAH.

We aim to study the pathologic features of SAH in comparison to alcoholic cirrhosis with >6 months abstinence prior to LT (AC) and evaluate their clinical outcomes.

Design: 45 patients with SAH who had liver transplantation from our pilot program and 21 patients with AC were evaluated. Trichrome, H&E, and iron stained slides were reviewed independently by 2 different blinded pathologists, who scored criteria as follows: 0 (none), 1 (mild/rare), 2 (moderate), and 3 (severe). Iron staining and fibrosis were scored on 0-4 scales and percent steatosis was quantified. Collagen density and Ki-67 ratio (Positive/total) were calculated using HALO software image analysis.

Results: Clinically, duration of alcohol consumption, length of abstinence prior to LT, MELD, Child-Turcotte stage, evidence of co-morbidity and hepatocellular carcinoma were significantly different while age, gender, BMI, grams of alcohol ingested per day were not significantly different. The one-year survival rate in SAH group and AC were 95% vs. 100% respectively. Histologically, the SAH cases showed significantly more steatosis, portal and lobular inflammation, Mallory-Denk hyaline, steatohepatitis, pericellular fibrosis, ductular reaction, cholate stasis, bile plugging, and collagen density (Table 1).

Table 1. Clinical and Pathologic Features in LT for SAH and AC patients (*statistically significant, ** Median (IQR), ***Mean)

Characteristic		AC (n = 21)	SAH (n = 45)	p Value
Age at transplant, y**		52.0 (51.0, 57.0)	49.0 (37.0, 56.0)	0.18
Male, n (%)		8 (38%)	14 (31%)	0.58
BMI**		28.0 (24.7, 30.7)	27.9 (25.0, 31.6)	0.73
Alcohol consumption duration, y**		20.0 (16.0, 28.5)	10.0 (7.0, 24.0)	0.020*
Standard drinks daily pre-abstinence**		70.0 (24.0, 299.0)	112.0 (80.0, 168.0)	0.36
Length of abstinence (days)**		423.0 (242.0, 1035.0)	61.0 (29.0, 124.0)	<0.001*
MELD at listing**		24.0 (13.0, 28.0)	35.0 (32.0, 39.0)	<0.001*
MELD at transplantation**		28.0 (26.0, 30.0)	34.0 (32.0, 38.0)	<0.001*
Child-Turcotte-Pugh	A	6 (29%)	0 (0%)	<0.001*
	B	5 (24%)	5 (11%)	
	C	10 (48%)	40 (89%)	
Co-morbidity, n (%)		6 (29%)	0 (0%)	<0.001*
Hepatocellular carcinoma, n (%)		4 (19%)	1 (2%)	0.016*
Steatosis (%) **		0.0 (0.0, 25.0)	10.0 (0.0, 25.0)	0.024*
Portal inflammation (0-3)***		1	2.37	<0.001*
Lobular inflammation (0-3) ***		0.67	2.42	<0.001*
Steatohepatitis (0-3) ***		0.048	1.47	<0.001*
Mallory -Denk bodies (0-3) ***		0.04	1.62	<0.001*
Pericellular fibrosis (0-3) ***		0.43	2.2	<0.001*
Portal fibrosis (0-4) ***		2.71	3.33	0.10
Ductular reaction (0-3) ***		0.38	1.93	<0.001*
Cholate stasis (0-3) ***		0.095	1.24	<0.001*
Bile plugging (0-3) ***		0.19	1.33	<0.001*
Iron deposition (0-4) ***		0.71	0.78	0.85
Cirrhosis, n (%)		17(81%)	43(96%)	0.055
Ki 67 Ratio***		0.012	0.006	0.21
Collagen Density (%) **		0.3 (0.1, 0.4)	0.4 (0.2, 0.5)	0.037*

Conclusions: Histologic changes in SAH cases show more advanced liver disease than those seen in AC patients, however 1 year outcomes were similar. Distinct histologic findings may be used for diagnosis when clinical history is unavailable. This also provides further bases to investigate the mechanisms of alcohol induced liver injury.

1597   Post-Transplant Acute Cellular Rejection of Liver: Comparison Between Immunohistochemical Markers Using Digital Image Analysis
Sepideh Besharati[1], Ahmet Gurakar[1], Robert A. Anders[2], Amy Kim[1], Qingfeng Zhu[2], Kyle Jackson[1], Andrew Cameron[1], Jacqueline Wang[1]
[1]Johns Hopkins University, Baltimore, MD, [2]Johns Hopkins, Baltimore, MD

Disclosures: Sepideh Besharati: None; Ahmet Gurakar: None; Robert A. Anders: None; Amy Kim: None; Qingfeng Zhu: None; Kyle Jackson: None; Andrew Cameron: None; Jacqueline Wang: None

Background: Acute cellular rejection (ACR) after liver transplantation is a serious complication which is shown to be associated with higher risk of graft failure. Markers of immune response have shown to predict graft complication including ACR. The aim of this study is to

evaluate the immune response of ACR compared to non-ACR cases from percutaneous liver biopsy specimens obtained from liver transplant recipients.

Design: This retrospective study included 53 liver transplant recipients who had a liver biopsy for abnormal liver enzymes. 27 of these patients had ACR and 26 patients did not have ACR but other causes of abnormal liver enzymes. Formalin-fixed paraffin-embedded blocks were retrieved from institutional pathology archive. H&E and immunohistochemistry staining (FOXP3, CD38, CD4, CD8, and PD-L1) were performed for all cases.

The stained slides were digitalized at 20X using NonoZoomer slide scanner and uploaded and annotated in HALO image analysis software. In order to make the tissue area matched in two groups of non-rejected cases (biopsy) and rejected cases (fine needle aspiration), we used pseudo-needle aspiration annotation (diagonal strip of whole tissue with 500-micron diameter) instead of whole slide biopsy annotation. The positive cells were quantified in the annotated tissue part and cell density was defined as cell count divided by tissue area (μ2). Biomarker expression levels were compared using Kruskal-Wallis test. A 2-sided α level of 0.05 was used to indicate statistical significance.

Results: Table 1 indicates clinical and positive cell density of immunohistochemical markers in rejected and non-rejected cased. Among clinical data, mean value of BMI and ALT was significantly different between two groups (P <0.05 and <0.001 respectively).CD4 and CD38 cell density were higher in non-ACR than ACR, and similar trend was noted in CD8. (P values<0.001). PD-L1 cell density was significantly higher in ACR compared to non-ACR (P <0.001), with FOXP3 cell density also higher in ACR cases although not statistically significant. (Figure 1).

Table 1. Clinical and immunohistochemistry stain positive cell density of liver biopsy in ACR vs Non-ACR patients.

	Non- ACR, N=26	ACR patients, N=27	P value
Age, mean	59.3	59.42	0.98
Male (%)	44.45	65.38	0.26
BMI, mean	30.21	25.76	0.03*
ALT, mean	60.07	251.04	<0.001*
AST, mean	80.77	165.04	0.18
HCC, n (%)	12(46.15)	13(48.14)	0.88
HCV, n (%)	14(53.85)	17(63)	0.5
Immunohistochemistry			
FOXP3, median (IQR)	19.07 (11.13 – 43.48)	34.85 (17.65 – 56.07)	0.14
CD38, median (IQR)	71.46 (47.88 – 116.95)	8.27 (3.39 – 21.01)	<0.001*
CD4, median (IQR)	599.92 (392.52 – 1024.17)	417.75 (293.67 – 561.65)	<0.05*
CD8, median (IQR)	344.87 (181.78)	288.26 (161.58)	0.24
PD-L1, median (IQR)	51.59 (26.42 – 118.34)	204.46 (88.20 – 488.98)	<0.001*

Figure 1 - 1597

Comparison between ACR and non-ACR cases in terms of CD8, CD4, CD38, FOXP3 and PDL1 positive cells density in liver biopsy
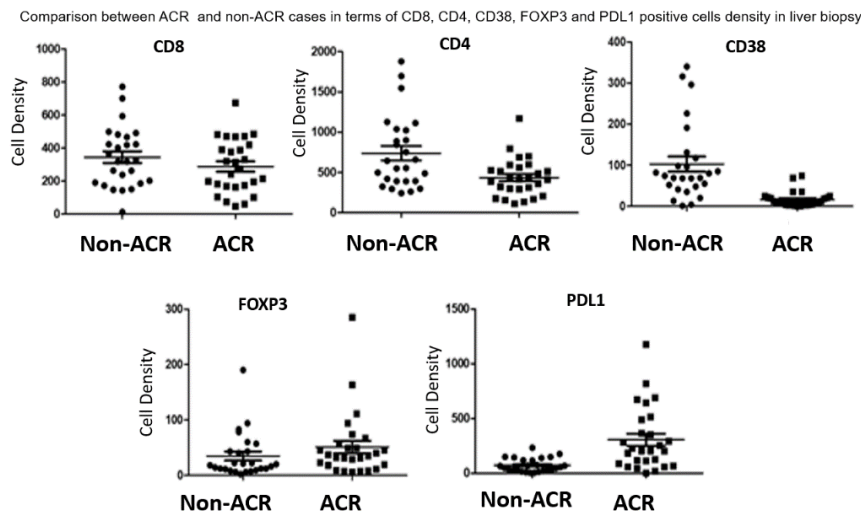
Conclusions: This preliminary study points to the immune mechanism involved in ACR.

1598 Heterozygous Alpha-1 Antitrypsin Deficiency Potentiates Liver Fibrosis with Other Chronic Liver Diseases

Margaret Black[1], Maureen Whitsett[2], Ira Jacobson[2], Yvelisse Suarez[3], Neil Theise[3]
[1]NYU, Long Island City, NY, [2]New York University Langone Health, New York City, NY, [3]NYU Langone Health, New York, NY

Disclosures: Margaret Black: None; Maureen Whitsett: None; Ira Jacobson: None; Yvelisse Suarez: None; Neil Theise: None

Background: Alpha-1 antitrypsin deficiency (AATD) arises from inherited autosomal co-dominant *SERPINA1* mutations that lead to liver and lung disease. Clinical manifestations within the liver are variable and include chronic hepatitis, cirrhosis, and the development of hepatocellular carcinoma. While the risk of liver disease with homozygous AATD is established, the prevalence of clinically significant liver disease in heterozygotes is not well described. Accumulating evidence suggests that heterozygous AATD (HAATD) acts as a co-factor for other liver diseases, but little is known about its effect on pathologic fibrosis. We investigate the stage of liver fibrosis in patients with histologic evidence of HAATD compared to controls with a wide range of chronic liver diseases.

Design: Our database was retrospectively searched to obtain 23 liver biopsy and resection specimens with evidence of chronic liver disease and intracytoplasmic α1 anti-trypsin (AAT) globules stained by immunohistochemistry. The group with histologic evidence of possible HAATD was compared to control cases of liver biopsies obtained from patients with chronic liver disease without evidence of AAT globules. Clinicopathologic data included age, gender, race, genotype, chronic liver disease type (chronic cholestatic disease, fatty liver disease, Hepatitis B or C, auto-immune hepatitis, hemochromatosis, and unknown cause), liver disease stage, and clinical follow-up. Statistical analyses were performed to assess correlation between clinicopathologic variables and disease groups.

Results: Compared to controls, subjects in the HAATD cohort had a higher rate of stage 4 fibrosis (52.17% vs 21.67%, *p* = 0.017). The control specimens were relatively evenly distributed among stages 1-4 fibrosis (Table). Of the 7 HAATD patients who underwent subsequent genetic testing, 6 patients were found to have heterozygous *SERPINA1* mutations (5 PI*MZ, 1 PI*SZ). There were no significant differences in age, race, or gender between control and HAATD groups.

Clinicopathologic Factor	HAATD	Control	p-value
Age			
Age < 60	14 (60.87%)	71 (59.17%)	1.0000 (N.S.)
Age >= 60	9 (39.13%)	49 (40.83%)	
Race			
White	17 (73.91%)	76 (63.33%)	0.8515 (N.S.)
Black	1 (4.35%)	13 (10.83%)	
Asian	2 (8.70%)	12 (10.00%)	
Hispanic	1 (4.35%)	11 (9.17%)	
Other	2 (8.70%)	8 (6.67%)	
Gender			
M	16 (69.57%)	60 (50.00%)	0.1109 (N.S.)
F	7 (30.43%)	60 (50.00%)	
Stage			
1	3 (13.04%)	37 (30.83%)	0.01652
2	2 (8.70%)	28 (23.33%)	
3	6 (26.09%)	29 (24.17%)	
4	12 (52.17%)	26 (21.67%)	

Conclusions: Histologic and immunohistochemical evidence of AAT globules was associated with a higher stage of concurrent liver disease. These results add to the growing body of literature which suggests that HAATD may potentiate the progression of concurrent liver diseases. In addition, histologic and immunohistochemical evidence of AAT globules may be useful in the early diagnosis of HAATD.

1599 Evaluation of Liver Zonation Patterns Utilizing Argininosuccinate Synthetase (ASS1) and Glutamine Synthetase (GS) Immunostains in Cirrhosis and Focal Nodular Hyperplasia (FNH)

Katherine Boylan[1], John Hart[1]
[1]The University of Chicago, Chicago, IL

Disclosures: Katherine Boylan: None; John Hart: None

Background: ASS1 is a urea cycle enzyme essential for ammonia metabolism and is restricted to zone 1 hepatocytes. GS plays a role in maintaining amino acid balance and is restricted to zone 3 hepatocytes. Altered expression of GS has been reported in cirrhosis and in FNH, but there are no studies of ASS1 as a zone 1 marker in these disorders. This study aims to investigate alterations in zone 1 and zone 3 hepatocyte distributions in cirrhosis of various etiologies and FNH utilizing ASS1 and GS immunostains.

Design: Native livers and lobectomy cases of cirrhosis (n=14), FNH (n=8), and normal liver (n=3) were selected. Etiologies of cirrhosis included chronic venous outflow obstruction (cardiac, n=2), chronic hepatitis (macronodular, n = 8, HCV, HBV & AIH), steatohepatitis (micronodular, n=2), and biliary (biliary, PBC, n=2). Consecutive sections were stained with ASS1 and GS. The ASS1 antibody was obtained from ProteinTech and performed at 1:2000 dilution utilizing the Leica system.

Results: Cardiac cirrhosis showed near total extinction of GS staining with scattered positive staining of debris in Kupffer cells and in hepatocytes adjacent to fibrous septa and remaining central veins. There was diffuse expansion of strong ASS1 staining throughout the nodules. All macronodular cirrhosis cases exhibited preserved zone 3 GS staining around central veins, as well as migration of zone 3 hepatocytes to the periphery of some nodules. ASS1 revealed expansion of zone 1 with strong staining throughout each nodule. Micronodular cirrhosis showed minimal patchy GS staining at the periphery of nodules, with preserved ASS1 strong staining at the periphery of nodules and diffuse moderate expansion of zone 1 throughout the nodules. Biliary cirrhosis showed expansion of zone 3 GS hepatocytes, as well as expansion of zone 1 ASS1 hepatocytes, such that hepatocytes in the centers of nodules expressed both markers. FNH cases showed map-like expansion of GS zone 3 hepatocytes, with preservation of zone 1 ASS1+ hepatocytes next to septa, and zone 2 hepatocytes negative for both markers.

Figure 1 - 1599
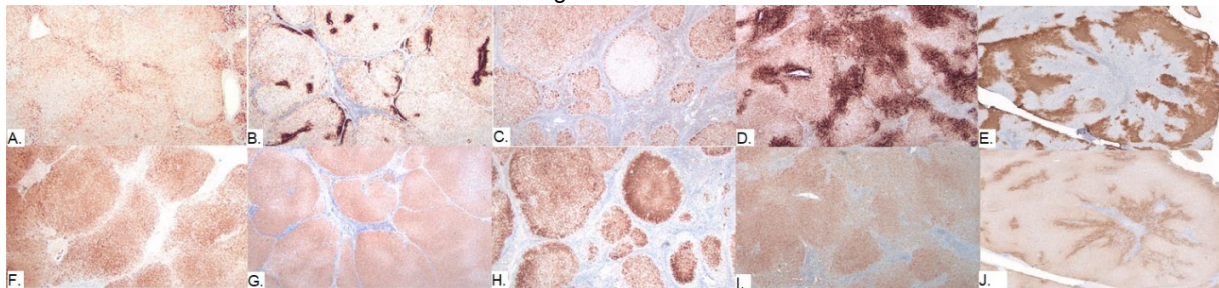
Figure 1. Representative sections of liver; top row stained with glutamine synthetase (GS), and bottom row stained with argininosuccinate synthetase (ASS1) immunohistochemical stains. A & F) Cardiac cirrhosis. B & G) Macronodular cirrhosis. C & H) Micronodular cirrhosis. D & I) Biliary cirrhosis. E & J) Focal nodular hyperplasia.

Conclusions: Each etiology of cirrhosis exhibits a distinctive pattern of GS (zone 3) and ASS1 (zone 1) expression reflecting the pathologic processes responsible for cirrhosis development. The staining patterns provide insight into mechanisms of hepatic injury and suggest clinical utility in evaluating cryptogenic cirrhosis cases. ASS1 staining in FNH reveals retention of zone 1 hepatocytes, despite the expansion of GS+ zone 3 hepatocytes.

1600   Positive Antimitochondrial Antibodies in Patients without Primary Biliary Cholangitis Who Underwent Liver Biopsies: A Thirteen-Year Experience in a Large Hospital Network
Lawrence Browne[1], Mojgan Hosseini[2], Jingjing Hu[3], Soora Wi[4]
[1]TPMG Kaiser, Orinda, CA, [2]University of California San Diego, La Jolla, CA, [3]University of California San Diego, San Diego, CA, [4]Kaiser TPMG, Berkeley, CA

Disclosures: Lawrence Browne: None; Mojgan Hosseini: None; Jingjing Hu: None; Soora Wi: None

Background: Antimitochondrial antibodies (AMA) are considered to have a high degree of specificity for the diagnosis of primary biliary cholangitis (PBC) [e.g., Most assays = 95 % sensitive and 98 % specific for PBC. Clin Liver Dis. 2008;12(2):261]. "False positivity" for AMA is a recognized phenomenon, but .the percentage of false positives and the histologic diagnostic findings in those patients who underwent a liver biopsy, resection, or FNA who do not have PBC are not well described.

Design: The electronic records of a large hospital system were reviewed for all AMA tests performed between 2/3/2005 and 6/26/2018. The positive results were cross-matched to those patients who underwent a liver biopsy, resection, or FNA during that time period +1 year. The liver diagnoses were reviewed to determine which cases were consistent with PBC and/or an obstructive biliary process versus other liver conditions.

Results: A total number of 63,348 AMA tests were performed between 2/3/2005 and 6/26/2018. 2341 AMA tests (3.7%) were positive. Of the positive tests, 914 patients (39%) had a liver pathology sample. 5% of liver biopsies were morphologically consistent with PBC or an obstructive biliary process. The remaining diagnoses were classified for our study as follows: Hepatitis C (HCV) = 41%; Hepatitis B (HBV) = 6%; Steatohepatitis/Fatty liver disease = 5%; Iron overload = 2%; Primary liver malignancy = 4%; Metastatic neoplasm = 14%; Benign tumor or cyst = 3%; Nonspecific diagnoses and Nondiagnostic specimens = 20%.

Conclusions: False-positive AMA results are important to recognize for liver biopsies that are not morphologically consistent with a diagnosis of PBC. The most common liver diagnosis in patients with a positive AMA who also had a liver pathology sample in our system carried a diagnosis of HCV. PBC represented a very small subset of diagnoses. The AMA testing did not appear to drive the liver sampling in many cases, as is evinced by the large number of patients in our cohort undergoing biopsies for diagnostic confirmation of metastases. Liver pathologists should be aware of the high rate of potential "false positive" AMA results in patients undergoing liver sampling for a spectrum of reasons.

Limitations of our study include the fact that FNAs generally cannot rule out a diagnosis of PBC, although FNA represent a minority of the samples reviewed. A further limitation is that it is unknown what % of positive AMA test results specifically drove liver sampling in our system.

1601 Histologic Characteristics of Adjacent Mass Effect Differ in Primary and Metastatic Liver Neoplasms

Caroline Bsirini[1], Raul Gonzalez[2], Diana Agostini-Vulaj[1]
[1]University of Rochester Medical Center, Rochester, NY, [2]Beth Israel Deaconess Medical Center, Boston, MA

Disclosures: Caroline Bsirini: None; Raul Gonzalez: None; Diana Agostini-Vulaj: None

Background: Liver neoplasms, whether primary or metastatic, may cause adjacent liver parenchymal changes referred to as mass effect (ME), typified by bile ductular reaction, sinusoidal dilation, and edematous portal tracts with neutrophils. Although this phenomenon is well known, it has received little scrutiny. This study aims to analyze whether histologic changes of ME in the liver differ depending on the type and origin of causative neoplasm.

Design: We identified 166 cases of primary or metastatic liver neoplasms. Clinicopathologic features analyzed included age, sex, portal changes, inflammatory milieu, hepatocyte atrophy, cholestasis, sinusoidal dilation, acidophil bodies, ductular reaction, interface with liver parenchyma, and maximum distance of mass effect changes seen adjacent to neoplasm (when possible). Statistical analyses were performed using Fisher's exact test, with P-values of <0.05 considered significant.

Results: Our cohort included 36 (22%) primary liver neoplasms, including hepatocellular carcinoma (HCC) (26, 72%) and hepatocellular adenoma (HCA) (10, 28%), along with 130 (78%) metastatic neoplasms, including colorectal adenocarcinoma (59, 46%), breast carcinoma (29, 22%), lung adenocarcinoma (16, 12%), urothelial carcinoma (16, 12%), and melanoma (10, 8%). Compared with primary liver neoplasms, sinusoidal dilation and cholestasis were more commonly seen in metastatic liver neoplasms (P=0.024 and P=0.019, respectively) (Fig. 1). The interface between tumor and normal liver in the metastatic group was more commonly ill-defined (P<0.0001) (Table). Among primary neoplasms, HCC more often showed neutrophils in the background than HCA (P=0.0003). HCAs generally tended to show minimal adjacent changes (Fig. 2). Of the metastatic neoplasms, breast carcinoma notably demonstrated very minimal findings in >50% of cases, some of which displayed subtle sinusoidal tumor extension. Additionally, melanoma showed sinusoidal extension in 40% of cases. ME changes could be seen up to 1.8 cm away from the neoplasm.

Table 1. Histologic Features of Mass Effect Changes in Primary and Metastatic Liver Neoplasms

	Primary liver tumors n (%)	Metastatic liver tumors n (%)	P-value
Sinusoidal dilation	20 (55)	98 (75)	0.024
Sinusoidal blood	15 (42)	36 (28)	0.15
Ductular reaction	21 (58)	65 (50)	0.45
Cholestasis	17 (47)	102 (78)	0.019
Neutrophils	18 (50)	78 (60)	0.34
Lymphocytes	21 (58)	86 (66)	0.43
Acidophil bodies	5 (14)	31 (24)	0.26
Portal vein changes	2 (6)	3 (2)	0.3
Portal edema	1 (3)	6 (5)	1
Hepatocyte atrophy	9 (25)	33 (25)	1
Interface with liver parenchyma	Fibrotic capsule, 5 (14%) Ill-defined, 17 (47%) Well-delineated, 12 (33%) Not applicable, 2 (6%)	Ill-defined, 114 (87%) Well-delineated, 14 (11%) Not applicable, 2 (2%)	<0.0001

Figure 1 - 1601
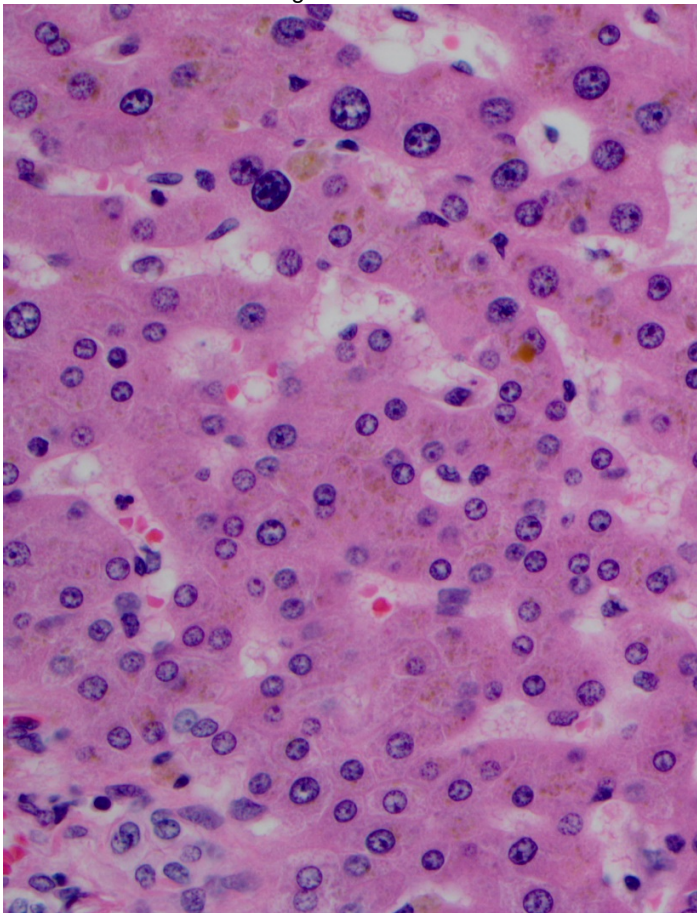
Figure 2 - 1601
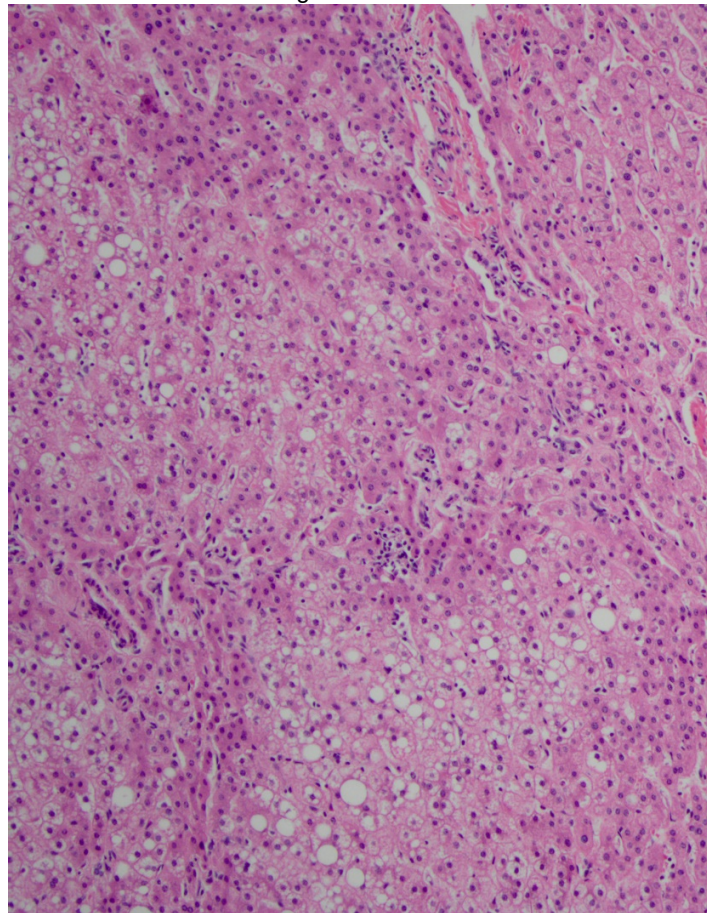
Conclusions: Our study demonstrates that different patterns of ME change can be observed depending on whether the adjacent neoplasm is primary or metastatic. Of note, sinusoidal dilation and cholestasis are more commonly seen in metastatic disease than primary liver neoplasms. Pathologist awareness of these different findings may be of utility in cases of liver biopsies where the targeted lesion is mostly or entirely unsampled.

1602 Molecular Confirmation of Alpha 1-Antitrypsin (AAT) Deficiency in Liver Transplant Setting: A Province-Wide Experience

Hussam Bukhari[1], Andre Mattman[2], Gordon Ritchie[3], Laura Burns[4], David Schaeffer[5], Hui-Min Yang[6]
[1]Vancouver, BC, [2]St Paul Hospital/University of British Columbia, Vancouver, BC, [3]St. Paul's Hospital/University of British Columbia, Vancouver, BC, [4]St. Paul's Hospital, Vancouver, BC, [5]Vancouver General Hospital, Vancouver, BC, [6]Vancouver General Hospital/University of British Columbia, Vancouver, BC

Background: Alpha 1-Antitrypsin deficiency is a hereditary autosomal recessive disorder which affects AAT, a plasma protease inhibitor, leading to increased risk of pulmonary and liver disease including the risk of developing hepatocellular carcinoma. The most commonly affected AAT alleles are the Pi*Z and Pi*S alleles. Patients suspected of harboring an AAT abnormality based on low serum concentration of the enzyme are confirmed via isoelectric focusing and/or PCR based DNA tests using peripheral blood samples. Determining AAT genotype via molecular analysis of Formalin-Fixed Paraffin-Embedded (FFPE) specimens is a novel approach that may aid in the detection of abnormal AAT alleles. We performed real-time PCR assay of FFPE liver explant tissue in specimens that showed PASD positive & AAT immunoreactive globules to determine proportion of aberrant AAT allele frequency in liver transplant patients in British Columbia.

Design: A total of 142 patients with end-stage liver disease had received liver transplants in British Columbia, Canada from May 1, 2016 to May 1, 2019. Of those patients,18 (12.68%) showed positivity for periportal PASD positive globules. The globules were immunohistochemically positive for AAT. The 18 patients were selected for real-time PCR analysis of FFPE hepatic explant tissue to detect S and Z allele variants. Sanger sequencing of rare alleles variants is to be performed if PCR proved negative. Of the 18 patients tested, 7 patients (38.9%) had a normal pre-transplant AAT serum levels, 3 patients (16.7%) had a low serum AAT levels and 8 patients (44.4%) were not tested preoperatively for AAT serum concentration. <

Results: Real-time PCR assay of the FFPE tissue was successful with all the tissue samples meet quality control parameters. All the patients included in the study elucidated Z allele variants; 2 of which are homozygous (11.1%) and 16 heterozygous (88.9%).

Conclusions: Screening for AAT deficiency using serum levels is not sufficiently sensitive to detect deficiency, especially in carriers of heterozygous alleles or rare alterations, frequently leaving an unsatisfying diagnosis of cryptogenic cirrhosis. If AAT genotyping was not performed preoperatively and the risk is high based on the histological presence of PASD/AAT positive globules in the explanted liver, then the underlying etiology could be confirmed via molecular testing of FFPE tissue. This may lead to an increase in detection and diagnosis of previously clinically underdiagnosed cases of nonspecific cirrhosis.

1603 Reproducibility of NAS Score and Correlation with Steatohepatitis Diagnosis

Joseph Burt[1], Stephen Lagana[1], Anne Koehne de Gonzalez[1], Michael Lee[2], Ladan Fazlollahi[1], Helen Remotti[3]
[1]New York-Presbyterian/Columbia University Medical Center, New York, NY, [2]Columbia University, Long Island City, NY, [3]Columbia University Medical Center, New York, NY

Background: The Nonalcoholic fatty liver disease Activity Score (NAS) is commonly used in therapeutic trials to evaluate changes in Nonalcoholic fatty liver disease (NAFLD). A cutoff NAS score ≥ 5 (Brunt criteria) may be mistaken as a surrogate for establishing the pathologic diagnosis of Nonalcoholic steatohepatitis (NASH), which takes into account other histologic features of the biopsy. This study aims to investigate the interobserver reproducibility of the NAS score, and the variation between final pathologic diagnosis and NAS score, among subspecialist liver-GI pathologists at a single academic medical center.

Design: 30 anonymized adult liver biopsies were examined by 4 pathologists. Cases were graded for degree of steatosis (0-3), lobular inflammation (0-3), hepatocyte ballooning (0-2), steatosis location, portal inflammation (0-2), fibrosis, the presence of Mallory-Denk bodies, and NAS Score (0-8). The NAS point scale was divided into 3 categories (≥ 5, 3-4, ≤2) corresponding to 3 diagnostic categories (steatohepatitis, borderline steatohepatitis, not steatohepatitis). The intra-class correlation coefficient (ICC) was calculated using two-way ANOVA for NAS score, final diagnosis, histologic features, and agreement between NAS and final diagnosis.

Results: A NAS ≥ 5 was seen in 18% of cases, while a final pathologic diagnosis of steatohepatitis was given in 23% of cases. Of cases diagnosed as steatohepatitis, 71% had NAS ≥ 5, 29% had NAS 3-4, and none had NAS ≤2. Of cases diagnosed as borderline steatohepatitis, 5% had NAS ≥ 5, 90% had NAS 3-4, and 5% had a NAS ≤2. Of cases diagnosed as not steatohepatitis, none had NAS ≥ 5, 25% had NAS 3-4, and 85% had NAS ≤2.

Variable	Interrater agreement (ICC)
NAS Score	0.73
Final diagnosis	0.68
Steatosis	0.73
Lobular inflammation	0.46
Ballooning	0.78
Steatosis location	0.23
Chronic portal inflammation	0.55
Fibrosis	0.87
Mallory-Denk bodies	0.66

Conclusions: NAS score showed better reproducibility than final diagnosis and good correlation with diagnosis (ICC 0.85). Greatest correlation was seen between a diagnosis of borderline steatohepatitis and a NAS 3-4, while 29% of cases diagnosed as steatohepatitis did not reach a NAS score ≥ 5. Greatest interrater agreement was seen with fibrosis staging and least with grading lobular inflammation and steatosis location. These data suggest NAS scoring is reproducible and useful for clinical NASH studies following response to treatment, but NAS scores may not correlate with pathologic diagnosis of NASH. Evaluation of scoring systems incorporating extent and pattern of fibrosis with NAS Score may show stronger correlation with NASH.

1604 Dynamic Changes in the Portal Tract Interstitium (Space of Mall) in Primary Sclerosing Cholangitis and Chronic Hepatitis C

Qing Chang[1], Sunjida Ahmed[2], Briana Zeck[2], Lilly Drohan[3], Xiaodong Li[4], Odise Cenaj[5], Wenqing Cao[5], Neil Theise[2]
[1]NYU Langone Health, Staten Island, NY, [2]NYU Langone Health, New York, NY, [3]Colgate University, Hamilton, NY, [4]UCI Medical Center, South Pasadena, CA, [5]New York University Langone Health, New York, NY

Disclosures: Qing Chang: None; Sunjida Ahmed: None; Briana Zeck: None; Lilly Drohan: None; Xiaodong Li: None; Odise Cenaj: None; Wenqing Cao: None; Neil Theise: None

Background: In 1906, Franklin Mall described a portal tract (PT) stromal vascular space, the "Space of Mall" (SoM). Recently, in vivo microscopy confirmed Mall's insights: fibroconnective tissues of the body, including biliary submucosae and the PT stroma, are a pre-lymphatic, reticular network of fluid-filled interstitial sinuses supported by a complex scaffold of thick collagen bundles (Benias et al *Sci Rep* 2018:8). Elastin fibers interlace with collagen. The fluid is rich in hyaluronic acid (HA). These components have been little studied in liver disease. We investigated changes in SoM matrix and fluid across all stages of Primary Sclerosing Cholangitis (PSC) and chronic hepatitis C (CHC).

Design: FFPE tissues from normal liver and liver biopsies/explants with all stages of PSC (n=8) and of Metavir F1-F4 CHC (n=12) were stained with H&E, Masson trichrome, Elastin Van Gieson (EVG). Multiplex chromogenic IHC assay (DISCOVERY Ultra, Ventana) stained for HA (brown); vimentin (magenta) and CD34 (teal) labeled endothelial and interstitial lining cells. D2-40 IHC showed lymphatic endothelium scored as 1+ to 4+ based on ease of identification, low to high power. Extra-PT sinusoidal HA (sHA) was semiquantitatively scored (1+: <10%, 2+: 10-25%, 3+: 25-50%, 4+: >50%). EVG distinguished fibrillary vs. amorphous elastin.

Results: Selected results are presented in Figs 1 and 2. Normal PTs show thick dense collagen bundles between which are spaces densely filled with HA and sHA present roughly confined to the limiting plate. HA shows PT spaces to be continuous through PT stroma. Collagen: normal in early PSC and in uninflamed CHC PT, but markedly diminished within CHC PT inflammatory infiltrates. sHA: early/intermediate PSC: 1+-4+, late PSC: 4+; CHC F1: 2+-3+, F2-F4: 4+ and often associated with CD34+ sinusoidal capillarization. D2-40: nearly absent in normal PT, 4+ in all stages of PSC and F1-F3 CHC, but 3+-4+ in cirrhotic CHC. Elastin: fibrillary in normal, absent in early/intermediate stage PSC, fibrillary and amorphous in non-inflamed CHC PT, though absent in portal inflammation. Increased in all advanced stages.

Figure 1 - 1604

Figure 1. Collagen and elastin composition in normal and early stages of PSC and CHC
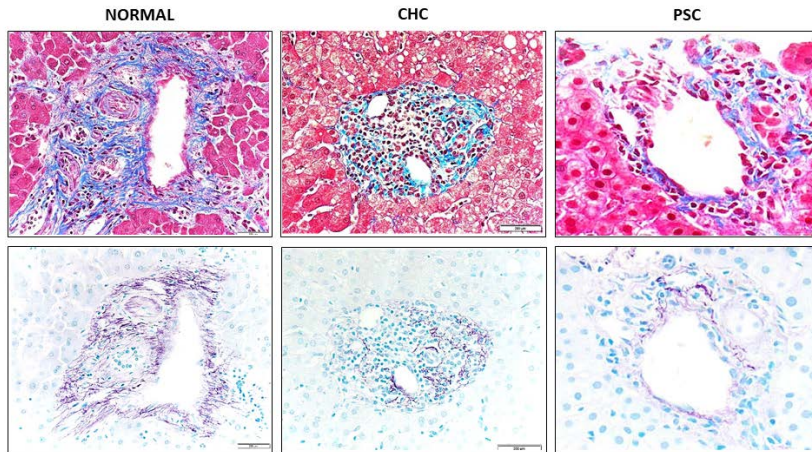
Figure 1 Legend. <u>Upper row</u>: Trichrome stain shows normal collagen bundles with very narrow space of Mall between them in normal tissue. In CHC collagen bundles appear normal in the absence of inflammation, but where inflammation is prominent the collagen becomes inapparent. In PSC portal tracts, with and without bile ducts, there is normal appearing collagen and interstitial spaces. <u>Lower row</u>: EVG stain highlights normal fibrillary elastin fibers throughout the portal tract stroma. Elastin is absent in the midst of CHC inflammation, but maintained in non-inflamed stroma. In PSC stromal elastin fibers are absent, leaving only blood vessel walls staining positive.

Figure 2 - 1604

Figure 2. Hyaluronic Acid in Portal Tract Interstitium/Space of Mall and in Sinusoids
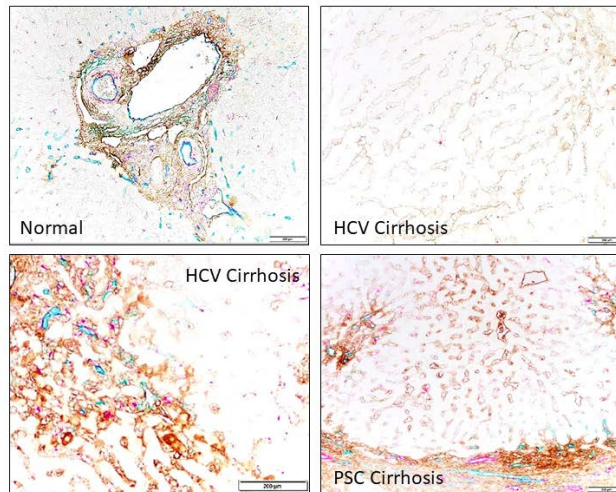
Figure 2 Legend. Multiplex chromogenic IHC assay stained for HA (brown); vimentin (magenta) and CD34 (teal) label endothelial and interstitial lining cells. <u>Upper Left</u>: Normal portal tract shows PT interstitium/space of Mall filled with HA; slight sinusoidal HA at limiting plate (10x) <u>Lower left</u>: Advanced stage CHC shows extensive that most prominent sinusoidal HA staining co-localizes with CD34 sinusoidal capillarization. <u>Upper, Lower Right</u>: Extensive sinusoidal HA in advanced liver disease.

Conclusions: HA stains confirm that spaces in PT stroma are not artifactual, but are those defined by Mall and, as he demonstrated, are one continuous space. PT mesenchymal components are not static in early or advanced stages of chronic biliary and hepatitic diseases, but show an underappreciated dynamic range of changes that are often disease specific.

1605 Obliterative Venopathy-like Changes in Routine Liver Biopsies without Known Portal Hypertension

Aastha Chauhan[1], Monica Sanchez-Avila[2], Dale Snover[2]
[1]University of Minnesota, Saint Paul, MN, [2]University of Minnesota, Minneapolis, MN

Disclosures: Aastha Chauhan: None; Monica Sanchez-Avila: None; Dale Snover: None

Background: Obliterative portal venopathy (OPV), also known as hepatoportal sclerosis (HPS) is regarded as the primary histological diagnosis for idiopathic non-cirrhotic portal hypertension (INCPH). INCPH is a rare clinical syndrome, defined by the presence of unequivocal clinical signs of portal hypertension (PH) with patent extrahepatic portal and hepatic veins, and no evidence of cirrhosis or any

other liver disease causing PH. The histological features of OPV include portal vein sclerosis, herniated portal veins, hypervascular portal tracts, and duplication of central veins (Guido et al. Histopathology 2019; 74:219-226). A prior study reported these changes in approximately 20% of biopsies from patients with elevated transaminases and no other known cause of liver disease (Guido *et al*,Liver Int. 2016; 36: 454-460). This study was undertaken to determine the frequency of these changes in random biopsies.

Design: We analyzed consecutive liver biopsies from January 2009 to December 2014, in adult patients who underwent biopsy for non-tumour lesions. Cases with stage 3 or 4 fibrosis were excluded.

Biopsies were evaluated for portal vein sclerosis, herniated portal veins, hypervascularized portal tracts, periportal abnormal vessels, and multiple central veins.

Results: A total of 100 consecutive biopsies with technically adequate biopsies were assessed. Of these, 82 were from females and 18 from males. Total number of evaluable portal tracts ranged from 1 – 18 per biopsy (mean 5). 35% of biopsies had at least one herniated portal vein and 45% had hypervascular portal tracts. 20% had both. Periportal abnormal vessels were not identified. For biopsies with herniation, 11 – 83% of portal tracts showed this change (mean 35%) and for hypervascularity 10 – 100% (mean 36%). Number of central areas ranged from 0 – 10 per biopsy (mean 2.8) and 15% of biopsies had duplicated central vein branches.

Conclusions: The presence of histological features of OPV is common in biopsies regardless of underlying pathology. Currently the clinical significance of these changes particularly in regard to current or future portal hypertension is unknown. Further study including correlation with laboratory data including coagulation studies and outcome should help determine the minimal number of these changes that may be of clinical significance.

1606 Immunotherapy Related Hepatitis: Histology, Lymphocytic Infiltrate Characterization and PD-L1 Staining Pattern

Jesus Chavez[1], Wendy Frankel[2], Clarissa Cassol[3], Christina Arnold[4], Dwight Owen[2], Wei Chen[2]
[1]The Ohio State University, Marble Cliff, OH, [2]The Ohio State University Wexner Medical Center, Columbus, OH, [3]The Ohio State University, Columbus, OH, [4]The University of Colorado, Denver, CO

Disclosures: Jesus Chavez: None; Wendy Frankel: None; Clarissa Cassol: None; Christina Arnold: None; Dwight Owen: *Advisory Board Member*, AstraZeneca; Wei Chen: None

Background: Immune checkpoint inhibitors (ICPIs) show sustained clinical response in multiple advanced malignancies. The activated T cells can lead to nonspecific immune system activation, with adverse events ranging from fatigue, dermatologic/mucosal toxicity to endocrinopathies and hepatotoxicity. Immunotherapy related hepatitis (IRH) can be seen as early as 8 weeks after therapy, but the associated histologic findings are not well defined. PD-L1 epithelial membranous staining was recently described as a specific finding in ICPIs interstitial nephritis, and we postulated that it could also be seen in IRH.

Design: We identified 5 patients on ICPIs therapy for metastatic cancer with a medical liver biopsy (bx) performed 01/2010 to 12/2018. H&E stained slides, pathology reports and laboratory data were reviewed. Immunohistochemistry for CD4, CD8, CD20 and PD-L1 was performed. The liver inflammatory infiltrate was semi-quantified using 40x fields (3 hot spots averaged). 7 cases of age-matched classic autoimmune hepatitis (AIH) cases were identified and evaluated for comparison. Patients with other explanations for the liver injury or history of liver transplant were excluded. Statistical analysis was performed using unpaired t-test.

Results: 5 cases of IRH were identified: 3 patients on anti PD-1, 1 on anti CTLA-4 and 1 receiving combined therapy. The ICPIs were for 2 melanomas, 2 lung adenocarcinoma and 1 breast cancer. On average, liver bx was performed 48 weeks after initial therapy and 12 weeks from last dose with the most common indication being mildly elevated liver function tests. We found a hepatitis pattern of injury with mild mixed portal and lobular inflammation and scattered dead hepatocytes; 3 cases demonstrated additional findings including glassy hepatocytes (combined therapy), lobular histiocytic aggregates (PD-1) and reactive hepatocytes (PD-1). In both IRH and AIH, the inflammatory infiltrate was predominantly CD8+ T lymphocytes, and IRH showed a trend of higher CD4:CD8 ratio (1:3 vs. 1:8, p=0.06) than AIH. PD-L1 staining was positive in 1 patient receiving anti PD-1 therapy (membranous staining in inflammatory cells and weak cytoplasmic in hepatocytes), but negative in all AIH cases.

Table 1. Lobular Immunostaining Pattern Score Comparison between Autoimmune Hepatitis (AIH) and Immunotherapy Related Hepatitis (IRH) Cases.

	CD4 (mean)	CD8 (mean)	CD4:CD8 (mean)	CD20 (mean)	PDL-1+/- (n)
AIH (n=7)	5.4	43.4	1:8	4	-
IRH (n=5)	6	18	1:3	1.8	+ (1)

Conclusions: The predominance of CD8+ T lymphocytes in liver bx of patients receiving ICPIs supports an immune mediated hepatic injury. Unlike ICPIs associated interstitial nephritis, membranous PD-L1 epithelial staining was not seen in IRH in this small cohort.

1607   C-Reactive Protein (CRP) is Superior to Serum Amyloid A (SAA) for Identifying Inflammatory Hepatic Adenomas

Zongming Eric Chen[1], Dhanpat Jain[2], Sanjay Kakar[3], Tsung-Teh Wu[1], Saba Yasir[1], Matthew Yeh[4], Michael Torbenson[1]
[1]Mayo Clinic, Rochester, MN, [2]Yale University School of Medicine, New Haven, CT, [3]University of California San Francisco, San Francisco, CA, [4]University of Washington Medical Center, Seattle, WA

Disclosures: Zongming Eric Chen: None; Dhanpat Jain: None; Sanjay Kakar: None; Tsung-Teh Wu: None; Saba Yasir: None; Matthew Yeh: None; Michael Torbenson: None

Background: Subtyping hepatocellular adenomas is an important part of patient management. For example, inflammatory hepatocellular adenomas are important to identify because they have an increased risk for hemorrhage and for beta-catenin activation. CRP and SAA immunostains are the standard methods to identify inflammatory hepatocellular adenomas. There is limited data comparing the sensitivity of these two stains.

Design: A multicenter, retrospective study examined the frequency of positive staining for SAA and CRP in inflammatory hepatocellular adenomas. The study included both biopsies and resection specimens. A subset analysis was also performed for cases with beta-catenin activation.

Results: Inflammatory hepatocellular adenomas were identified in 87 patients with an average age of 38 ± 12 years (75 women, 8 men, 4 unavailable). 32% were biopsy specimens. Based on beta-catenin and glutamine synthetase staining, 11 tumors also had beta-catenin activation (13%). Immunostains for SAA were positive in 79 of 85 (91%) cases, but were patchy or weak in 13 (15%) positive cases. In contrast, CRP was more sensitive, being positive in 84 of 86 (97%) cases. Put another way, 6% of all inflammatory hepatocellular adenomas were positive only for CRP (negative for SAA), while 1% were positive for SAA and negative for CRP. These findings were similar in the subset of 11 inflammatory hepatocellular adenomas that also had beta catenin activation: 8 were positive for both, 1 for CRP alone and 2 for SAA alone.

Conclusions: This is one of the largest series of inflammatory hepatocellular adenomas to specifically examine the sensitivity of SAA vs CRP for identifying inflammatory adenomas. In this study, CRP was more sensitive than SAA (97% positive vs 91% positive). SAA also had an additional 15% of cases that had weak, patchy, or equivocal staining. Overall, 11% of inflammatory adenomas also showed beta catenin activation. These beta catenin activated adenomas showed similar staining patterns with CRP and SAA. Thus, in pathology practices that choose to use a single stain, CRP is more sensitive than SAA.

1608   Utility and Limitations of Albumin RNAScope Detection of Albumin mRNA in the Diagnosis of Hepatobiliary Lesions and Metastatic Carcinomas in the Liver

Katrina Collins[1], Safina Hafeez[2], Saverio Ligato[3], Richard Cartun[2]
[1]The University of Texas MD Anderson Cancer Center, Houston, TX, [2]Hartford Hospital, Hartford, CT, [3]Hartford Hospital, Canton, CT

Disclosures: Katrina Collins: None; Safina Hafeez: None; Saverio Ligato: None; Richard Cartun: None

Background: Albumin messenger RNA *in situ* hybridization (RISH) is a sensitive and specific marker for identifying hepatocellular carcinoma (HCC) with a diagnostic sensitivity of nearly 100%. In contrast, intrahepatic cholangiocarcinomas (ICCs) show a variable sensitivity ranging from 45% to 99%. Extrahepatic cholangiocarcinomas (ECCs) and metastatic carcinomas, with rare exceptions, are usually negative. Bile duct adenomas (BDAs) and a few biliary hamartomas (BHs) have been reported to be positive, but focally and with a very low number of transcripts. The purpose of this study was to assess the utility and limitations of albumin RNAScope detection of albumin mRNA in a cohort of HCCs, ICCs, ECCs, BDAs, BHs and metastatic carcinomas to the liver. Furthermore, we tried to explain the reasons for the significant discrepancy in sensitivity of this marker in ICC as previously reported in the literature.

Design: We identified 122 cases of hepatobiliary lesions and metastatic carcinomas. Albumin RISH was performed on formalin-fixed, paraffin-embedded tissue sections using the RNAScope (Leica Biosystems, Buffalo Grove, IL) on the LEICA Bond III platform, using probe Hs-ALB-01 (Advanced Cell Diagnostics, Newark, CA) as well as negative (DapB) and positive probe (PPIB) for mRNA. Cytoplasmic, dot-like reactivity in more than 5% of tumor cells was regarded as positive. ICCs were classified according to the classification proposed by Hayashi *et al*. (PMID: 27259014) in small duct (SD), large duct (LD), and indeterminate (IND) subtypes.

Results: Albumin RISH was positive in all 17 HCCs and negative in all 28 non-hepatic carcinomas, 9 ECCs, 8 BDAs and 13 BDHs. Overall, 35 of 47 (74.4%) ICCs were positive for albumin mRNA, with the majority, 35/37 (94.6%), being of SD subtype and 2 of 3 (66.7%) on the IND subtype. Interestingly, only 1/7 (14.3%) LD subtype showed albumin mRNA, $P<0.003$ (Table 1).

Table 1. Albumin RNA ISH according to Histologic Subtype

Classification	Total cases (n)	Albumin mRNA ISH Positive (n)	Positive (%)	Negative (n)	Negative (%)	Tissue site Liver (n)	EH (n)	Biopsy (n)	Biopsy (%)	Resection (n)	Resection (%)
Hepatocellular carcinoma	17	17	100	0	0	17	0	10	58.8	7	41.1
Intrahepatic cholangiocarcinoma[a]	47	35	74.4	12	25.6	44	3				
Small duct subtype	37	35	94.6	2	5.4	36	1	20	54	17	46
Large duct subtype	7	1	14.3	6	85.7	6	1	5	71.4	2	28.6
Indeterminate subtype	3	2	66.7	1	33.3	2	1	2	66.7	1	33.3
Extrahepatic cholangiocarcinoma	9	0	0	9	100	0	9	3	33.3	6	66.7
Bile duct adenoma	8	0	0	8	100	8	0	7[b]	77.5	1	12.5
Bile duct hamartoma	13	0	0	13	100	13	0	9[b]	69.2	4	30.8
Non-hepatic carcinoma[c]	28	0	0	28	100	28	0	26	92.9	2	7.1
Total	122							82		40	

EH: Extrahepatic

[a]Albumin mRNA reactivity differed among the three subtypes assessed (p<0.003; Fischer-Exact)

[b]Wedge biopsies

[c] Included cases from the following sites: colon (6), extrahepatic cholangiocarcinoma metastasis to liver (4), hepatoid (1), breast (2), stomach (1), lung (2), pancreatic ductal (8), pancreatic acinic (2), and neuroendocrine (2)

Conclusions: Albumin RISH is a highly sensitive and specific for HCCs. It is highly sensitive and moderately specific in the diagnosis of ICC with small gland morphology, especially when included in a panel of immunohistochemical tests. However, a lack of reactivity, especially in adenocarcinomas with large duct morphology, does not exclude this diagnostic possibility. We propose that the variability in sensitivity of albumin RISH in ICCs could depend on the relative representation of the subtypes included in the previous studies.

1609 Targeted 37-Gene Panel Next Generation Sequencing for an Accurate Diagnosis of Infantile Cholestasis Syndrome and Correlation of Genotype to Phenotype
Ashim Das[1], Aditi Sharma[1], Arnab Pal[2], Sadhna Lal[2]
[1]PGIMER, Chandigarh, India, [2]Postgraduate Institute of Medical Education & Research, Chandigarh, India

Disclosures: Ashim Das: None; Aditi Sharma: None; Arnab Pal: None; Sadhna Lal: None

Background: Infantile cholestasis syndrome is a highly complex group of disorders. An accurate diagnosis is required for appropriate management to halt disease progression. However, diagnosis is often difficult because of similar phenotypic features with different genotypes and some entities like PFIC I and PFIC II can have both milder and severe forms. Next generation sequencing (NGS) using a customized gene panel can point the molecular alterations responsible for the disease.

Design: From a pool of 65 patients and 61 family members who were initially screened for a hotspot by DNA mass array, a total of 9 patients were randomly selected. DNA was isolated from blood to identify any germ line mutation. A panel of 37 genes (PFIC panel IAD148358 designed on ion ampliseq designer) with 877 amplicons was selected (Fig 1) which covered several categories of infantile cholestasis syndrome e.g bile acid synthetic defect and other metabolic disorders, canalicular transport defect, errors in tight junctions like citrin deficiency, and developmental defects like paucity of bile ducts. All the exonic areas were covered. Out of 9 samples, one was excluded because of low coverage. The data was interpreted using the Ion reporter (v5.10) and other software like SIFT, Exac, OMIM, Clinvar, Varsome and Mutation Tester.

Results: There was 99% coverage of target amplicons and the initial number of variants range from 144-179 (Table 1). In 3 cases with a Non-PFIC histology and an autosomal dominant inheritance pattern, an in-frame deletion in the exon was observed at chr20:10621886 leading to cDNA truncation of the *JAG* gene associated with Alagille syndrome. All were validated by Sanger sequencing (Fig.2). One case showed a heterozygous mutation with semi-dominant effect at chr8:59404935 (p.Pro398Ala) involving the *CYP7A1* gene responsible for defects in bile acid metabolism. *ABCB11* gene variation was seen in 2 cases with PFICII histology, one showed homozygous variation along with indel of *JAG1* gene and the other was a non-synonymous deleterious variation. *CFTR* mutation was observed in 2 cases, one showing additional *JAG1* mutation; histology revealed portal triaditis.

Patient ID	ACMG classification	Inheritance	Molecular inference	Protein change	Genotype	Gene	Histological
1. Ion Express_008	PVS1,PM2: Likely Pathogenic	Autosomal Dominant	**PIBD**	T975Lfs*9	Homozygous	JAG1 (20:10621886)	Non PFIC
2. Ion Express_012	PP3, BP6 Uncertain Significance	Autosomal Semi-dominant	**Bile acid synthetic defect**	p.Pro398Ala	Heterozygous	CYP7A1(chr8:59404935)	PIBD
3. Ion Express_006	PM1,PM2,PP3,BP1 Uncertain Significance	Autosomal Recessive	**PFIC II**	Glu942lys	Homozygous	ABCB11 (chr2: 169791926)	PFIC II
	PVS1,PM2: Likely Pathogenic	Autosomal Dominant	**PIBD**	T975Lfs*9	Homozygous	JAG1 (20:10621886)	
4. Ion Express_007	PVS1,PM2: Likely Pathogenic	Autosomal Dominant	**PIBD**	T975Lfs*9	Homozygous	JAG1 (20:10621886)	Non PFIC
5. Ion Express_003	Likely pathogenic PP5	Autosomal Recessive	**PFIC II**	p.ARG948Cys	Homozygous	ABCB11 chr2:169791908	PFIC-II
6. Ion Express_010	PM2,BP4, Uncertain Significance	Autosomal Recessive/Dominant	**uncertain**	V456A	Heterozygous	CFTRChr 7: 117188852	PIBD
	Uncertain significance		**PIBD**	5' UTR	Homozygous	Jag1 Chr20: 10654261	
7. Ion Express_004	PP3,BP4Uncertain Significance	Autosomal Recessive	**No deleterious mutations**	p.Pro9971Leu	Heterozygous	TJP2 chr9: 71863079	Non-PFIC
8. Ion Express 002	PM1,PP3 BP4 Uncertain Significance	Autosomal Recessive/Dominant	**Cystic fibrosis**	pLeu183leu p.Phe1413Leu	Heterozygous Heterozygous	i)CFTR chr7:117174387 ii) CFTR chr7:117305613	Portal triaditis

Figure 1 - 1609

Fig 1: 37 Gene panel for study of infantile cholestasis group of disorders

1.	BSEP deficiency	ABCB11	28	Neonatal ichthyosis-cholangitis syndrome	CLDN1
2.	FIC 1 deficiency	ATP8B	29	Neonatal sclerosing cholangitis	DCD2
3.	TJP2 deficiency	TJP2	30	Wilson's disease	ATP7B
4.	MDR3 deficiency	ABCB4	31	Cystic fibrosis	CFTR
5.	FXR deficiency	NR1H4	32	Epoxide hydrolase(bile transport)	EPHX1
6.	Citrin deficiency	SLC25A13	33	Dysfunctional intrahepatic bile ducts	HNF1B(Hepatocyte nuclear factor)
7.	Citrin deficiency	ASS	34		
8.	Transaldolase deficiency	TALDO	35	Polycystic kidney and hepatic disease	PKHD1
9.	Alagille syndrome	NOTCH2	36	Polycystic liver	PRKCSH
10.	Alagille syndrome	JAG 1	37	Bile acid transmembrane transporter	SLCO1A2/SLC25A13
11.	Gilbert syndrome	UTG1A1			
12.	Dubin-Johnson syndrome	ABCC2			
13.	Niemann-Pick disease type	NPC1			
14.	Niemann-Pick disease type	NPC2			
15.	GRACILE syndrome	BCS1L			
16.	Arthrogryposis-renal dysfunction-cholestasis syndrome	VSP33B			
17.	Crigler-Najjar syndrome	UTG1A1			
18.	Mc Cune Albright syndrome	GNAS			
Bile acid synthetic disorders					
19.	Delta (4)-3-oxosteroid 5-beta-reductase	AKR1D1			
20.	Bile acid CoA ligase	SLC27A5			
21.	Delta 3,3-beta-hydroxy- -5C27-steroid oxidoreductase	BASD1			
22.	Oxysterol 7 alpha-hydroxylase	CYP7B1			
23.	Bile acid CoA:amino acid N acyltransferase	BAAT			
24.	Alpha-methylacyl-CoA racemase	AMACR			
25.	Sterol 27-hydroxylase	CYP27A1			
26.	Cholestrol 7 alpha hydroxylase	CYP7A1			
27.	Delta 3B-hydroxy-c27 steroid dehydogenase	HSD3B7			

Figure 2 - 1609

Fig 2

Chromatogram   **Mapping with Reference Sequence**
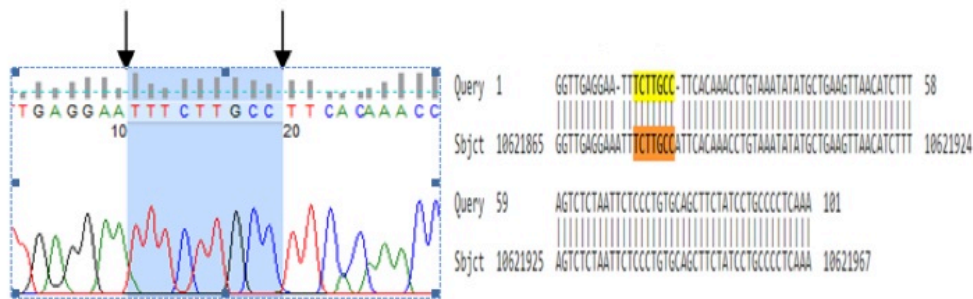
Conclusions: Targeted 37 gene panel NGS is a robust high throughput technique to screen known and unknown variants associated with infantile cholestasis syndrome. Correlation of histopathology with molecular findings is essential for an accurate diagnosis. This study provides initial data for the identification of causative mutations in our population

1610   Lymphocyte-Rich Hepatocellular Carcinoma: Features of the Immune Microenvironment and Clinical Course of a Reclassified Entity

Tony El Jabbour[1], Adam Gersten[2], Carlos Castrodad-Rodriguez[3], Xuchen Zhang[4], Ilke Nalbantoglu[5], Maria Westerhoff[6], Qiang Liu[7], Nicole Panarelli[8]

[1]Tony El Jabbour, Bronx, NY, [2]Montefiore Medical Center – Moses Division, Bronx, NY, [3]Montefiore Medical Center, Bronx, NY, [4]Yale University School of Medicine, Orange, CT, [5]Yale University School of Medicine, Woodbridge, CT, [6]University of Michigan, Ann Arbor, MI, [7]Montefiore Medical Center, Princeton Junction, NJ, [8]Montefiore Medical Center, Scarsdale, NY

Disclosures: Tony El Jabbour: None; Adam Gersten: None; Carlos Castrodad-Rodriguez: None; Xuchen Zhang: None; Ilke Nalbantoglu: None; Maria Westerhoff: None; Qiang Liu: None; Nicole Panarelli: None

Background: The most recent world health organization (WHO) classification groups lymphoepithelioma-like and lymphocyte-predominant hepatocellular carcinoma (HCC) under the new term, lymphocyte-rich HCC (L-RHCC). Lymphocytes outnumber malignant hepatocytes, in these rare tumors, and their prognosis appears better than conventional HCC, based on approximately 40 described cases. Features of the tumor microenvironment are promising biomarkers of response to immunomodulatory therapies, particularly in tumors with dense lymphocytic infiltrates. We aim, through this case series, to add to existing knowledge about L-RHCC, and further characterize its immune microenvironment.

Design: We searched the archives of three institutions for HCC's classified with any of the aforementioned terms. Clinical and histological data was extracted from pathology reports and electronic medical records. PD-L1 immunostain and in-situ hybridization (ISH) for Epstein-Barr virus (EBV) were performed using standard protocols. Each PD-L1 stain was independently scored by three authors.

Results: Four cases from two men and two women were included; their clinical and histologic features are summarized in Table 1. Tumors ranged in greatest dimension from 2.2-9.2 cm. One patient had multifocal disease. In situ hybridization for Epstein-Barr virus was negative in all tested cases (n=3). Tumor cell PD-L1 expression was minimal in three cases, but extensive in the last case (Fig. 1A, B). The corresponding tumor positive scores (TPS) were 1% (n=2), 3%, and 50%. In contrast, PD-L1 was highly expressed in tumor infiltrating lymphocytes of all cases (Fig. 1C, D), resulting in combined positive scores (CPS) ranging from 20-90. Both CPS and TPS were above the threshold for initiation of anti-PDL1 therapy in all cases. Patients had known underlying liver disease in 3 cases (HBV (n=1), HCV (n=2)), and one had no known liver disorder. One tumor occurred in a background of cirrhosis, but advanced fibrosis was absent in the other cases. Upon clinical follow-up, all patients were alive and free of metastatic disease.

Table 1. Clinical and Pathologic Features of Study Cases				
Features	Case 1	Case 2	Case 3	Case 4
Age, Sex	64, Male	47, Female	70, Male	53, Female
Tumor size (greatest dimension)	2.8 cm	2.2 cm	3.5 cm	5 lesions, largest 9.2 cm
Pathologic stage	pT2Nx	pT1Nx	pT1bNx	pT3Nx
Background liver disease	HCV with cirrhosis	HBV without fibrosis	HCV without fibrosis	None
EBV ISH	Negative	Negative	Negative	N/A*
TPS	1%	3%	50%	1%
CPS	20	70	90	50
Clinical outcome, follow-up interval	Alive: 3 years, 8 months	Alive: 9 years, 8 months	Alive: 2 months	Alive: 8 months
*N/A= not available				

Figure 1 - 1610
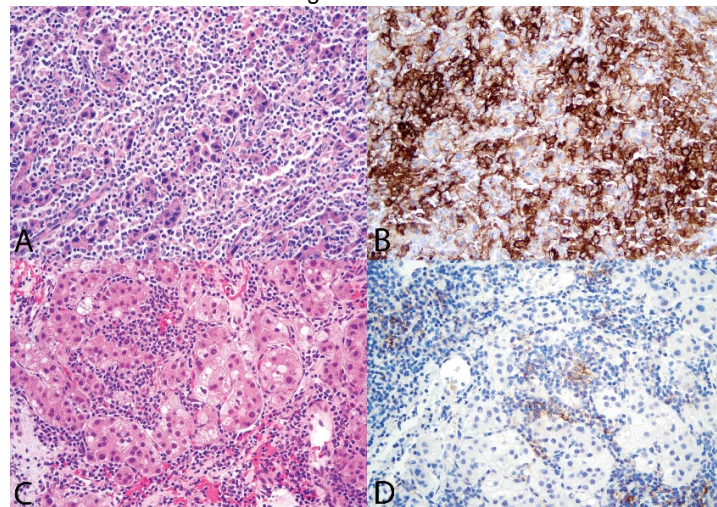
Conclusions: This series of lymphocyte rich HCCs proved to have relatively favorable prognosis and be unrelated to EBV, as has been reported in other series. High PD-L1 expression in the tumor immune infiltrate indicates that immune checkpoint inhibitor therapy may be beneficial to patients with these tumors.

1611 Transient Elastography versus Liver Biopsy: Discordance in Evaluations for Fibrosis and Steatosis from a Pathology Standpoint

Jiayun Fang[1], Jerome Cheng[2], Michael Chang[3], Joseph Ahn[4], Maria Westerhoff[2]
[1]University of Michigan Hospitals, Ann Arbor, MI, [2]University of Michigan, Ann Arbor, MI, [3]Portland VA Medical Center, Portland, OR, [4]Oregon Health & Science University, Portland, OR

Disclosures: Jiayun Fang: None; Jerome Cheng: None; Michael Chang: None; Joseph Ahn: None; Maria Westerhoff: None

Background: Transient elastography (TE) is a non-invasive method of evaluating liver fibrosis and steatosis. Biopsy (BX), on the other hand, remains the gold standard for fibrosis, steatosis, and can also help exclude other conditions. Known sources of discrepancy between TE and BX include BMI>28 kg/m^2 and conditions that increase liver stiffness, such as inflammation (ALT>100), congestive hepatopathy, and cholestasis. The goal of this study was to assess how frequent these causes are in practice and the role of BX findings.

Design: Patients (pts) with TE and liver BX within 1 month of each other were identified from the database. BMI, BX indications, TE results (liver stiffness measurement and assessment: F0-F4; degree of steatosis via controlled attenuation parameter), and liver-related lab values were recorded. Histology review included diagnosis, fibrosis (stage 1-4 Batts & Ludwig for chronic hepatitis; Brunt system for NAFLD), % steatosis, BX length, and number of portal tracts (PT). Major discrepancy in fibrosis was defined as F3 or F4 on TE, when BX showed stage 0-1. Discordance for steatosis was defined as moderate to severe steatosis on TE when no or mild steatosis present on BX, or no steatosis according to TE when >66% seen by BX.

Results: Eighty-four pts (mean 51 yrs; 52% female) received TE and BX within 1 month of each other. BX was performed for workup of abnormal LFTs or due to a TE result of possible cirrhosis. Mean BX length was 2.4 cm with 17 PT. Overall, TE and BX showed major discordance in fibrosis and/or steatosis in 42%. Major discordance for fibrosis occurred in 35% (n=30), most commonly due to BMI>28 (43%) or combination of BMI>28 with another cause (23%) (see Table). Alone or with other causes, ALT>100 occurred in 20%, cholestasis in 13%, drug injury in 13%, and vascular outflow obstruction in 10%. Steatosis by TE and BX were discrepant in 21% (n=18): 12 showed mild steatosis (10-33%) on BX but "moderate to severe steatosis" on TE. Three BX with NASH and >66% steatosis were "no to minimal steatosis" by TE; 3 BX showed no steatosis but were "moderate to severe steatosis" on TE.

Causes of Discrepancy between TE and Biopsy in Fibrosis Assessment	% Cases (n=30 for Total Discrepancies between TE and Biopsy)
BMI >28 kg/m^2	43%
Vascular outflow obstruction on Biopsy	3.3%
Cholestasis on Biopsy	6.7%
Drug injury pattern on Biopsy	3.3%
Unknown	10%
Combination:	
• BMI >28 kg/m^2 + ↑ALT	10%
• Cholestasis + BMI >28 kg/m^2	6.7%
• Drug + BMI >28 kg/m^2	3.3%
• Vascular outflow obstruction + BMI >28 kg/m^2	3.3%
• Drug + ↑ALT	6.7%
• Vascular outflow obstruction + ↑ALT	3.3%

Conclusions: Liver BX may not only be submitted for primary diagnosis, but to confirm TE fibrosis and steatosis results. In our study, 35% of TE fibrosis evaluations were of major discordance with BX (66% with BMI>28). Pathologists can also assist in identifying known but unexpected causes of discordance through their diagnoses of vascular outflow obstruction, drug injury, cholestasis, and hepatitis.

1612 Identification of Histological and Clinical Features Associated with Antibody-Mediated Rejection (AMR) in Liver Allografts

Catherine Forse[1], Morteza Tarokh[2], Scott Robertson[2], Daniel Roberts[2], Lisa Yerian[2], Chao Tu[2], Bijan Eghtesad[2], Koji Hashimoto[2], Federico Aucejo[3], Daniela Allende[4]
[1]The Ottawa Hospital - University of Ottawa, Ottawa, ON, [2]Cleveland Clinic, Cleveland, OH, [3]Cleveland Clinic, Shaker heights, OH, [4]Cleveland Clinic, Lerner College of Medicine of Case Western University School of Medicine, Avon Lake, OH

Background: The diagnosis of AMR is challenging and requires correlation of histological features, C4d immunohistochemistry and donor specific antibodies (DSA). The aim of the study was to identify clinical and/or histologic features useful in the diagnosis of AMR according to published criteria (Demetris AJ et al., 2016).

Design: IRB approval was obtained. All liver biopsies with available C4d immunohistochemistry were retrospectively identified from a pathology database (2010-2018). Clinical data was obtained from chart review. H&E stained slides were reviewed and biopsies were classified into three groups: definitive for AMR, suspicious for AMR, and negative for AMR. Classification as definitive for AMR included all the following: clinical suspicion for AMR, positive DSA, positive C4d stain, compatible histology, and response to therapy. Suspicious for AMR was defined as some but not all of the following: positive DSA, positive C4d stain, and compatible histology. Biopsies negative for AMR included none of these features.

Results: 134 liver biopsies from 107 patients were included. Cases were divided into definitive for AMR (n=6), suspicious for AMR (n=58), or negative for AMR (n=70) categories. In multinomial logistic regression analysis, patient age, gender and donor gender were not significantly different among the groups. The etiology of chronic liver disease in the explant, liver enzymes, type of graft, ischemic time, and complications were not significantly different among the groups. Histologic findings are summarized in Table 1. Endothelial cell hypertrophy/ swelling ($p<0.001$), microvascular disruption/ interstitial hemorrhage ($p=0.038$), patchy endotheliitis ($p=0.006$), diffuse bile ductular proliferation ($p=0.024$), minimal to mild portal inflammation ($p=0.033$), mixed inflammatory infiltrates with eosinophils ($p=0.002$), absent to patchy lobular inflammation ($p=0.022$), regenerative hepatocellular changes ($p=0.023$), and canalicular and/or hepatocellular cholestasis ($p=0.053$) were significantly associated with a definitive diagnosis of AMR.

Table 1.

	[All cases] N=134	Negative for AMR N=70	Definitive for AMR N=6	Suspicious for AMR N=58	P-value overall
Portal Inflammation, N (%):					0.033
Absent	15 (11.2%)	14 (20.0%)	0 (0.00%)	1 (1.72%)	
Minimal	79 (59.0%)	38 (54.3%)	4 (66.7%)	37 (63.8%)	
Mild	36 (26.9%)	16 (22.9%)	2 (33.3%)	18 (31.0%)	
Moderate	3 (2.24%)	2 (2.86%)	0 (0.00%)	1 (1.72%)	
Severe	1 (0.75%)	0 (0.00%)	0 (0.00%)	1 (1.72%)	
Type of Portal Inflammation, N (%):					0.002
Not applicable	15 (11.2%)	14 (20.0%)	0 (0.00%)	1 (1.72%)	
Lymphocyte-predominant	73 (54.5%)	40 (57.1%)	2 (33.3%)	31 (53.4%)	
Plasma cell-predominant	4 (2.99%)	2 (2.86%)	0 (0.00%)	2 (3.45%)	
Mixed lymphoplasmacytic with eosinophils	42 (31.3%)	14 (20.0%)	4 (66.7%)	24 (41.4%)	
Interface Activity, N (%):					0.815
Absent	118 (88.1%)	62 (88.6%)	5 (83.3%)	51 (87.9%)	
Present	16 (11.9%)	8 (11.4%)	1 (16.7%)	7 (12.1%)	
Lobular Inflammation, N (%):					0.022
Absent	45 (33.6%)	30 (42.9%)	2 (33.3%)	13 (22.4%)	
Patchy	69 (51.5%)	30 (42.9%)	2 (33.3%)	37 (63.8%)	
Diffuse	6 (4.48%)	1 (1.43%)	1 (16.7%)	4 (6.90%)	
Sinusoidal	14 (10.4%)	9 (12.9%)	1 (16.7%)	4 (6.90%)	
Perivenulitis, N (%):					0.301
Absent	117 (87.3%)	64 (91.4%)	5 (83.3%)	48 (82.8%)	
Patchy	10 (7.46%)	4 (5.71%)	0 (0.00%)	6 (10.3%)	
Diffuse	7 (5.22%)	2 (2.86%)	1 (16.7%)	4 (6.90%)	
Hepatocellular Injury, N (%):					0.396
Absent	68 (50.7%)	39 (55.7%)	1 (16.7%)	28 (48.3%)	
Few	46 (34.3%)	21 (30.0%)	4 (66.7%)	21 (36.2%)	
Many	10 (7.46%)	4 (5.71%)	1 (16.7%)	5 (8.62%)	
Necrosis	10 (7.46%)	6 (8.57%)	0 (0.00%)	4 (6.90%)	

Regenerative hepatocellular changes, N (%):					0.023
Absent	51 (38.1%)	34 (48.6%)	2 (33.3%)	15 (25.9%)	
Present	83 (61.9%)	36 (51.4%)	4 (66.7%)	43 (74.1%)	
Endotheliitis, N (%):					0.006
Absent	103 (77.4%)	61 (87.1%)	2 (40.0%)	40 (69.0%)	
Patchy	26 (19.5%)	9 (12.9%)	3 (60.0%)	14 (24.1%)	
Diffuse	4 (3.01%)	0 (0.00%)	0 (0.00%)	4 (6.90%)	
Lymphocytic and or necrotizing.arteritis, N (%): Absent	134 (100%)	70 (100%)	6 (100%)	58 (100%)	.
Endothelial cell hypertrophy/ swelling, N (%):					<0.001
Absent	107 (79.9%)	64 (91.4%)	1 (16.7%)	42 (72.4%)	
Present	27 (20.1%)	6 (8.57%)	5 (83.3%)	16 (27.6%)	
Sinusoidal dilatation, N (%):					0.278
Absent	119 (88.8%)	59 (84.3%)	6 (100%)	54 (93.1%)	
Present	15 (11.2%)	11 (15.7%)	0 (0.00%)	4 (6.90%)	
Microvascular disruption interstitial hemorrhage, N (%):					0.038
Absent	109 (81.3%)	61 (87.1%)	3 (50.0%)	45 (77.6%)	
Present	25 (18.7%)	9 (12.9%)	3 (50.0%)	13 (22.4%)	
Fibrin thrombi, N (%):					1.000
Absent	132 (98.5%)	69 (98.6%)	6 (100%)	57 (98.3%)	
Present	2 (1.49%)	1 (1.43%)	0 (0.00%)	1 (1.72%)	
Portal stromal edema, N (%):					0.041
Absent	132 (98.5%)	70 (100%)	5 (83.3%)	57 (98.3%)	
Present	2 (1.49%)	0 (0.00%)	1 (16.7%)	1 (1.72%)	
Leukocyte sludging or margination, N (%): Absent	134 (100%)	70 (100%)	6 (100%)	58 (100%)	.
Intimal hyperplasia in arteries, N (%):					0.478
Absent	133 (99.3%)	70 (100%)	6 (100%)	57 (98.3%)	
Present	1 (0.75%)	0 (0.00%)	0 (0.00%)	1 (1.72%)	
Foam cell change in arteries, N (%): Absent	134 (100%)	70 (100%)	6 (100%)	58 (100%)	.
Bile duct injury, N (%):					0.088
Absent	80 (59.7%)	49 (70.0%)	4 (66.7%)	27 (46.6%)	
Focal	44 (32.8%)	17 (24.3%)	2 (33.3%)	25 (43.1%)	
Diffuse	10 (7.46%)	4 (5.71%)	0 (0.00%)	6 (10.3%)	
Senescent changes, N (%):					1.000
Absent	132 (98.5%)	69 (98.6%)	6 (100%)	57 (98.3%)	
Focal	2 (1.49%)	1 (1.43%)	0 (0.00%)	1 (1.72%)	
Bile ductular proliferation, N (%):					0.024
Absent	78 (58.2%)	48 (68.6%)	2 (33.3%)	28 (48.3%)	
Focal	37 (27.6%)	15 (21.4%)	1 (16.7%)	21 (36.2%)	
Diffuse	19 (14.2%)	7 (10.0%)	3 (50.0%)	9 (15.5%)	
Bile duct loss, N (%):					0.346
Absent	129 (96.3%)	69 (98.6%)	6 (100%)	54 (93.1%)	
Present	5 (3.73%)	1 (1.43%)	0 (0.00%)	4 (6.90%)	
Cholestasis, N (%):					0.053
Absent	98 (73.1%)	56 (80.0%)	2 (33.3%)	40 (69.0%)	
Canalicular	17 (12.7%)	7 (10.0%)	2 (33.3%)	8 (13.8%)	
Hepatocellular	11 (8.21%)	4 (5.71%)	0 (0.00%)	7 (12.1%)	
Mixed	8 (5.97%)	3 (4.29%)	2 (33.3%)	3 (5.17%)	
Fibrosis, N (%):					0.742
Absent	95 (71.4%)	51 (72.9%)	4 (66.7%)	40 (70.2%)	
Portal/periportal	23 (17.3%)	13 (18.6%)	1 (16.7%)	9 (15.8%)	
Perivenular	6 (4.51%)	2 (2.86%)	0 (0.00%)	4 (7.02%)	
Bridging fibrosis	5 (3.76%)	2 (2.86%)	1 (16.7%)	2 (3.51%)	
Cirrhosis	4 (3.01%)	2 (2.86%)	0 (0.00%)	2 (3.51%)	
Steatosis, N (%):					0.740
No	100 (74.6%)	50 (71.4%)	5 (83.3%)	45 (77.6%)	
Yes	34 (25.4%)	20 (28.6%)	1 (16.7%)	13 (22.4%)	

Conclusions: Clinical features are not helpful in differentiating patients with AMR from those without AMR. A variety of histologic findings beyond those described (Demetris AJ et al., 2016) can be seen in definitive AMR cases. The high frequency of mixed infiltrates with eosinophils and endotheliitis seen in our AMR cases highlights the histologic overlap and/or coexistence of acute cellular rejection in many of these cases.

1613 Focal Adhesion Kinase (FAK) Overexpression and Prognostic Implication in Pediatric Hepatocellular Carcinoma

Paola Francalanci[1], Isabella Giovannoni[2], Cristiano De Stefanis[1], Ilaria Romito[1], Chiara Grimaldi[1], Aurora Castellano[1], Anna Alisi[1]
[1]Bambino Gesù Children's Hospital, Roma, Italy, [2]Bambino Gesù Children's Hospital, Rome, Italy

Disclosures: Paola Francalanci: None; Isabella Giovannoni: None; Cristiano De Stefanis: None; Ilaria Romito: None; Chiara Grimaldi: None; Aurora Castellano: None; Anna Alisi: None

Background: Liver cancer comprises 1-2% of pediatric solid cancers. Pediatric HCC is extraordinary and it may originate either in healthy or in cirrhotic livers.

Focal adhesion kinase (FAK), a tyrosine kinase, has been shown to be overexpressed and to correlate with aggressiveness in adult HCC. Inhibition of FAK decreases HCC invasiveness by down-regulating Enhancer of Zeste homolog 2 (EZH2), an epigenetic controller, that acts in transcriptional repression of a large number of genes via histone 3 methylation of lysine 27 (H3K27me3).

Design: Available pediatric slides from institutional files were retrieved. HE, PAS, PAS-D and Masson trichrome were reviewed. Immunofluorenscence for FAK, H3K27me3, EZH2 and PCNA; and immunohistochemistry for β-catenin, Glypican3 and Glutamine Synthetase were performed. Genomic DNA from FFPE HCCs and paired normal liver tissues were extracted. Mutation screening was done using DNA sequencing of *CTNNB1*. Copy number evaluation of *FAK* was investigated using multiplex ligation-dependent probe amplification (MLPA).

Results: Seventeen HCCs from 2009 to 2018 were identified (8 F and 9 M, age range: 1m-33y, median 9y) and compared with 8 age-matched healthy livers (CTRL). Six HCCs developed in healthy liver and 11 on a cirrhotic background. Quantitative analysis of immunofluorescence data showed that FAK is overexpressed in HCCs and among them this protein is significantly higher in cirrhotic HCCs than in a healthy milieu (**Figure 1**). Accordingly to FAK, the levels of EZH2 were significantly increased in HCCs from a cirrhotic background. MLPA displayed duplication in majority of probes-spanning 8q arms, containing *FAK* gene, in 3 samples of cirrhotic HCCs, but no anomalies were found in non-cirrhotic HCC. Spearman's correlation analysis showed that FAK, EZH2, H3K27me3, and PCNA expression did not correlate with the expression of nuclear β-Catenin, Glypican-3 and GS6, metastasis or survival data. On the other hand, the expression of FAK, EZH2, and PCNA significantly inversely correlated with tumor size. In fact, Spearman's correlation coefficients for FAK was -0.51 ($p < 0.05$); for EZH2 was -0.48 ($p < 0.05$); for PCNA was -0.51 ($p < 0.05$).

Figure 1 - 1613
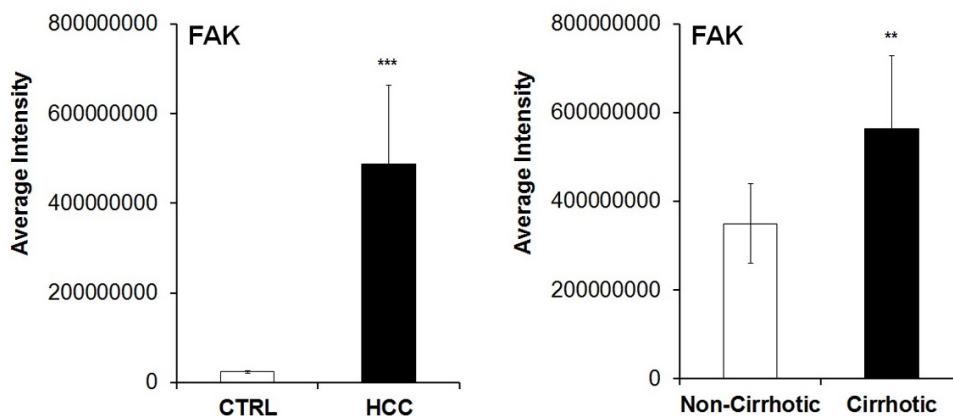
Conclusions: FAK is overexpressed in pediatric HCCs and the more significant up-regulation is in small HCC in a background of cirrhotic liver. Inhibition of FAK may offer an effective strategy to protect against HCC development. These data deserve further investigations.

1614 Perineural Invasion in Hepatocellular Carcinoma is Rare and Not Associated with Outcome

Lanisha Fuller[1], Daniel Owen[1], Danielle Carpenter[2], Raul Gonzalez[3], Rondell Graham[4], Cynthia Guy[5], Daniel Roberts[1], Michael Schild[6], Daniela Allende[7]

[1]Cleveland Clinic, Cleveland, OH, [2]St. Louis University School of Medicine, St. Louis, MO, [3]Beth Israel Deaconess Medical Center, Boston, MA, [4]Mayo Clinic, Rochester, MN, [5]Duke University, Chapel Hill, NC, [6]Duke University Medical Center, Durham, NC, [7]Cleveland Clinic, Lerner College of Medicine of Case Western University School of Medicine, Avon Lake, OH

Disclosures: Lanisha Fuller: None; Daniel Owen: None; Danielle Carpenter: None; Raul Gonzalez: None; Rondell Graham: None; Cynthia Guy: None; Daniel Roberts: None; Michael Schild: None; Daniela Allende: None

Background: According to the 8th edition AJCC Cancer Staging Manual, T-category staging of hepatocellular carcinoma (HCC) is largely based on tumor size and the presence of vascular invasion. Even though multiple clinical and pathologic features have been proposed as prognostic factors by the World Health Organization (WHO), the significance of perineural invasion (PNI) remains unknown. The aims of the study are to characterize HCC with PNI and to assess its impact on patient outcome.

Design: With Institutional Review Board approval, a retrospective search of pathology databases at our institution was conducted (1992-2019) for HCC with and without PNI. The population of HCC with PNI was enriched by collecting additional cases from three outside institutions. Clinical data was obtained from electronic medical records. A control group of HCC without PNI (matched by tumor grade, AJCC TNM stage, and presence/absence of cirrhosis) was identified. H&E-stained slides were reviewed, and cases of combined HCC-cholangiocarcinoma were excluded.

Results: Clinical and pathologic findings are summarized in the Table. In our institution, six HCC cases with PNI were identified (6/891, <1%), and five additional cases were collected from other institutions. HCC with PNI was not significantly associated with any of the clinical or pathologic parameters investigated versus our control population. When controlling for tumor grade, stage, and the presence/absence of cirrhosis, PNI did not impact survival or overall outcome.

Table: Summary of clinical and pathologic findings

	HCC with PNI (N=11)	HCC without PNI (N=24)	*P*-value
Mean age (range)	68 (60-79)	65 (45-82)	p=NS
Gender (M:F)	8:3	19:5	p=NS
Location	R=5 L=3 B=3	R=14 L=3 B=7	p=NS
Focality	Unifocal=7 Multifocal=4	Unifocal=13 Multifocal=11	p=NS
Tumor size in cm (mean, +/- SD)	5.2 (+/- 2.2)	5.7 (+/- 5.7)	p=NS
Tumor differentiation grade	Well=1 Moderate=7 Poor=3	Well=3 Moderate=14 Poor=7	p=NS
LVI (small vessel) present	9/11	14/24	p=NS
Satellitosis	0/11	2/24	p=NS
Cirrhosis	Yes=7 No=4	Yes=12 No=12	p=NS
Background chronic liver disease	HBV=1 HCV=4 NAFL=2 NASH=1 Alcohol=1 PSC=1 Biliary obstruction=1	HBV=2 HCV=4 HCV/Alcohol=5 NAFL=3	p=NS

		NASH=4 Alcohol=1 None/unknown=5	
AJCC 8th ed. pT Stage	pT1=1 pT2=8 pT4=2	pT1=2 pT2=18 pT4=4	p=NS
Resection Type	Total=4 Partial=7	Total=12 Partial=12	
Margin status	Negative=10 Positive=1	Negative=22 Positive=2	p=NS
Outcome	Alive=6 Dead=4 No FU=1	Alive=10 Dead=10 No FU=4	p=NS
Survival in months (mean +/- SD)	33.3 (+/- 22.5)	43.4 (+/- 40.8)	p=NS

R=right, L=left, B=both lobes, FU=follow up, NS=not significant

Conclusions: PNI is extremely rare in HCC but still occurs in the absence of a combined cholangiocarcinoma component. There was no association between PNI and any of the clinical and pathologic parameters investigated. When controlling for tumor differentiation grade, tumor stage, and the presence/absence of cirrhosis, there was no significant difference in survival and overall outcome.

1615   Lucocyte Chemotactic Factor 2 (LECT2) Amyloidosis in Liver Transplant

Armando Gamboa-Dominguez[1], Norma Uribe-Uribe[2], Alejandra Gutierrez-Carreon[3]
[1]INCMNSZ, Mexico City, DF, Mexico, [2]Mexico City, FDM, Mexico, [3]INCMNSZ, Mexico City, Tlalpan, Mexico

Disclosures: Armando Gamboa-Dominguez: None

Background: Amyloidosis LECT2 (ALECT2) is more prevalent in Hispanic decedents and it has a variable globular distribution in the liver. Its identification in graft samples obtained for the assessment of macrovesicular steatosis, could provide an unbiased prevalence estimation.

Aim: Identify the prevalence of ALECT2 in graft time zero biopsies and liver explants, its associated conditions, evolution of deposits and clinical findings.

Design: A retrospective review of procured time zero biopsy and liver explant from 2000 to 2018 was performed in a third level setting. Cases with suspected amyloid deposits were submitted to Congo red stain under polarized microscope. Immunohistochemistry for amyloid A, LECT2, Kappa and Lambda were performed when the histochemical stain was positive. Clinical charts were reviewed as well as subsequent biopsies and liver function tests. Liver tissue area with amyloid deposits was calculated in every sample.

Results: 300 liver transplants were performed and time zero biopsies of grafts were obtained in 227. ALECT2 was identified in 2/227 time zero grafts (0.8%), and in 3/300 liver explants (1%). Associated conditions to end-stage liver disease, demographic data and evolution is summarized in table. Both transplanted patients with ALECT2 grafts, had one and three subsequent liver biopsies showing increase of globular deposits after one and thirteen years (Figures). Area occupied by amyloid in the patient with the largest follow-up was 30% of the sampled tissue and, it was located in portal tracts, lobules and pericentral zone without biochemical or clinical manifestations (Apple green birrefringence image). Globular deposits in explanted livers were mainly observed in fibrotic tracts, pericentral zones and focally in vessels walls. Two of these patients had colonic and duodenal biopsies that did not show amyloid. No recurrences of ALECT2 were observed 24 months after liver transplant. Amyloid deposits were LECT2 positive and negative for amyloid A, Kappa and Lambda.

Case	Gender	Age	End Stage Liver Disease	ALECT2	Follow-up Years	Amyloid deposits
1	M	53	Hepatitis C virus	Graft	1	Portal, pericentral
2	M	49	Hepatitis C virus	Graft	13	Portal, lob cluster
3	M	66	Alcoholism	Explant	1	No recurrence
4	M	70	Autoimmune hepatitis	Explant	2	No recurrence
5	F	60	Primary biliary cholangitis	Explant	2	No recurrence

Table: Cases of ALECT2 amyloidosis in transplanted patients in 18 years.
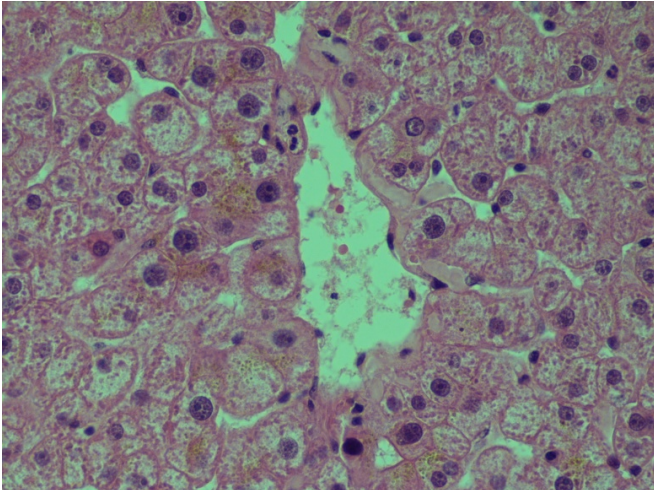
Figure 1 - 1615   Figure 2 - 1615
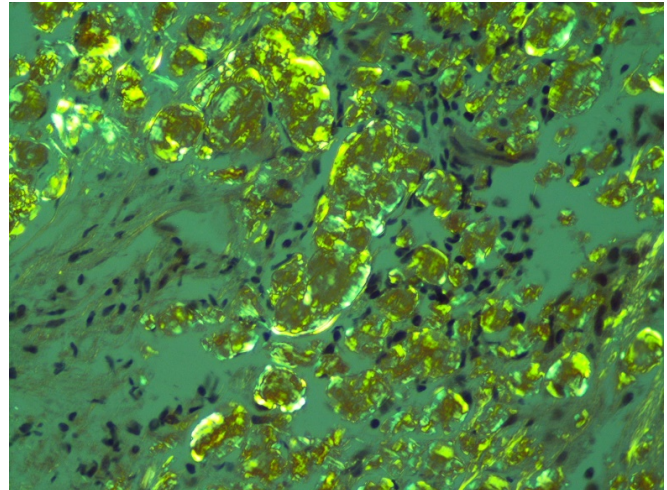
Conclusions: The prevalence of ALECT2 is 0.8% in liver donors and 1% in explanted livers in Mexican patients. Transplant team should carefully review the pericentral zone in graft time zero biopsies because in both organs these small deposits were missed in the present study. Besides the documented increase of ALECT2 deposits in iatrogenic hepatic amyloidosis, no repercusion was documented on liver function tests or in graft sintetic function.

1616   Emergence of Alveolar Echinococcosis (Echinococcus Multilocularis Infection) in Western Canada Presenting with Cystic Liver Lesions: Diagnostic Pathological Pitfalls and Confirmatory Testing

Safwat Am Girgis[1], Stan Houston[1], Ethology Unit Department Biology[2], Kinga Kowalewska-Grochowska[1]
[1]University of Alberta Hospital, Edmonton, AB, [2]University of Pisa, Pisa, Italy

Disclosures: Safwat Am Girgis: None; Stan Houston: None; Ethology Unit Department Biology: None; Kinga Kowalewska-Grochowska: None

Background: Echinococcus multilocularis, a tapeworm infection of canids and rodents, can infect humans producing continuously growing tumour-like polycystic mass (Alveolar Echinococcosis), the vast majority involving the liver. Only two cases of human disease have been reported in continental North America prior to 2013. Between 2013 and 2019, several more cases have been diagnosed in the province of Alberta in Western Canada.

Design: Patients presenting with suspected cystic liver tumors between 2013 and 2019 in the province of Alberta were clinically reviewed. The pathologic material included needle core biopsy, fine needle aspiration cytology and surgical resections. The diagnosis of AE was further confirmed by PCR testing and/or serology.

Results: A total of 14 cases (7 females + 7 males) have been diagnosed over the past 6 years. Age ranged from 20-80 years. Most patients were asymptomatic, some presented with nonspecific abdominal symptoms; all were further investigated by abdominal imaging, serology and biopsy. Most cases (8/14) were diagnosed on needle core biopsy while the remaining six were diagnosed by surgical resection. Of these, two showed extrahepatic involvement, including diaphragm (2), pleura (1) and peritoneum (1). One case was a resection of suspect metastatic colorectal adenocarcinoma in recently diagnosed patient. Another was an incidental finding in an explanted liver from a patient who underwent liver transplantation for HCV cirrhosis. All cases showed microcystic spaces with markedly necrotic and granulomatous background. The spaces were lined by lamellated strongly PAS and GMS positive membranes. No protoscolices were seen in any of the cases. All cases were confirmed by serology and/or PCR according to WHO criteria.

Conclusions: Alveolar echinococcosis is an emerging infectious disease in North America, and early detection is of key importance to patient survival. All cases presented with necrotic granulomatous changes in the liver. Recent emergence of human AE in North America emphasizes the need for diagnostic awareness amongst pathologists in order to recognize and diagnose the disease without delay. Suspected cases require confirmation by PCR and serology regardless of the histologic features.

1617 Polyglucosan-Like Hepatocellular Inclusions are Associated with Polypharmacy

Iván González[1], Kathleen Byrnes[2]
[1]Washington University School of Medicine, St. Louis, MO, [2]Washington University in St. Louis, St. Louis, MO

Disclosures: Iván González: None; Kathleen Byrnes: None

Background: Ground-glass (GG) hepatocyte inclusions are classically seen in chronic Hepatitis B (HBV) infection. They also occur in a range of other settings including storage disorders or cyanamide therapy. However, there is a subset where a clear etiology cannot be elucidated (Gastroenterology 2006;131:713-8, *Am J Surg Pathol* 2006;30:1085-90). In this retrospective study we aimed to characterize the clinical characteristics and electron microscopic findings associated with GG hepatocytes.

Design: All cases of GG hepatocytes from 2000-2019 were retrieved from our files. Pertinent clinical information was obtained via chart review. Electron Microscopy was performed in our department.

Results: Of the 60 cases available for re-review, 85% were excluded due to a positive serology for HBV. Of the remaining 9 cases, 67% (n=6) were men with a mean age of 49 years (range: 2 - 69). The clinical indications for biopsy ranged from increased liver function test (n=5), cirrhosis per imaging (n=2), and follow-up biopsy (n=2). Elevated liver function tests (AST and ALT) were present in 6 patients (pts). One pt reported alcohol abuse however was not on cyanamide therapy. In the 6 pts with available medication history, there was a mean number of 8.2 (range, 3-14) medications used. The most common medications included immunosuppressive medications (n=4), health supplements (n=3), and antibiotics (n=3; table 1). Histologically, GG inclusions mostly involved zones 1-2 (56%, n=5). The inclusions were all diastase sensitive by PAS-D. All showed some chronic portal inflammation. Two had minimal lobular inflammation. They had varying degrees of fibrosis with 3 cases of periportal fibrosis. There were no definitive features of drug induced liver injury. Electron microscopy performed on one case showed intracytoplasmic vacuoles entrapping organelles (figure 1).

| Table-1. Association of Medication Class and Patients with Ground-Glass Hepatocyte	
Medication Class	**Number of Patients, n (%)**
Immunosuppression	4 (66.7%)
Supplement	3 (50%)
Antibiotics	3 (50%)
Antihypertensive	2 (33.3%)
Antihistamine	2 (33.3%)
Corticosteroid	2 (33.3%)
Antidepressant	2 (33.3%)
Benzodiazepine	2 (33.3%)
Levothyroxine	2 (33.3%)

Figure 1 - 1617
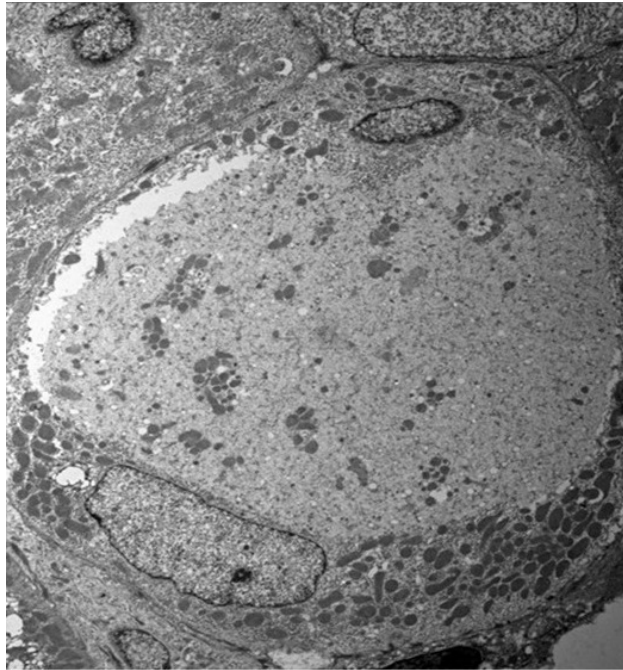
Figure-1. Intracytoplasmic pale vacuoles entrapping organelles.

Conclusions: GG inclusions in patients with negative HBV serology are rare. It affects predominantly men and a wide age range of pts. As described in the literature, immunosuppression is associated with a subset. It also is associated with polypharmacy with health supplement and antibiotic usage being the most common medications. Whether this represents a defect in hepatocyte metabolism as a result of medication injury is unclear, but seems likely given that the majority of pts were taking multiple drugs. Our findings highlight the importance of recognizing this rare entity and raising the possibility of polypharmacy in this subset of pts.

1618 Utilization of the Oncoscan Dx Platform as a Diagnostic Tool for Well-Differentiated Hepatocellular Lesions

Ashley Greer[1], Jennifer Hauenstein[2], Debra Saxe[3], Stewart Neill[4], Alyssa Krasinskas[5], Brian Robinson[6]
[1]Emory, Decatur, GA, [2]Emory University, Smyrna, GA, [3]Emory University School of Medicine, Atlanta, GA, [4]Emory University Medicine, Decatur, GA, [5]Emory University, Atlanta, GA, [6]Avondale Estates, GA

Background: Hepatocellular carcinoma (HCC) is one of the leading causes of cancer-related deaths, with a mortality rate of roughly 32,000 individuals this past year in the US alone. Hepatocellular adenomas (HCA), in contrast, are largely considered benign neoplasms, have very low malignant potential, and their management is often devoid surgical or oncologic intervention. While the outcomes between these two lesions are contrasted, histologically, there can be extensive overlap. This is particularly the case with well-differentiated HCC, where there is only mild nuclear atypia, focal expansion of hepatic plates, and scant mitotic activity. Unfortunately, immunohistochemical stains, which are often used to differentiate benign versus malignant lesions, are of little utility. However, genetically these lesions are quite distinct. Studies have shown that HCC contain a wide variety of chromosomal alterations, such as gains at chromosomal regions 8q, 1q, 20q, 7q, Xq, 5p, and 17q, and/or losses at 16q, 17p, 4q, 8p, 1p, 13q, and 16p, whereas HCA only rarely shows chromosomal abnormalities.

Design: Expert liver pathologists selected three well-differentiated HCCs and three HCAs with significant histologic overlap. DNA was extracted from lesional tissue obtained from FFPE samples (10 microdissected unstained slides) and analyzed on Oncoscan DX platform (335,000 probes) to assess for chromosomal gain, loss, or loss of heterozygosity (LOH). Gains and losses include those greater 50 kb in length and containing less than 25 probes; CNLOH are those areas greater than 3000 kb in length and containing more than 100 markers.

Results: As predicted, the HCCs showed increased genomic instability compared with the HCAs (7,11 and 26 aberrations for the three HCC vs 0, 1 and 1 for the three HCAs)(Figure 1). Moreover, chromosomal alterations mapped to previously described alterations detected in HCC 1q, 6p, 7q, 8p, 8q, 9p, 9q, 13q, 16p, 17p, 21p.

Conclusions: Chromosomal aberrations (gain, loss and LOH) detected on microarray can be used to differentiate well-differentiated hepatocellular lesions. This can be clinically valuable when hepatocellular lesions cannot be classified definitively as adenoma or carcinoma based on morphologic findings or immunohistochemistry. The overall genomic instability of the lesion, while helpful to the pathologist in rendering a correct diagnosis, can hopefully help clinicians determine the aggressiveness of the lesion and direct appropriate care.

1619   The Process of Liver Regeneration after Acute Autoimmune Hepatitis-Associated Hepatic Necrosis

Shaomin Hu[1], John Hart[1]
[1]The University of Chicago, Chicago, IL

Disclosures: Shaomin Hu: None; John Hart: None

Background: Hepatic progenitor cells possess the regenerative ability to differentiate towards either hepatocytes or cholangiocytes. In this study we investigated the dynamic histologic changes within the periportal parenchyma following acute hepatic necrosis to delineate the process of restoration of normal hepatic anatomy, with a primary focus on autoimmune hepatitis (AIH).

Design: We identified 34 needle biopsy and native liver resection cases with acute hepatic necrosis (from 5% to 90%) caused by AIH (n=19), drug/toxin-induced (n=12) and ischemic (n=3) liver injury. Arginase-1 & CK7 immunostains were utilized to identify & grade (0-4) bile ductular reaction (CK7+ abortive ductal profiles in the periportal stroma), intermediate hepatocytes (CK7+ and arginase-1+ large polypoid cells emanating from ductules) and neo-hepatocytes (CK7+ and arginase-1+ smaller isolated cells within zone 1).

Results: The 19 AIH cases were first evaluated. By 1 week after disease onset (n=5), a ductular reaction was evident in 5 of 5 cases, with intermediate hepatocytes just starting to appear in 2 (Fig.1 & 2). After 2.5 weeks (n=12), the degree of ductular reaction decreased & intermediate hepatocytes appeared, and were numerous in 11 cases (92%). Beyond 1 year (n=2), the ductular reaction & intermediate hepatocytes were no longer present and normal hepatic anatomy was restored. Neo-hepatocytes developed after intermediate hepatocytes became evident and were spatially adjacent to them, supporting that they represent newly generated mature hepatocytes. The sequence of ductular reaction followed by generation of intermediate hepatocytes and then neo-hepatocytes was also observed in severe drug/toxin induced acute hepatitis cases (n=12). Ductular reaction and intermediate hepatocytes were not identified in any of the cases collected within 5 days of disease onset (n=3), indicating that this much time is required for regeneration to begin. Eight patients progressed to liver failure & required liver transplant. In all of these cases an exuberant ductular reaction was observed but intermediate hepatocytes were minimal (n=1) or absent (n=7), and no neo-hepatocytes were identified.

Figure 1 - 1619
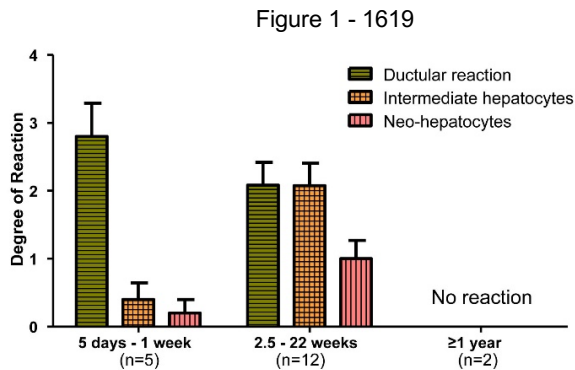
Figure 1. Degree of ductular reaction, intermediate hepatocyte and neo-hepatocyte response after acute autoimmune hepatitis-associated hepatic necrosis.

Figure 2 - 1619
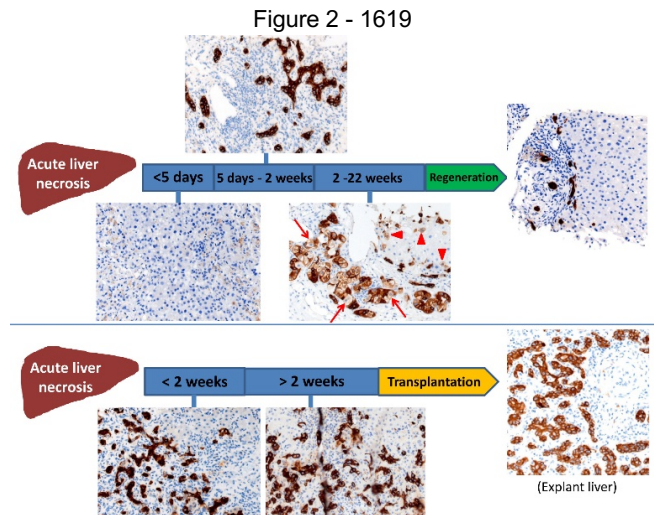
Figure 2. Histologic sequence model of liver regeneration (**top**) and failure (**below**) after significant hepatocyte necrosis. 1) A ductular reaction appears about 5 days after disease onset; 2) this in turn leads to generation of intermediate hepatocytes at about 2 weeks; 3) if generation of intermediate hepatocytes is robust neo-hepatocytes appear indicating the start of maturation into differentiated hepatocytes to restore lobular parenchyma. 4) Failure to generate intermediate hepatocytes results instead in exuberant ductular reaction but no recovery of hepatocyte volume, eventuating in liver failure and necessity for liver transplantation. CK7 immunostains were used to identify ductular reaction, intermediate hepatocytes (**arrow**) and neo-hepatocytes (**arrowhead**) (original magnification 20x).

Conclusions: It appears that in patients with acute onset of severe hepatic necrosis if a robust intermediate hepatocyte response is not evident in a biopsy taken more than 2.5 weeks after disease onset the patient will likely require a liver transplant. This is particular true if a marked bile ductular reaction is evident.

1620 Unclassified Primary Liver Carcinoma Including Intermediate Cell Carcinoma: Proposal for Diagnostic Categories and Criteria for Diagnosis

Alexander Kikuchi[1], Dhanpat Jain[2], Michael Torbenson[3], Tsung-Teh Wu[4], Matthew Yeh[5], Sanjay Kakar[1]
[1]University of California San Francisco, San Francisco, CA, [2]Yale University School of Medicine, New Haven, CT, [3]Mayo Clinic Rochester, Rochester, MN, [4]Mayo Clinic, Rochester, MN, [5]University of Washington Medical Center, Seattle, WA

Disclosures: Alexander Kikuchi: None; Dhanpat Jain: None; Michael Torbenson: None; Tsung-Teh Wu: None; Matthew Yeh: None; Sanjay Kakar: None

Background: Some primary liver carcinomas (PLC) cannot be classified as hepatocellular carcinoma (HCC), cholangiocarcinoma (CC) or combined HCC-CC. These most commonly occur as part of otherwise typical HCC, CC or HCC-CC, but can pose diagnostic problems if they form a major component. Rarely, this unclassified component may comprise nearly all the tumor. WHO 2019 does not include the category of liver tumors with 'stem cell features', but includes intermediate cell carcinoma (INT), without providing detailed diagnostic criteria. Definition of INT is variable across studies, and have included scirrhous HCC as well as HCC with CK7/CK19 staining(PMID 14739102;26969740). This study proposes a practical approach to PLCs that defy definite categorization.

Design: HCC, CC and HCC-CC cases, as well cases in which diagnosis of HCC vs CC was not clear based on morphology and immunohistochemistry(IHC) were reviewed for significant stem cell-like (SCL), INT or PLC-poorly differentiated (PLC-PD) components (defined as $\geq$25% on at least one section; tumors with <25% of these components were excluded). SCL component was defined as small uniform tumor cells without polygonal 'hepatoid' appearance and lacking clear glandular differentiation. INT areas had moderate cytoplasm and overlapping features of HCC and CC; when poorly differentiated (marked nuclear atypia), these cases were categorized as PLC-PD. By definition, discrete well-formed glands or mucin typical of CC were not present. Tumors with abundant stroma, hepatoid appearance, positive with $\geq$2 hepatocellular markers(HepPar, GPC3) and/or diffuse staining with arginase-1(Arg) were considered scirrhous HCC and excluded.

Results: SCL features were seen in 3 cases:2 HCC, 1 HCC-CC (proportion 25-60%). INT component was seen in 6 cases:3 HCC-CC (all resections;proportion 25-30%), 3 biopsies (entirely INT). PLC-PD was seen in 4 cases:1 HCC-CC (resection;proportion 25%),1 resection with entire PLC-PD and 2 biopsies(entirely PLC-PD).

		Morphology	Hepatocellular markers	CK7/CK19/MOC31
SCL-like,n=3		Uniform small cells at periphery of HCC nests or cords/nests/trabeculae in fibrous stroma	HepPar, Arg: 0/3, GPC: 1/3	Each positive in 1 case
INT, n=6		Moderate cytoplasm, moderate atypia. (a) Hepatoid cells in fibrous stroma, IHC negative for HCC, n=2 (b) Solid nests/ sheets with or without pseudoacini in fibrous stroma, overall features not enough for scirrhous HCC, n=4	(a) Hep Par, Arg, GPC: 0/2.(b) Hep Par: 2/4, GPC: 1/4, Arg 0/4	(a) CK7, MOC31: 1/2, CK19: 0/2 (b) CK7, CK19: 4/4
PLC=PD, n=4		Similar to INT but marked nuclear atypia	Hep Par, Arg, GPC: 0/4.	CK7: 4/4; CK19, MOC31: 3/4

Conclusions: Distinction of HCC and CC has important treatment implications, but some PLCs cannot be clearly categorized as HCC or CC when SCL, INT or poor differentiated components comprise a major portion of tumor in the biopsy/resection. This study proposes definite categories with specific morphologic and IHC criteria. Use of standardized definitions is necessary to ensure uniformity in diagnosis, characterize and compare genetic changes across studies, and study the prognostic impact of SCL, INT and PLC-PD components.

1621 Human Polyomaviruses 6 and 7 and Merkel Cell Polyomavirus are Hepatotropic Viruses

Faisal Klufah[1], Ghalib Mobaraki[2], Emil Chteinberg[1], Ernst-Jan Speel[3], Raed Alharbi[4], Véronique Winnepenninckx[1], Anna Kordelia Kurz[5], Iryna Samarska[6], Axel zur Hausen[6]

[1]Maastricht University Medical Center, Maastricht, Limburg, Netherlands, [2]Maastricht UMC+, Maastricht, Netherlands, [3]Maastricht University Medical Centre, Maastricht, Limburg, Netherlands, [4]Albaha University, Albaha, Saudi Arabia, [5]University Hospital RWTH Aachen, Aachen, Nordrhein-Westfalen, Germany, [6]Maastricht University Medical Centre+, Maastricht, Limburg, Netherlands

Disclosures: Faisal Klufah: None; Ghalib Mobaraki: None; Emil Chteinberg: None; Ernst-Jan Speel: None; Raed Alharbi: None; Véronique Winnepenninckx: None; Anna Kordelia Kurz: None; Iryna Samarska: None; Axel zur Hausen: None

Background: Cholangiocarcinoma (CCA) is a rare biliary duct malignancy with poor prognosis. Recently, the presence of human polyomavirus 6 (HPyV6) has been reported in the bile of different hepatobiliary diseases, in particular frequently detected in the bile of CCA patients including high viral load (Chan et al., 2017). Here, we investigated the prevalence of the novel HPyVs (HPyV6, HPyV7, and MCPyV) in CCA by using diverse molecular techniques in order to assess a possible role of HPyVs in CCA.

Design: 56 formalin fixed and paraffin embedded tissues of 19 CCA patients were included in this study. Screening for HPyVs was conducted using degenerated primers as published recently (Chan et al., 2017). In addition, HPyV-specific PCRs were performed to amplify HPyV6, HPyV7 & MCPyV. All PCR products were sequenced. DNA Fluorescence in situ hybridization (FISH), RNA(RISH) and immunohistochemistry (IHC) were used to assess the presence of HPyV6, HPyV7, and MCPyV on the DNA, transcriptional and translational level.

Results: Screening with degenerated primers was validated by testing positive control plasmids containing MCPyV, HPyV6, 7, 9, NJPyV, WUV, CaPyV plasmids which all revealed specific PCR bands as confirmed by sequence analysis. Seventeen (90%) of 19 CCAs were tested positive for HPyV7 by degenerated PCR, compared to 3 (16%) and MCPyV in 5 (26%). The presence of HPyV7 DNA was confirmed by HPyV7 specific FISH in 5 of 13 CCAs. Also, the presence of HPyV6 DNA was confirmed by HPyV6 specific FISH in 3 of 12 CCAs and MCPyV FISH confirmed in 4 of 7. RISH confirmed the presence of HPyV6 on the single cell level within the histomorphological context. In addition, using diverse monoclonal antibodies (HPyV7 STAg 2T10, HPyV6 STAg 1T1, MCPyV LTAg CM2B4) for IHC revealed the expression of viral proteins within these tissues.

#	Case ID	G	Age	Dx	Deg FA1 PCR	HPyV6				HPyV7			MCPyV			FISH	IHC
						PCR	IHC	FISH	RNA-ish	PCR	IHC	FISH	PCR				
						sTAg 123bp	1T1 sTAg		LTAg	sTAg 181bp	2T10 sTAg		M1/M2 178bp	VP1 351bp	LT3 308bp		LTAg
1	1	F	67	iCCA	HPyV7	-	+++	nd	nd	+	+++	+	+	+	+	+	+1
2	2	M	59	iCCA	-	W+	+	W+	+	-	-	-	-	-	-	-	nd
3	3	F	68	iCCA	HPyV7	-	-	nd	nd	-	++	W+	-	-	-	nd	nd
4	4	F	29	iCCA	-	W+	+++	W+	nd	+	++	W+	-	-	-	nd	nd
5	6	M	74	iCCA	MCPyV	-	+	-	nd	+	++	-	-	-	-	+	+1
6	7	M	64	pCCA	MCPyV	-	+++	-	-	W+	+++	+	-	-	W+	+	+2
7	8	F	64	pCCA	HPyV7	-	-	-	-	-	+++	-	-	-	-	nd	nd
8	9	M	45	pCCA	MCPyV	-	++	-	-	-	++	-	+	-	-	-	+1
9	11	F	50	dCCA	HPyV7	-	nd	-	nd	-	-	-	-	-	-	nd	-
10	12	M	70	iCCA	HPyV7	-	nd	-	-	+	++	-	-	-	-	nd	nd
11	13	M	69	iCCA	HPyV7	-	nd	nd	nd	-	+++	nd	-	-	-	nd	nd
12	14	M	70	iCCA	HPyV7	-	+++	-	nd	W+	+++	-	-	-	-	nd	nd
13	15	F	71	iCCA	HPyV7	+	+++	+	W+	-	+++	+	-	-	-	nd	nd
14	16	F	64	iCCA	HPyV7	-	-	nd	-	-	-	nd	-	-	-	-	nd
15	17	M	59	pCCA	HPyV7	-	+	nd	nd	+	+++	nd	-	-	-	nd	nd
16	19	M	69	iCCA	HPyV7	-	-	nd	nd	+	+++	nd	+	-	+	+	+1
17	20	M	71	iCCA	HPyV7	-	+	nd	nd	+	+++	nd	-	-	-	nd	nd
18	21	F	63	iCCA	HPyV7	-	+	-	nd	+	+++	-	-	-	-	nd	nd
19	22	M	61	iCCA	HPyV7	-	nd	nd	nd	-	nd	nd	-	-	-	nd	nd
		F:8 M:11		iCCA:14 pCCA:4 dCCA:1	HPyV7:14 MCPyV:3	3/19	11/15	3/11	2/7	10/19	15/18	5/13	3/19	1/19	3/19	4/7	5/6

Conclusions: Our results reveal that CCA and non-neoplastic liver tissues contain HPyV7, HPyV6 and MCPyV. HPyV7 was found to be more prevalent than HPyV6. Of interest, FISH, RISH, and IHC shows HPyV6 &7 and MCPyV in CCA cells as well as non-neoplastic hepatocytes. Follow-up studies are needed to understand the possible role of these viruses in the tumorigenesis of CCA. In addition, further studies on the potential contribution of these viruses to inflammatory liver diseases are warranted.

1622   Clinicopathologic Characteristics of Scirrhous Hepatocellular Carcinomas with or without Steatohepatitic Features

Hironori Kusano[1], Masayuki Okudaira[1], Yutaro Mihara[1], Taro Shioga[1], Shinji Mizuochi[1], Yoshinao Kinjo[1], Yoshiki Naito[1], Jun Akiba[2], Osamu Nakashima[3], Hirohisa Yano[1]
[1]Kurume University School of Medicine, Kurume, Fukuoka, Japan, [2]Kurume University Hospital, Kurume, Fukuoka, Japan, [3]Kurume University Hospital, Kurume, Japan

Background: Scirrhous and steatohepatitic hepatocellular carcinomas (HCCs) have been defined as morphological subtypes of HCC in the most recent WHO classification. Both subtypes show intratumoral fibrosis and their histological characteristics are overlapping. In this study, we investigated clinicopathologic characteristics of HCCs showing intratumoral fibrosis with or without steatohepatitic features.

Design: We reviewed 1550 HCC nodules resected at our institute from 2003 to 2019. Among these HCCs, 98 nodules (6.3%) showed more than 50% of tumor nests with interstitial fibrosis which were defined as scirrhous HCCs (SHCCs). SHCCs were further classified into steatohepatitic SHCC and non-steatohepatitic SHCC. The diagnosis of steatohepatitic SHCCs were made if the SHCCs fulfilled three of the following four criteria: intratumoral steatosis (more than 5% of tumor cells), tumor cell ballooning, tumor cells containing Mallory-Denk body-like intracytoplasmic material, intratumoral inflammatory infiltrations. Patients with solitary HCC treated with curative resection who have no previous treatment were included in the survival analysis.

Results: There is no significant difference between conventional (n=563) and scirrhous (n=57) HCCs in overall survival. In 98 SHCCs, 40 SHCCs (41%) showed steatohepatitic features. Steatohepatitic SHCCs are likely to show steatosis (steatohepatitic/non-steatohepatitic 47.5%/24.1%, P=0.0162), ballooning (steatohepatitic/non-steatohepatitic 47.5%/10.3%, P<0.0001), and Mallory-Denk bodies (steatohepatitic/non-steatohepatitic 15.0%/1.7%, P=0.0121) in non-neoplastic liver tissue. Patients with steatohepatitic SHCCs are more likely to have diabetes mellitus (steatohepatitic/non-steatohepatitic 60.0%/39.7%, P=0.0475) and no chronic hepatitis B virus infection (steatohepatitic/non-steatohepatitic 12.5%/32.8%, P=0.0219). There is no significant difference between steatohepatitic (n=20) and non-steatohepatitic (n=37) SHCCs in overall survival.

Conclusions: Steatohepatitic feature is not a significant prognostic factor, but closely related to their background liver disease.

1623 Diagnostic Utility of p-S6RP Immunohistochemistry in Antibody-Mediated Rejection in Liver Allograft Biopsies

Stanley Kwong[1], Wei Zheng[2], Brian Cone[3], Gregory Fishbein[4], Hanlin Wang[3]
[1]Department of Pathology and Laboratory Medicine, David Geffen School of Medicine at UCLA, Los Angeles, CA, [2]University of Emory, Atlanta, GA, [3]David Geffen School of Medicine at UCLA, Los Angeles, CA, [4]UCLA Health, Los Angeles, CA

Background: The diagnosis of antibody-mediated rejection (AMR) of liver allografts requires positive C4d immunohistochemistry (IHC) and positive donor-specific antibodies (DSA) as recommended by the Banff Working Group. It is known, however, that C4d IHC has low sensitivity and specificity in liver allografts, is prone to interobserver variability, and does not correlate well with DSA. The aim of this study was to investigate the diagnostic value of a new immunomarker, p-S6RP, which has shown promise as an AMR biomarker in cardiac and lung allografts recently.

Design: A total of 148 posttransplant liver biopsies from 148 patients were included in this study. C4d and p-S6RP IHCs were performed on each biopsy. HLA class I and II DSA status was obtained from our HLA laboratory for each case. Both C4d and p-S6RP IHCs were scored based on the extensiveness of positive staining in endothelial cells of portal microvasculature (portal veins and capillaries) as recommended by the Banff Working Group: 0% staining, negative (0); ≤ 10% staining, minimal (1+); >10% to ≤50%, focal (2+), >50%, diffuse (3+). The sensitivity and specificity of each stain as a biomarker of positive DSA status were calculated.

Results: The data for DSA, p-S6RP and C4d are summarized in the Table. The sensitivities and specificities for p-S6RP are as follows: ≥1+, 74% and 55%; ≥2+, 41% and 87%; and 3+, 17% and 97%. The sensitivities and specificities for C4d are as follows: ≥1+, 36% and 71%; ≥2+, 28% and 78%; and 3+, 16% and 87%. If 2+ is used as a cut-off, 75 p-S6RP cases (50%) were concordant with DSA status, among which 48 (32%) were p-S6RP+/DSA+ and 27 (18%) were p-S6RP-/DSA-. Of discordant cases, 4 (3%) were p-S6RP+/DSA- and 69 (47%) were p-S6RP-/DSA+. For C4d, 57 cases (39%) were concordant with DSA status, among which 33 (22%) were C4d+/DSA+ and 24 (16%) were C4d-/DSA-. Of discordant cases, 7 (5%) were C4d+/DSA- and 84 (57%) were C4d-/DSA+.

Table. Summary of DSA, p-S6RP and C4d data

p-S6RP	DSA Positive	Negative	Total	C4d	DSA Positive	Negative	Total	
0	30	17	47	0	75	22	97	
1+	39	10	49	1	9	2	11	
2+	28	3	31	2	14	3	17	
3+	20	1	21	3	19	4	23	
Total	117	31	148	Total	117	31	148	

Conclusions: If 2+ is chosen as a cut-off for positivity, p-S6RP appears to show better sensitivity, specificity, and concordance with DSA status in comparison with C4d. p-S6RP has the potential to be an adjunct IHC marker in the evaluation of liver allograft biopsies for AMR, especially in cases with equivocal C4d IHC.

1624 The Diagnostic Value of HSP70 and Glypican 3 in Hepatocellular Carcinoma: A Revisit

Hongjie Li[1], Ilke Nalbantoglu[2], Dhanpat Jain[1], Xuchen Zhang[3]
[1]Yale University School of Medicine, New Haven, CT, [2]Yale University School of Medicine, Woodbridge, CT, [3]Yale University School of Medicine, Orange, CT

Background: Diagnosing well differentiated hepatocellular carcinoma (WD-HCC) based solely on H&E examination can be challenging. Overexpression of at least two markers among heat shock protein-70 (HSP70), Glypican-3 (GPC3), and glutamine synthetase (GS) has been suggested (EASL Clinical Practice Guidelines and the 5th edition of WHO digestive system tumors) to be a useful adjunct in diagnosing WD-HCC. The aim of this study is to evaluate of the diagnostic value of HSP70 and GPC3 in the diagnosis of HCC.

Design: We retrospectively reviewed 33 cases of well- to moderated-differentiated (MD) HCCs from our pathology database archives. The final diagnosis in each case had been established based on histopathologic analysis. Cases where immunohistochemistry (IHC) for these two markers (HSP70 and GPC3) had been performed at the time of diagnosis were selected.

Results: We included 17 WD-HCCs and 16 MD-HCCs (**Table**). Although positive staining with HSP70 was more commonly seen in MD-HCC compared to WD-HCC (25% vs 6%, p=0.3419), the result is not statistically significant. GPC3 positivity was seen more commonly in WD-HCC compared to MD-HCC (24% vs 13%, p=0.4117) with no statistical significance. Positive staining with at least one marker (HSP70 and/or GPC3) was more commonly seen in MD-CC compared with WD-HCC (69% vs 29%, P=0.0238). In addition, positive staining with both HSP70 and GPC3 was more commonly seen in MD-HCC (44%) compared with WD-HCC (044% vs 0%, P=0.0021).

	Well-differentiated HCC	Moderately-differentiated HCC	p value	sensitivity	specificity
HSP70	1 (6%)	4 (25%)	0.3419	6%	75%
GPC3	4 (24%)	2 (13%)	0.4117	24%	88%
GPC3 and/or HSP70	5 (29%)	11 (69%)	0.0238	29%	31%
Both GPC3 and HSP70	0 (0%)	7 (44%)	0.0021	0%	56%

Conclusions: Either single or combined use of HSP70 and GPC3 has a low sensitivity in diagnosing WD-HCC and despite the recommendations, they are seldom useful in challenging cases. The utility of these stains is limited in our relatively small cohort. Further exploration with a larger number of cases will help establish the true sensitivity of these markers for the diagnosis of WD- HCC.

1625 A Clinicopathologic Study of Multiple Hepatocellular Adenomas in North America

Hongjie Li[1], Pallavi Patil[1], Sanjay Kakar[2], Matthew Yeh[3], Michael Torbenson[4], Mario Strazzabosco[1], Xuchen Zhang[5], Dhanpat Jain[1], Silvia Vilarinho[1], Tsung-Teh Wu[6]
[1]Yale University School of Medicine, New Haven, CT, [2]University of California San Francisco, San Francisco, CA, [3]University of Washington Medical Center, Seattle, WA, [4]Mayo Clinic Rochester, Rochester, MN, [5]Yale University School of Medicine, Orange, CT, [6]Mayo Clinic, Rochester, MN

Background: Hepatocellular adenomas (HCAs) are benign often solitary liver tumors with many subtypes, association with oral contraceptives in women and anabolic steroid/androgen in men. Multiple HCAs (³2) and adenomatosis (³10) are uncommon. The goal of the study was to evaluate subtypes, predisposing conditions and background liver disease in cases with multiple HCAs.

Design: HCAs (biopsies and resections) from participating institutions were reviewed for patient demographics, size and number of lesions, subtype, predisposing liver disease, status of background liver and associated HCC. HCAs were subtyped based on accepted criteria as inflammatory HCA (I-HCA), beta-catenin activated HCA (B-HCA), HNF-1 alpha inactivated HCA (H-HCA), and unclassified HCA (U-HCA). Cases with incomplete information regarding HCA subtype were excluded.

Results: A total of 175 of HCAs were identified and included in the study of which 81(46.3%) patients had multiple HCAs, including 15 (8.6%) cases with adenomatosis (Table). There was no significant difference with regards to age and HCA size range and HCA subtypes between the groups; however, there were more men in the adenomatosis group compared to others. One patient demonstrated more than one subtype (H-HCA and B-HCA). Malignant transformation into hepatocellular carcinoma was identified in all groups, with a relatively high

incidence in adenomatosis. MODY1 and congenital portal vein absence were identified as the predisposing cause in 2 patients with multiple HCAs.

Number of Adenoma	Age range (mean)	Gender M : F	Size range (cm)	Total	Types					More than 1 subtype	Background liver disease (# of case)	Associated HCC
					H-HCA	I-HCA	B-HCA	Mixed HCA	NOS			
1 HCA	11-64 (35)	10:84	1-14	94	24 (25%)	40 (42%)	9 (10%)	7 (7%)	14 (15%)	0 (0%)	Steatosis (71%) Granulomas (29%)	9 (9%)
³2 HCAs	16-55 (35)	1:65	0.2-17.5	66	10 (15%)	26 (39%)	1 (2%)	1 (2%)	27 (41%)	1 (2%)	MODY1 (1) Congenital Portal Vein absence (1)	2 (3%)
³10 HCAs	15-63 (39)	4:11	0.1-17.5	15	4 (27%)	5 (33%)	0 (0%)	1 (7%)	5 (33%)	0 (0%)	None	3 (20%)

Conclusions: This is a large series of multiple HCAs from United States and shows that these are not uncommon and constitute about 46.3% of all HCA patients. The distribution of various HCA subtypes in this group is similar to those with solitary lesions, but incidence of malignant transformation seems higher in patients with multiple adenomas and especially adenomatosis. While few patients have background liver disease or a predisposing cause, the vast majority of these patients do not have an identifiable predisposing cause or liver disease.

1626 Clinicopathological Characterization of T-cell Lymphomas in Liver

Philippa Li[1], Jiehao Zhou[2], Andrew Evans[3], Dongwei Zhang[3], Zenggang Pan[4], Xiaoyan Liao[3]
[1]Yale University, New Haven, CT, [2]Indiana University School of Medicine, Indianapolis, IN, [3]University of Rochester Medical Center, Rochester, NY, [4]Yale University School of Medicine, New Haven, CT

Disclosures: Philippa Li: None; Jiehao Zhou: None; Andrew Evans: None; Dongwei Zhang: None; Zenggang Pan: None; Xiaoyan Liao: None

Background: Hepatic T cell lymphomas (TCL) are rare, comprising approximately 12% of all lymphomas in liver. The clinicopathologic features are not fully understood.

Design: TCLs diagnosed in liver specimens between 2000 and 2019 were identified retrospectively from three large academic institutions. The histomorphologic features were reviewed and the lymphoma diagnoses were confirmed according to 2016 WHO Classification. Clinical information including radiographic findings, liver function test, and survival data was collected. R value, defined as Alanine aminotransferase/upper limit of normal: Alkaline phosphatase/upper limit of normal, was applied to designate a pattern of liver injury (hepatitic if R>5, cholestatic if R <2, and mixed if 2≤R≤5).

Results: A total of 41 surgical cases were retrieved from 35 patients (10 females and 25 males), with a median age of 54 (range 3-75), including 3 pediatric. Six patients had 2 specimens each. Eleven (34%) patients were diagnosed as hepatosplenic T cell lymphoma (HSTCL), 13 (37%) peripheral T cell lymphoma, not otherwise specified (PTCL, NOS), and 11 (34%) others (Table 1). In 24 of 36 specimens, there were no mass lesions on imaging studies but abnormal liver function tests (17 cholestatic, 6 hepatitis, 1 mixed). Interestingly, all HSTCL showed no mass lesion on image, a typical sinusoidal infiltration pattern on histology, and liver function test mostly cholestatic (R<2, n=8/11). Similar pattern was seen in majority of patients with PTCL NOS, namely no mass lesion (n=9/13) and cholestatic liver injury (n=7/13). Twelve specimens had mass lesions, correlating with either normal liver function test (n=8/12) or cholestatic liver injury (n=4/12); majority of those cases (n=8/12) were "others". Morphological analysis in 33 cases revealed 20 (60%) lymphoma cells were small or small-to-medium in size, with a portal or sinusoidal infiltration pattern, which mimics a reactive/inflammatory process. Patients with HSTCL had the worst prognosis with median survival day of 37, followed by PTCL NOS with a median survival day of 72.

Table 1. Clinicopathologic Features of T cell Lymphomas in Liver

	# Patients	Age (range)	Gender	Imaging findings mass vs. none	R value	Outcomes	Follow-up days (range)
HSTCL	11	39 (4-71)	1F; 10M	none	1 normal; 2 hepatitic; 8 cholestatic	9 DOD; 2 lost to follow/up	37 (1-215)
PTCL, NOS	13	55 (26-73)	3F; 10M	4 mass; 9 none	3 normal; 3 hepatitic; 7 cholestatic	8 DOD; 3 alive, 2 lost to follow-up	72 (14-2600)
AITL	2	75; 43	1F; 1M	1 mass; 1 none	1 normal; 1 hepatitic	1 alive; 1 DOD	658; 747
ALCL	2	71; 62	2M	2 mass	2 cholestatic	both DOD	52; 360
CTCL	2	73; 53	1F; 1M	1 mass; 1 none	2 cholestatic	both DOD	850; 152
PTLD	1	46	1F	none	mixed	DOD	4
EBV+ TCLPD/PTLD*	1	9	1F	none for EBV+TCLPD; mass for PTLD	hepatitic, normal	DOD	321
T-ALL	1	38	M	mass	normal	lost to follow-up	N/A
T-PLL	1	55	1F	mass	normal	DOD	2505
HSTCL-like, unclassified#	1	3	F	mass	normal	DOD	107

Abbreviations:

HSTCL: Hepatosplenic T cell lymphoma; PTCL, NOS: Peripheral T cell lymphoma, not otherwise specified; AITL: Angioimmunoblastic T-cell lymphoma; ALCL: Anaplastic large cell lymphoma; CTCL: Cutaneous T cell lymphoma; PTLD: Post-transplant lymphoproliferative disorder; EBV+ TCLPD: EBV positive T/NK cell lymphoproliferative disorder of childhood; T-ALL: T-cell acute lymphoblastic leukeamia; T-PLL: T-cell prolyphocytic leukemia; N/A: Not applicable; DOD: Died of disease

* This pediatric patient had EBV+TCLPD before developing fatal hepatic PTLD after bone marrow transplant

\# This pediatric patient had mixed lineage T/myeloid acute leukemia, with recurrence in liver as HSTCL-like lymphoma

Conclusions: This case series, the largest reported to date, described the frequencies, clinical findings, and histomorphological correlations of TCLs in liver. Understanding the clinicopathologic features is essential for a timely and accurate diagnosis, especially to differentiate from other conditions such as reactive lymphocytosis.

1627   Immunosuppressive Function of CD14-Myeloid-Derived Suppressor Cells Is Promoted by Tumor-Derived IFNB1 in Hepatocellular Carcinoma

Yongchao Li[1], Yaohong Wang[1], Shuyu E[1], Nour Yadak[2], Richa Jain[3], Ian Clark[4], Mahul Amin[5], Meiyun Fan[6]
[1]University of Tennessee Health Science Center, Memphis, TN, [2]UTHSC, Bartlett, TN, [3]Banner-University Medical Center, Tucson, AZ, [4]University of Tennessee, Memphis, TN, [5]Methodist University Hospital, Memphis, TN, [6]The University of Tennessee Health Science Center, Memphis, TN

Disclosures: Yongchao Li: None; Yaohong Wang: None; Shuyu E: None; Nour Yadak: None; Ian Clark: None; Mahul Amin: *Consultant*, Urogen; *Consultant*, Advanced Clinical; *Advisory Board Member*, Cell Max; *Advisory Board Member*, Precipio Diagnostics; Meiyun Fan: None

Background: Infiltration of myeloid-derived suppressor cells (MDSCs) in hepatocellular carcinoma (HCC) is often associated with poor prognosis due to functional suppression of CD8-T cells. Integrated analyses of multiple data platforms of HCC in the TCGA database and available single cell RNA-seq (ScRNA-seq) data from Gene Expression Omnibus (GEO) of tumor infiltrating lymphocytes (TILs) and peripheral blood mononuclear cells (PBMCs) implicates an important role of tumor- derived IFNB1 (Interferon Beta 1), as a consequence of transcriptional activation of 9p21.3 locus, in promoting CD14+ MDSC-mediated suppression of CD8+ T cells. The aim of this study is to investigate the impact of tumor-derived IFNB1 (interferon beta 1) on distribution and functional status of CD14-MDSCs in HCC **(Fig1).**

Design: 30 cases of previously diagnosed of poorly differentiated/undifferentiated HCC were selected and Formalin-Fixed Paraffin-Embedded (FFPE) tissue blocks were collected and sectioned at 4 µm. ScRNA-seq datasets of TILs and PBMCs from Gene Expression Omnibus (GEO) were analyzed to identify immune cells responsive to IFNB1. RNAscope assay were performed on patient FFPE slides to detect the expression of IFNB1 in tumor cells, the expression of immune suppressive genes induced by IFNB1 in CD14-MDSCs and exhaustion markers of CD8-T cells. IHC on FFPE were used to examine the distribution patterns of CD14-MDSCs and CD8-T cells.

Results: 1) RNAscope assay detected IFNB1 mRNA in poorly differentiated HCC tumor cells that coexpress CDKN2A, a surrogate marker of epigenetic activation of the IFNB1-encoding 9p21.3 loci **(Fig2A)**. 2) Among TILs, CD14-MDSCs were found to be associated with expression of IFNB1 responsive genes in tumors expressing CDKN2A. 3) Comparing to other immune cells, CD14-MDSCs exhibited strongest response to IFNB1 treatment *in vitro*, manifested by magnitude and number of transcription induction **(Fig2B)**. 4) IFNB1 induces expression in CD14-MDSCs of several genes known to inhibit CD8-T cells, including LILRB2, LILRB4 and CD274.

Figure 1 - 1627
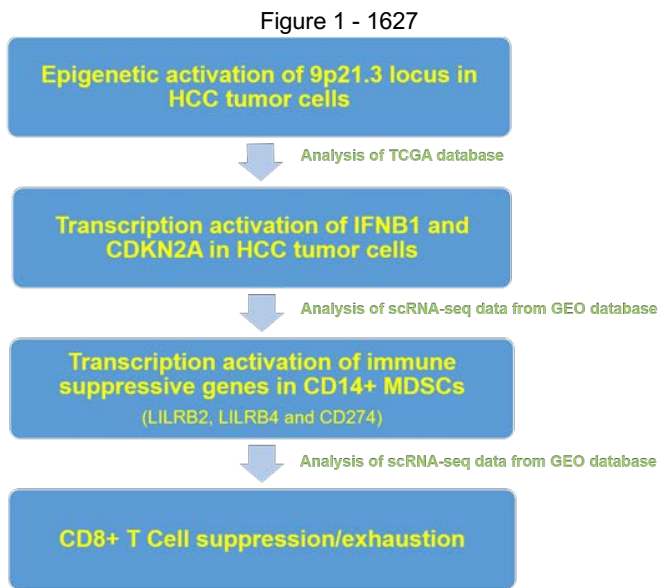
Fig 1. Tumor-derived IFNB1 drives suppression of CD8+ T effector cells by inducing expression of immune suppressive gene in CD14+ MDSCs.

Figure 2 - 1627
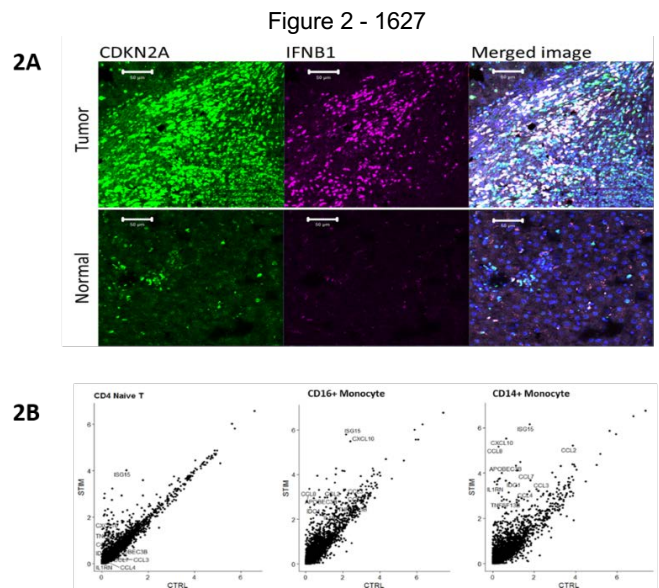
Fig 2A. Detection of correlated expression of CDKN2A and IFNB1 HCC tumor cells by the RNAscope ISH Assay on FFPE tissues. **2B.** CD14+ MDSCs exhibited strongest response to IFNB1 (100 U/mL, 6 h), manifested by magnitude and number of genes induced by IFNB1. Single cell RNA-seq Data were retrieved from GSE96583.

Conclusions: Transcription activation of IFNB1 in HCC tumor cells likely plays an important role in suppressing CD8- T cells through CD14-MDSCs. Targeting immune IFNB1-induced genes in CD14-MDSCs could be a novel strategy to enhance anti-tumor cytolytic activity of CD8-T cells.

1628   Hepatitic Variant of Graft-Versus-Host Disease: Prevalence and Comparison with Clinicopathologic Features of the Classic Variant

Tom Liang[1], Stephen Dong[2], Shefali Chopra[3]
[1]LAC + USC Medical Center/Keck Medical Center of USC, Los Angeles, CA, [2]Keck Hospital of USC and LAC-USC Medical Center, Los Angeles, CA, [3]University of Southern California, San Marino, CA

Disclosures: Tom Liang: None; Stephen Dong: None; Shefali Chopra: None

Background: Graft versus host disease (GVHD) of the liver occurs after allogenic hematopoietic stem cell transplantation presenting as a cholestatic disease. Hepatitic variant has been described with a differential diagnosis of drug induced liver injury (DILI) and infection. This study was undertaken to see what percentage of cases are hepatitic and compare clinicopathologic features.

Design: 51 cases of liver biopsy with diagnosis of GVHD from 41 patients were identified. Age, ethnicity, disease , therapy, time of biopsy from transplant time, conditioning regimen, HLA status, therapy, response, other organs involved, hepatitis status, bilirubin, ALP, AST, and ALT were recorded. Cases were reviewed and classified as classic or hepatitic variant. Cases with confounding causes (e.g. DILI, infection) were excluded.

Results: 16 cases (15 patients) had moderate portal inflammation with interface and significant lobular inflammation and were the hepatitic variant. 25% of hepatitic cases had ductular reaction, apoptosis, and endotheliitis present. No case had ductopenia. The median AST was 179, ALT 190, ALP 156, and bilirubin 0.5.

35 cases (26 patients) had mild portal inflammation, no interface and absent to mild lobular inflammation and were the classic variant. 8.6% of classic cases had ductular reaction, 5.7% had apoptosis, and none had endotheliitis. Ductopenia was seen in 5.7% cases. The median AST was 93, ALT 156, ALP 294 and bilirubin 1.3.

42 out of 51 cases had biopsies >100 days after transplant. 31% were in the hepatitic group, and 69% were in the classic group. All cases in both groups responded to treatment with increased immunosuppression.

When cases were divided based on ALT values irrespective of histologic criteria, those with ALT > 200 U/L had significantly shorter time to GVHD manifestation (241 vs 408 days, p < 0.01) and were associated with reduced intensity conditioning (RIC) regimen compared to myeloablative therapy (43% vs 18%, p < 0.01).

Conclusions: 36.6% (15/41) patients had hepatitic variant of GVHD. Hepatitic variant had ductular reaction, endotheliitis, and apoptosis in 25% cases. The Hepatitic variant was associated with higher AST and ALT values, but lower bilirubin and ALP when compared to the classic variant. There was no significant histological differences or utility of separating cases into acute and chronic GVHD based on 100 days after transplant. Cases with higher ALT values were associated with RIC regimen and had shorter time to GVHD manifestation.

1629 Whole Slide Image Education Module Improves Donor Liver Frozen Section Diagnosis Accuracy for Liver Transplantation

Yen-Yu Lin[1], Yu-Cheng Lee[2], Wei-An Lai[1], Ching-Yeuh Yang[1], Hsin-Yi Chang[3], Hsiang-Sheng Wang[1], Yu-Ju Su[4], Yi-Chen Yeh[5]
[1]Taipei Veterans General Hospital, Taipei, Taiwan, [2]Taipei Veterans General Hospital, Yonghe District, New Taipei City, Taiwan, [3]VGHTPE, Taipei, Taiwan, [4]Far Eastern Memorial Hospital, New Taipei City, Taiwan, [5]Taipei, Taiwan

Disclosures: Yen-Yu Lin: None; Yu-Cheng Lee: None; Wei-An Lai: None; Ching-Yeuh Yang: None; Hsin-Yi Chang: None; Hsiang-Sheng Wang: None; Yu-Ju Su: None; Yi-Chen Yeh: None

Background: During the process of liver transplantation, evaluating the quality of the donor liver by frozen section can provide valuable information. Specifically, the extent of macrosteatosis of the liver tissue has been shown to correlate with the transplantation outcome. Providing specific training and easily accessible reference images may improve the diagnosis accuracy of the duty pathologist performing this task.

Design: From 2009 to 2019, all liver transplantation cases in a single center with intra-operative frozen section of the donor liver were reviewed, and the original frozen sections were scanned using a high-throughput slide scanner. Two pathologists reviewed the original slides and the whole slide images (WSI). The percentage of tissue area affected by macrosteatosis was determined by the two pathologists, referencing the original diagnosis made at the time of surgery when such percentage was mentioned in the report. The cases were then categorized into mild (0-30%), moderate (31-60%) or severe (61-100%) macrosteatosis. These cases were then segregated into one training set and one testing set. Six pathology residents were invited to view the WSI training set, make diagnoses, followed by a discussion session, and then view the testing set.

Results: A total of 35 liver transplantation cases were reviewed. There was a trend toward a correlation between moderate or severe macrosteatosis of the donor liver and poor initial graft function (defined as serum AST or ALT >2500 U/L in the first 3 days or total bilirubin > 10 mg/dL on day 7 post-transplantation), but the difference was not statistically significant (Fisher's exact test, p=0.14). The frozen section slides of 25 cases were judged to be of sufficient quality to be included in the education module (13 for training, 12 for testing). When the pathology residents viewed the training set, their evaluation of macrosteatosis extent was concordant with the consensus in 89.5% of cases. After the discussion session, their evaluation of the testing set was concordant with the consensus in 95% of cases (Table 1).

Table 1. Result of resident education with the liver graft frozen section education module

	Training Set	Testing Set
Consensus Ratio of Negative/Mild, Moderate and Severe Macrosteatosis Cases	11:2:0	10:2:0
Correct Resident Classification of Macrosteatosis	60/67 (89.5%)	57/60 (95%)
Average Difference in Macrosteatosis Percentage Estimation Compared to Consensus	2.75	3.61

Conclusions: Inexperienced pathologists tend to over-estimate the macrosteatosis extent of a donor liver frozen section. Our WSI education module can reduce such diagnosis bias. It can also serve as a convenient on-site reference and may improve the diagnosis accuracy of duty pathologists when evaluating donor liver graft tissue.

1630 The Liver Biopsy in Antimitochondrial Antibody Positive Patients without Primary Biliary Cirrhosis

Mira Lotfalla[1], Rondell Graham[1], Roger Moreira[1], Taofic Mounajjed[1]
[1]Mayo Clinic, Rochester, MN

Disclosures: Mira Lotfalla: None; Rondell Graham: None; Roger Moreira: None; Taofic Mounajjed: None

Background: Antimitochondrial (M2) antibody (AMA) is specific for primary biliary cirrhosis (PBC) but has also been described in individuals without PBC. Although the clinical features of AMA-positive individuals without PBC have been described, their liver histology has not been well characterized. We aim to characterize the histologic patterns seen in liver biopsies of AMA-positive individuals who do not have PBC.

Design: Our electronic clinical records were retrospectively searched from 1992 to 2017 for AMA-positive patients. Only patients with a liver biopsy were included. In general, a positive AMA with an associated elevation in alkaline phosphatase was considered diagnostic of PBC; however, the clinical records and lab results for all patients were reviewed and used in conjunction with the liver biopsy to classify the liver disease. AMA was obtained by either Indirect Immunofluorescence (1992-2000) or Enzyme Immunoassay (2000-2017).

Results: A total of 575 AMA-positive patients were identified and classified into 3 categories: (1) patients with established PBC, (2) patients with overlap syndrome: PBC/autoimmune hepatitis (AIH), (3) patients with neither PBC nor PBC/AIH (non-PBC group). The non-PBC group numbered 34 patients (6% of the AMA-positive cohort), while the majority had PBC (n=493; 86%) or overlap syndrome (n=48, 8%). The clinical characteristics of the 3 groups are summarized in the table .
The liver biopsy in the non-PBC group showed chronic hepatitis (AIH: n=12 [35%], hepatitis C: n=4 [12%], undetermined etiology: n=3 [9%]), non-alcoholic steatohepatitis (n=8, 24%), primary sclerosing cholangitis (n=2, 6%), cryptogenic cirrhosis (n=2, 6%), fulminant hepatitis A (n=1, 3%), steatosis (n=1, 3%), and nonspecific findings ((n=1, 3%). Fourteen (41%) patients had advanced (bridging or greater) fibrosis.

Clinical characteristic of AMA-positive patients				
	Age at time of first biopsy in years (average, range)	Female : Male ratio	Average follow-up period (years)	Survival rate
PBC	56 (26-85)	5.3 : 1	8	79%
Overlap	52 (29-78)	7 : 1	9	77%
Non-PBC	55 (25-79)	7.5 : 1	5	85%

Conclusions: Although AMA is specific for PBC, 6% of our patients did not have PBC (false positives) during an average follow-up period of 5 years that included a liver biopsy. The most common histology associated with this finding is chronic hepatitis (AIH and hepatitis C) and steatohepatitis. AMA positivity in this setting might represent non-specific biologic variation, or could be attributed to other autoimmune conditions or possible technical testing artifacts.

1631 Imaging Mass Spectrometry is Accurate in Differentiating Bile Duct Adenoma from Intrahepatic Cholangiocarcinoma

Hsiang-Chih (Sean) Lu[1], Iván González[2], Nathan Patterson[3], Audra Judd[3], Michelle Reyzer[3], Deyali Chatterjee[4], Ilke Nalbantoglu[5]
[1]Washington University School of Medicine in St. Louis, St. Louis, MO, [2]Washington University School of Medicine, St. Louis, MO, [3]Vanderbilt University School of Medicine, Nashville, TN, [4]Washington University in St. Louis, St. Louis, MO, [5]Yale University School of Medicine, Woodbridge, CT

Disclosures: Hsiang-Chih (Sean) Lu: None; Iván González: None; Nathan Patterson: None; Audra Judd: None; Michelle Reyzer: None; Deyali Chatterjee: None; Ilke Nalbantoglu: None

Background: Bile duct adenomas (BDAs) are benign neoplasms typically discovered incidentally. They are usually small (<1 cm), subcapsular, well circumscribed, and composed of narrow tubules lined by bland epithelium with a fibrous stroma. The absence of pleomorphism, mitosis, and the configuration of the glands are helpful in distinguishing it from adenocarcinoma. Occasionally, the lesion may be larger, irregular and more cellular, causing confusion with a well-differentiated intrahepatic cholangiocarcinoma (iCCa), particularly when dealing with a small biopsy. Currently there are no good markers to distinguish between the two entities. However, the distinction is critical as it dictates the treatment and prognosis of the patients.

Design: Imaging mass spectrometry (IMS) is a novel method in mapping biological compounds in tissue sections. IMS allows mapping of multiple biomarkers simultaneously without using antibodies, generating an unbiased discovery of unique signatures of a particular disease entity. It can improve the sensitivity and specificity at a lower cost than conventional immunohistochemistry that relies on multiple antibodies. In this study, we set out to determine the accuracy of IMS in differentiating BDA and iCCa. We first utilized IMS from a set of training cases to build a classification model, and then applied it to test cases that were different from the training set.

Results: We first performed IMS in the training set of 13 unequivocal BDAs and 14 unequivocal iCCa. The MS peaks that were significantly different between the two were used to build a classification model with machine learning using a support vector machine algorithm with a linear kernel. The classification model was then applied to a test set consisting of 6 BDAs (all less than <1 cm) and 6 iCCa (2 well-, 3 moderately-, and 1 poorly-differentiated). Depending on the size of the lesion, 5 to 20 measurements (150-μm diameter each) were performed per case in the test set. Of the 145 measurements, only 5 spots from two iCCa (1 well- and 1 poorly-differentiated) were misclassified as BDA. All the measurements from BDAs were correctly classified. The accuracy of the classification model is 0.9655 with a Kappa of 0.9227.

Conclusions: Our study shows that IMS is accurate in differentiating BDA and iCCa. The utilization of this technique may be helpful in clinical practice to categorize borderline/atypical bile duct lesions, which are difficult to classify based on histomorphology alone.

1632 Hepatocellular Carcinoma in Non-Cirrhotic Livers Frequently Arises Through Transformation of Hepatocellular Adenoma

Kelsey McHugh[1], Daniela Allende[2], Rondell Graham[3], Carlos Romero-Marrero[4], Gianina Flocco[4], Daniel Roberts[4]
[1]Cleveland Clinic, Lakewood, OH, [2]Cleveland Clinic, Lerner College of Medicine of Case Western University School of Medicine, Avon Lake, OH, [3]Mayo Clinic, Rochester, MN, [4]Cleveland Clinic, Cleveland, OH

Disclosures: Kelsey McHugh: None; Daniela Allende: None; Rondell Graham: None; Carlos Romero-Marrero: None; Gianina Flocco: None; Daniel Roberts: None

Background: Hepatocellular carcinoma (HCC) arising without background cirrhosis is a rare phenomenon, and most examples have no clear etiology. The published rate of malignant transformation in hepatocellular adenoma (HCA) ranges from 3 to 10.6%, but its diagnosis can be difficult in cases where the majority of the lesion has been transformed. We reviewed all non-cirrhotic HCC diagnosed at our institution over a 13-year period and evaluated for the presence of precursor HCAs.

Design: Electronic review of pathology and medical records was conducted from 2007 to 2019 to identify resection specimens containing HCC without background cirrhosis. Slides were reviewed, and the diagnosis of HCA was based solely on histomorphology. All identified HCAs were subtyped using immunohistochemistry (glutamine synthetase, beta catenin, CRP, SAA, and LFABP), according to the World Health Organization classification scheme. Consensus was achieved by 3 authors (KEM, DA, DER) through simultaneous review.

Results: Thirty-four HCCs were identified in patients without cirrhosis. Twenty-five (74%) occurred in males, and nine in females (27%). Age at resection ranged from 34 to 88 years (mean of 68.8 years), and there was no significant difference in the average age of male and female patients. Tumor sizes ranged from 3.2 to 19 cm (mean of 8.7 cm) and included 13 (38%) well-differentiated, 15 (44%) moderately differentiated, and 6 (18%) poorly differentiated HCCs. Four (12%) patients had positive viral hepatitis serologies. Sixteen HCCs (47.1%) arose through transformation of definitive (n=14) or borderline (n=2) HCAs. Immunophenotyping these HCA precursors revealed the following subtypes: 8 (50%) inflammatory, 5 (31%) beta-catenin activated, 1 (6%) HNF1A-activated, and 2 (12%) unclassified. During this study period, the calculated rate of malignant transformation in HCAs at our institution was 12.1%.

	HCC with definite or borderline HCA (n=16)	HCC without HCA (n=18)	p-value
Patient Data			0.3360
Male	13	12	
Female	3	6	
Mean age (range), yrs	68.7 (34-88)	68.5 (48-82)	0.9592
HBV	0	1	1.00
HCV	2	1	
Tumor Data			
Mean size (range), cm	8.3 (3.2-18.8)	9.1 (3.5-1.8)	0.6271
Well-differentiated	9 (56%)	4 (22%)	0.0181
Modoerately differentiated	7 (44%)	8 (44%)	
Poorly differentiated	0	6 (33%)	
HCA subtype			
Inflammatory	8 (50%)	-	
Beta-catenin activated	5 (31%)	-	
HNF1A-activated	1 (6%)	-	
Unclassified	2 (13%)	-	

Conclusions: HCC without background cirrhosis frequently arises through malignant transformation of HCAs, and precursor lesions may be under-recognized at the time of initial histopathologic review. While beta-catenin activated HCAs are classically associated with the highest risk of HCC, inflammatory HCAs (without beta-catenin activation) most frequently showed malignant transformation in our cohort.

1633 Aberrant MFAP5, IMP3, BAP1, and p53 Immunohistochemistry Patterns Are Highly Specific for Primary Intrahepatic Cholangiocarcinoma

Kelsey McHugh[1], Daniela Allende[2], Lei Zhao[3], John Hart[4], Xuefeng Zhang[5]
[1]Cleveland Clinic, Lakewood, OH, [2]Cleveland Clinic, Lerner College of Medicine of Case Western University School of Medicine, Avon Lake, OH, [3]Brigham and Women's Hospital, Harvard Medical School, Boston, MA, [4]The University of Chicago, Chicago, IL, [5]Cleveland Clinic, Beachwood, OH

Disclosures: Kelsey McHugh: None; Daniela Allende: None; Lei Zhao: None; Lei Zhao: None; John Hart: None; Xuefeng Zhang: None

Background: Distinguishing benign bile duct proliferations from cholangiocarcinoma is a diagnostic challenge due to significant cytomorphologic overlap between benign reactive atypia and bland biliary malignancies. There are few diagnostic immunohistochemical (IHC) markers of use in this endeavor. In this study, we aim to determine if MFAP5, IMP3, BAP1 and p53 staining differs significantly in benign versus malignant bile duct proliferations.

Design: Electronic pathology records review was conducted from 2005 to 2019 to identify benign and malignant bile duct lesions. On a single representative block from each lesion, the following IHC panel was performed: MFAP5, IMP3, BAP1, p53, and Ki67. For each stain, "normal" staining was defined as the following: MFAP5, no loss of staining in stroma surrounding lesional glands; IMP3, <1% epithelial staining; BAP1, retained staining in >90% of lesional nuclei; p53, wild type staining. Any staining that did not fit within the parameters of "normal" staining was considered "abnormal." Ki67 proliferation index was "eyeballed" at a single high-power hotspot.

Results: A total of 79 cases were identified: 18 bile duct adenomas (BDA), 17 bile duct hamartomas (BDH), and 44 intrahepatic cholangiocarcinomas. All cases were stained with MFAP5 and IMP3. 39 cases were stained with BAP1, p53, and Ki67. The specificity of an abnormal staining pattern for diagnosing cholangiocarcinoma with MFAP, IMP3, BAP1, or p53 is as follows: 88.6%, 88.6%, 94.4%, and 94.1%, respectively. The sensitivities are 88.6%, 40%, 20%, and 15% respectively. The average Ki67 was 1.4% (range, 0 to 5%) in BDA/BDH, and 41.5% (range, 5 to 100%) in intrahepatic cholangiocarcinomas. When MFAP5, IMP3, BAP1, and p53 are considered as an immunopanel, 20/20 (100%) intrahepatic cholangiocarcinomas demonstrated abnormal staining with at least 1 of the 4 markers. Only 3/17 (17.6%) BDA/BDHs demonstrated abnormal staining with at least 1 marker. As a panel, the sensitivity and specificity of these 4 stains for cholangiocarcinoma is 100% and 82.4%.

Stain	Specificity (%)	Sensitivity (%)
MFAP5	88.6	88.6
IMP3	88.6	40
BAP1	94.4	20
p53	94.1	15
Four marker panel	82.4	100

Conclusions: "Abnormal" staining patterns with MFAP5, IMP3, BAP1, and p53 are specific to cholangiocarcinoma, and may be of clinical use in distinguishing between benign and malignant bile duct proliferations.

1634 A Truncating Variant of 17-Beta Hydroxysteroid Dehydrogenase13 Protein Protects Against Severe Histopathological Progression of Liver Injury and Cancer Development: Quantitative Next-Generation Sequencing-Based-Analysis and Meta-Analysis

Mohammad Mohammad[1], Yirui Hu[2], Guoli Chen[1], Jinhong Li[3], Jianhong Li[1]
[1]Geisinger Commonwealth School of Medicine, Danville, PA, [2]Geisinger Health Systems, Danville, PA, [3]Geisinger, Danville, PA

Disclosures: Mohammad Mohammad: None; Yirui Hu: None; Guoli Chen: None; Jinhong Li: None; Jianhong Li: None

Background: HSD17B13 (rs72613567) is a loss-of-function variant producing truncated protein with reduced enzymatic activity that was recently discovered to be associated with protection from chronic liver disease. Our objective is to investigate the strength of association between HSD17B13 loss-of-function and susceptibility to severe liver injury, fibrosis, and development of hepatocellular carcinoma to further assess its potential as a new therapeutic target.

Design: An exome sequence data of HSD17B13 variant in liver diseases, in addition to studies and substudies investigating the effects and safety of truncating HSD17B13 have been searched on four main databases (PubMed, Embase, Cochrane Library, and web of science) dating until September- 2019. Odds ratios (ORs) and 95% confidence intervals (CIs) were initially calculated from all enrolled 12 studies with adjustment for age & sex. Severity of liver diseases was assessed histologically and classified according to the fibrosis stage. Meta-analysis with random-effects was performed to estimate the pooled effect size. The pooled OR is considered statistically significant if 95% CI did not contain 1. Each included study's pooled estimates and measures of variability were used to generate forest plots. Publication bias was evaluated by Egger's test. Variability between included studies was assessed by heterogeneity tests using I2 statistic. All analyses were conducted using RStudio (Version 1.0.136) using the 'Meta' and 'Metafor' package.

Results: In a total of (5664) liver disease cases and (303139) control patients, the truncating HSD17B13 variant was a protective factor across all liver disease types (OR = 0.74, 95% CI: 0.69 to 0.79). When stratified by etiology of liver disease, truncating HSD17B13-variant was associated with lower risk of non-alcoholic liver disease (OR = 0.69, 95% CI: 0.60 to 0.78); alcoholic liver disease (OR = 0.77, 95% CI: 0.71 to 0.84); Advanced alcoholic liver disease (cirrhosis) (OR = 0.82, 95% CI: 0.72 to 0.93); Hepatitis C (OR = 0.71, 95% CI: 0.60 to 0.85) and liver cancer (OR = 0.72, 95% CI: 0.53 to 0.97). There was no heterogeneity observed (I2=0, p>0.05).

Conclusions: By summarizing the amount of data, this study provides unequivocal evidence of the truncating HSD17B13 (rs72613567) variant as a strong modifier of the pathological progression of chronic liver diseases demonstrating protection from liver fibrosis and cancer development, and thus a new emerging therapeutic target.

1635 Hepatitis A: A Contemporary Retelling

Mohamed Mustafa[1], Wassim Abdallah[2], Nathan Shelman[2], Raj Vuppalanchi[2], Samala Niharika[2], Romil Saxena[2]
[1]Indianapolis, IN, [2]Indiana University School of Medicine, Indianapolis, IN

Disclosures: Mohamed Mustafa: None; Wassim Abdallah: None; Nathan Shelman: None; Samala Niharika: None; Romil Saxena: None

Background: Existing series describe an abundance of portal plasma cells (PCs) in hepatitis A (HAV) with significant "spill over" into the limiting plate, features that overlap with autoimmune hepatitis (AIH). Liver biopsies for HAV are performed if disease course is unusual, there is chronic liver disease or competing etiology. We describe 15 such cases.

Design: A clinical database was used to identify HAV patients with a liver biopsy, and obtain clinical and laboratory data. Biopsies were reviewed for severity of portal, interface and lobular inflammation (mild, moderate, severe respectively). The percentage of PCs in portal tracts was graded as 1 (<10%), 2 (10-50%), or 3 (>50%). An overall diagnosis was rendered with an aim to identify features of HAV and distinguish it from AIH.

Results: There were 15 patients: 10 males, 5 females; 22-69 years old (median, 56), 3 patients, <45 years of age; Caucasian, 14; Asian 1. All patients were positive for anti-HAV IgM. Known risk factors were active intravenous drug use, 4; food borne transmission, 2; contact with known HAV, 3 and travel to endemic area,1. Biopsies were performed for persistently abnormal liver tests (LTs), 3; rebound in LTs after initial improvement, 2; very severe disease, 1 (known AIH); fulminant liver failure, 2 (one each with hepatitis B (HBV) and hepatitis C (HCV)); positive serum anti-smooth muscle antigen (ASMA), 2; chronic liver disease, 3 (NASH,2; AIH,1); positive anti-mitochondrial antibody (AMA),1; abnormal LTs, 1. Underlying diseases were fatty disease, 2; AIH, 2; HBV, 1 and HCV,1. Serum anti-nuclear antibody (ANA) was positive in 1 (performed in 9), ASMA in 11 (performed in 13) and AMA in 1 (performed in 9) patients, respectively. Eight biopsies showed severe, 2 biopsies, moderate and 1, mild hepatitis, respectively. Submassive necrosis was seen in 1 (patient with HBV), zone 3 necrosis in 1 (patient with positive ANA) and steatohepatitis in 1 biopsy respectively. PCs comprised 10-50% of portal inflammatory infiltrate in 8, and <10% in 7 cases. Small clusters of PCs were present in lobules in most cases.

Conclusions: 1) Many HAV patients have serum ASMA, raising suspicion for AIH. Biopsy diagnosis is required to initiate steroid therapy. 2) Most cases show severe hepatitis with many portal PCs and marked "spill over". In portal tracts, PCs are not the predominant component. Small cluters of PCs are often seen in lobules. 3) Significance of autoantibodies in HAV and criteria to distinguish it from AIH need refinement.

1636 Prevalence of Histological Features of Fibrosis Regression in Patients with Resected Hepatocellular Carcinoma

Christine Orr[1], Lina Chen[2], Tao Wang[1]
[1]Queen's University/Kingston Health Sciences Centre, Kingston, ON, [2]Queen's University, Kingston, ON

Disclosures: Christine Orr: None; Lina Chen: None; Tao Wang: None

Background: Hepatocellular carcinoma (HCC) is the most common primary liver cancer. Liver cirrhosis, the end-stage of chronic liver disease, is a major risk factor for the development of HCC. Cirrhosis is partially reversible through repair and can regress, which can lead to downstaging of fibrosis. However, the risk for HCC remains elevated in patients with partial regression of advanced fibrosis. To our knowledge, no study has investigated the prevalence of histological features of fibrosis regression in patients with resected HCC.

Design: We retrospectively identified 39 HCC resection cases from 36 patients performed at our institution from 2003-2018 and collected clinical-pathologic information from the patient records. Slides were reviewed blinded to the clinical information. The non-neoplastic liver parenchyma was evaluated by Masson trichrome for features of background liver disease and features of regression as exemplified by the hepatic repair complex (HRC). Specifically these features include perforated delicate septa, isolated thick collagen fibers, delicate periportal fibrous spikes, hepatic vein remnants with prolapsed hepatocytes, hepatocytes within portal tracts or split septa, minute regenerative nodules, and aberrant hepatic veins.

Results: Of the 39 HCC resections, 18 had a prior history of liver disease (4 HBV, 11 HCV, 3 alcoholic liver disease). Ages ranged from 35 to 84 with a predominantly male population (31 males vs 8 females). 32 cases showed at least two features of HRC. The most frequent HRC features identified were perforated delicate septa and hepatocytes within portal tracts or split septa, both of which were seen in 100% of cirrhotic livers (table 1). Of the 7 cases with no features of HRC all had no prior history of liver disease and 5 cases did not exhibit any fibrosis. 11 cases showed 7-8/8 features of HRC; 8 of these cases had prior known liver disease, and 8 cases were not cirrhotic (fibrosis stage 1-3).

Table 1. Laennec Fibrosis Stage and Presence of HRC Features										
Laennec Fibrosis Stage	N	Perforated Delicate Septa	Isolated Thick Collagen Fibers	Delicate Periportal Fibrous Spikes	Hepatic Vein Remnants with Prolapsed Hepatocytes	Hepatocytes within Portal Tracts or Split Septa	Minute Regenerative Nodules	Aberrant Parenchymal Veins	Portal Tract Remnants	Avg # of HRC
0	5	0 (0%)	0 (0%)	0 (0%)	0 (0%)	0 (0%)	0 (0%)	0 (0%)	0 (0%)	0
1	11	5 (45%)	7 (64%)	7 (64%)	4 (36%)	8 (73%)	1 (9%)	7 (64%)	8 (73%)	4.3
2	2	2 (100%)	2 (100%)	2 (100%)	2 (100%)	2 (100%)	1 (50%)	2 (100%)	2 (100%)	7.5
3	11	11 (100%)	6 (55%)	9 (82%)	2 (18%)	11 (100%)	5 (45%)	9 (82%)	8 (73%)	5.5
4a	3	3 (100%)	1 (33%)	2 (67%)	2 (67%)	3 (100%)	1 (33%)	1 (33%)	2 (67%)	5
4b	3	3 (100%)	1 (33%)	2 (67%)	0 (0%)	3 (100%)	3 (100%)	2 (67%)	3 (100%)	5.7
4c	4	4 (100%)	2 (50%)	2 (50%)	0 (0%)	4 (100%)	3 (75%)	4 (100%)	3 (75%)	5.5
Total:		28 (72%)	18 (46%)	24 (62%)	10 (26%)	31 (79%)	14 (36%)	25 (64%)	26 (67%)	

Conclusions: 32 of 39 HCC resections at our institution showed features of hepatic repair complex. Cases with a prior history of liver disease were more likely to show HRC regardless of fibrotic stage. These findings support that fibrosis repair and regression is a common and ongoing phenomenon in liver disease. It also suggests that some cases of HCC in "non-cirrhotic" livers may in fact represent cases of regressed cirrhosis.

1637 SF-1 Expression in Hepatocellular Carcinoma (HCC): A Potential Diagnostic Pitfall

Daniel Owen[1], Rifat Mannan[2], Jordan Reynolds[1], Daniel Roberts[1], Lisa Yerian[1], Daniela Allende[3]
[1]Cleveland Clinic, Cleveland, OH, [2]Perelman School of Medicine at the University of Pennsylvania, Philadelphia, PA, [3]Cleveland Clinic, Lerner College of Medicine of Case Western University School of Medicine, Avon Lake, OH

Disclosures: Daniel Owen: None; Rifat Mannan: None; Jordan Reynolds: None; Daniel Roberts: None; Lisa Yerian: None; Daniela Allende: None

Background: The differential diagnosis of HCC includes primary adrenocortical neoplasms. Significant morphologic overlap exists between these two neoplasms, including focal reticulin loss, leading to possible diagnostic error. SF-1, a steroid receptor protein involved in normal adrenal development and steroidogenesis, is often used to support a diagnosis of adrenocortical neoplasms in this differential.

Published literature on this topic is limited, with only 18 reported cases of HCC that were all negative for SF-1 by immunohistochemistry (IHC). The study aim is to analyze the expression of SF-1 in HCC arising in cirrhotic and non-cirrhotic liver.

Design: IRB approval was obtained. 90 HCC cases were identified from retrospective review of pathology databases (2004-2019) at our institution. Whole tissue sections from formalin fixed paraffin embedded blocks were used from HCCs arising in non-cirrhotic liver (45 cases) and matched HCCs arising in cirrhotic liver (45 cases) according to age, gender, AJCC tumor stage and grade. Cases of fibrolamellar HCC were excluded. A tissue microarray containing 66 cases of adrenocortical neoplasia (22 adenomas and 44 carcinomas) was also studied for comparison. All cases and controls were evaluated with SF-1 (R&D Systems, N1665, 1:100), arginase-1 (Ventana, SP156, predilute) and glypican-3(Cell Marque, 1G12, predilute). Hepatocyte (Dako, OCH1E5. 1:200), CD10 (Cell Marque, 56C6, predilute), Melan A (Biogenix, A103, 1:40) and inhibin (AbDSerotec, R1, 1:50) was also performed on a selected case.

Results: The study population characteristics and IHC results are listed in Table 1. Of the 90 HHCs in the study population, single HCC in non-cirrhotic liver was positive for SF1 (1/90, ~1%) (Figures 1 and 2) and glypican 3. In this case CD10 showed a canalicular staining pattern and hepatocyte, Melan A and inhibin were negative. As expected, arginase-1 was positive in nearly all HCC cases (94%) and glypican-3 was variably expressed in 63% of HCC cases. Of the adrenocortical neoplasms, 72% were positive for SF-1 (48/66), and none were positive for arginase-1 or glypican-3.

Table 1. Clinicopathologic and immunohistochemical profiles of HCC and adrenal neoplasms.

	Hepatocellular Carcinoma										Adrenal Neoplasm	
	Tumor Differentiation			Tumor Stage				Background Cirrhosis		All	ACA	ACC
	well	moderately	poorly	1	2	3	4	No	Yes			
Numer of Cases	17	64	9	35	45	5	5	45	45	90	22	44
Average Age	61	69	66	68	63	75	75	67	63	65		
Percent Male	76%	63%	67%	66%	67%	80%	40%	69%	62%	66%		
Percent Female	24%	38%	33%	34%	33%	20%	60%	31%	38%	34%		
SF-1 Positive	0	0	1 (11)	0	0	0	1 (20)	1 (2)	0	1 (1)	22 (100)	26 (59)
Arginase 1 Positive	17 (100)	60 (94)	8 (89)	34 (97)	43 (96)	4 (80)	4 (80)	42 (93)	43 (96)	85 (94)	0	0
Glypican 3 Positive	8 (47)	40 (63)	9 (100)	19 (54)	34 (76)	0	4 (80)	22 (49)	35 (78)	57 (63)	0	0

ACA: adrenocortical adenoma; ACC: adrenocortical carcinoma. Figures in parentheses indicate percentage per number of cases.

Figure 1 - 1637
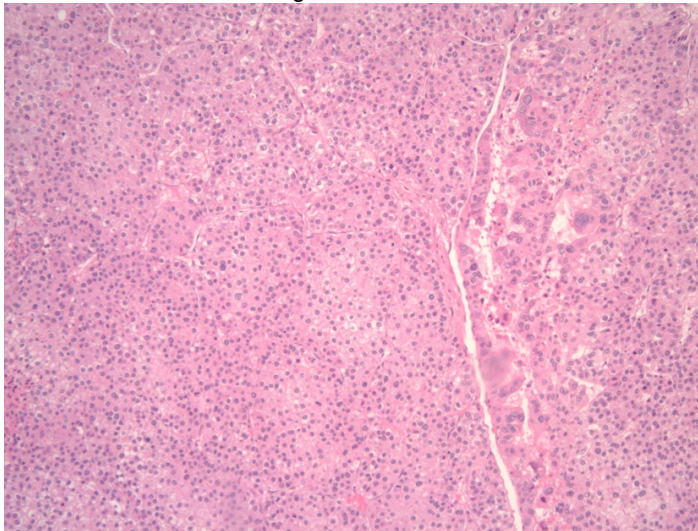
Figure 2 - 1637
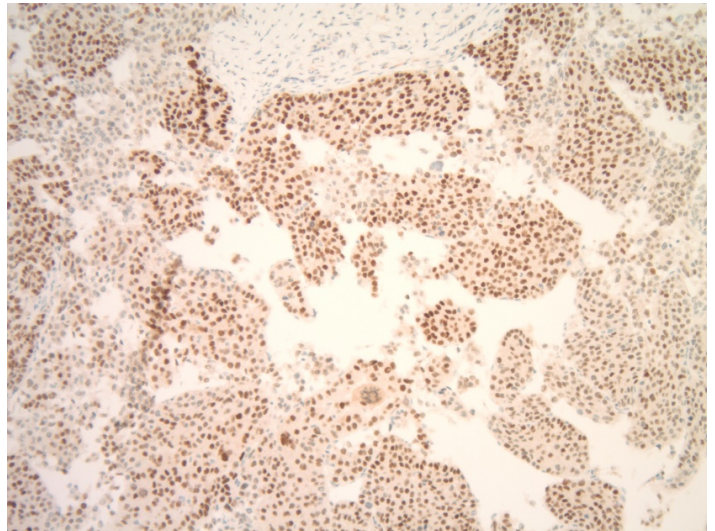
**Conclusions:** The distinction between HCC and adrenocortical neoplasia can be challenging. SF-1 positivity is a rare finding in HCC but remains a potential diagnostic pitfall. In such cases, an IHC panel approach that includes expression of primary hepatocellular markers (arginase1, glypican3), CD10 and lack of adrenocortical markers (Melan A and inhibin) are helpful in accurately classifying the tumor as HCC.

1638 HNF-1β Immunohistochemistry is More Sensitive and Specific than CRP in the Diagnosis of Cholangiocarcinoma

Pallavi Patil[1], Romulo Celli[2], Dhanpat Jain[1], Xuchen Zhang[3]
[1]Yale University School of Medicine, New Haven, CT, [2]Guilford, CT, [3]Yale University School of Medicine, Orange, CT

Disclosures: Pallavi Patil: None; Romulo Celli: None; Dhanpat Jain: None; Xuchen Zhang: None

Background: Intrahepatic cholangiocarcinoma (iCCA) is often a diagnosis of exclusion on liver biopsies as there is no specific immunohistochemical (IHC) marker that can aid its diagnosis. C-reactive protein (CRP) IHC has been recently suggested as helpful for the diagnosis of iCCA. Hepatocyte nuclear factor (HNF)-1β- is a transcription factor that plays a critical role in liver development and differentiation, is expressed in the pancreatico-biliary ductal system and kidney tubules. The aim of this study was to evaluate the diagnostic value of HNF-1β and CRP IHC in the diagnosis of iCCA.

Design: Cases of iCCA (biopsy and resections) and combined hepatocellular-cholangiocarcinoma (cHCC-CCA) (resections) were identified from our pathology archives. The diagnosis of all cases was confirmed with slide review and clinical follow-up. CRP and HNF-1β IHCs were reviewed and scored as positive when expressed in >=5% cells, cytoplasmic for CRP and nuclear for HNF-1β. IHC expression was scored for intensity (mild to strong) and percentage of positive cells, >=5 to 25% score 1, >=25 to 50% score 2, >=50% score 3. Statistical analysis was performed using a 2x2 table and Chi square test.

Results: Cases of iCCA (n=56) and cHCC-CCA (n=9) were identified and included in the study. HNF-1β was expressed in 56 (100%) of iCCAs compared to CRP in 39 of 54 (72%) cases (Figure 1). (Table 1). The expression of HNF-1β was diffuse (score 3) and strong compared to CRP (p=0.0001) in iCCA cases. In cases of cHCC-CCA, CRP was expressed in 8 of 9 (89%) and HNF-1β was expressed in 100% cases in the cholangiocarcinoma (CCA) component (Figure 2). The hepatocellular carcinoma (HCC) component of cHCC-CCA was present for evaluation in 5 of 9 cases, where CRP was expressed in all and HNF-1β in none.

| Cohort (n)	IHC score	CRP n(%)	HNF-1 Beta n(%)	p value
iCCA (56)	0 (negative)	15 (27)	0 (0)	
	1+	3 (5)	1 (2)	
	2+	5 (9)	4 (7)	
	3+	31 (57)	50 (91)	0.0001
	Total positive	39 of 54 (72)	55 of 55 (100)	0.0001
CCA in-cHCC-CCA (9)	0 (negative)	1 (11)	0 (0)	
	1+	0 (0)	2 (20)	
	2+	5 (56)	3 (30)	
	3+	3 (33)	4 (40)	1.0000
	Total positive	8 (89)	9 (100)	1.0000
HCC in cHCC-CCA (5)	0 (negative)	0 (0)	5 (100)	
	1+	0 (0)	0 (0)	
	2+	0 (0)	0 (0)	
	3+	5 (100)	0 (0)	0.0079
	Total positive	5 (100)	0 (0)	0.0079
Total CC (65)	0 (negative)	16 (25)	0 (0)	
	1+	3 (5)	3 (5)	
	2+	10 (16)	7 (11)	
	3+	34 (54)	54 (84)	0.0002
	Total positive	47 of 63 (75)	64 of 64 (100)	0.0001

Figure 1 - 1638
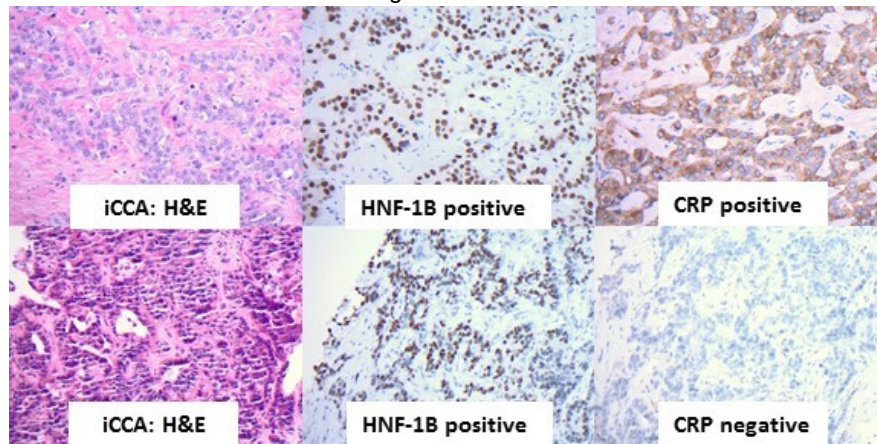
Figure 2 - 1638
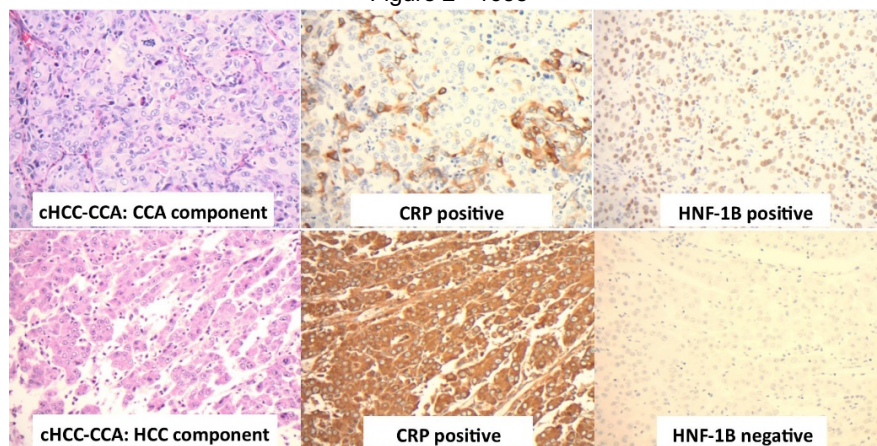
Conclusions: Our study shows that HNF-1β is a sensitive and specific marker of iCCA and cholangiocarcinoma component of cHCC-CCA compared to CRP. HNF-1β IHC can be used in clinical practice for identifying cholangiolar differentiation in adenocarcinomas or cases suspected to be cHCC-CCA.

1639 Multi-Institutional Study of Clinicopathological Features of Hepatocellular Adenomas in the United States

Pallavi Patil[1], Hongjie Li[1], Sanjay Kakar[2], Tsung-Teh Wu[3], Matthew Yeh[4], Michael Torbenson[5], Xuchen Zhang[6], Dhanpat Jain[1]
[1]Yale University School of Medicine, New Haven, CT, [2]University of California San Francisco, San Francisco, CA, [3]Mayo Clinic, Rochester, MN, [4]University of Washington Medical Center, Seattle, WA, [5]Mayo Clinic Rochester, Rochester, MN, [6]Yale University School of Medicine, Orange, CT

Disclosures: Pallavi Patil: None; Hongjie Li: None; Sanjay Kakar: None; Tsung-Teh Wu: None; Matthew Yeh: None; Michael Torbenson: None; Xuchen Zhang: None; Dhanpat Jain: None

Background: HCAs are subtyped as inflammatory HCA (I-HCA), beta-catenin activated HCA (B-HCA), HNF-1 alpha inactivated HCA (H-HCA), unclassified HCA (U-HCA), mixed (I-HCA + B-HCA, and H-HCA + B-HCA). There are limited large series of HCAs from the United States. The goal of the study was to compile a large multi-institutional HCA database and describe the clinicopathologic features and subtype distribution of HCA from United States.

Design: HCAs (resections) from participating institutions were reviewed for patient demographics, size and number of lesions, HCA subtype, molecular data, predisposing liver disease, status of background liver and associated HCC. HCAs were subtyped based on accepted criteria as I-HCA, B-HCA, H-HCA, and U-HCA. Cases with incomplete information regarding HCA sub-type were excluded. Any hepatocellular carcinoma (HCC) arising in HCA were recorded. Cases that could not be reliably classified as HCC or HCA were called hepatocellular neoplasms of uncertain malignant potential (HUMP).

Results: A total of 175 cases of HCAs were included in the study. There were 91% female patients and 9% male patients. Median age was 35 years (range 5-74). Median size was 7 cm (range 0.1-17.5). Percentage of HCAs by subtype was I-HCA 40%, B-HCA 6%, H-HCA 22%, U-HCA 26%, mixed I-HCA + B-HCA 5%, mixed H-HCA + B-HCA 1%. Cases with HUMP comprised 2% of reviewed cases and were excluded from the HCA subtype percentages. HCC was found in 8% cases arising from B-HCA 14%, H-HCA 29%, U-HCA 36%, and mixed I-HCA + B-HCA 21%. Multiple adenomas (>2) were identified in 46% of patients. Description of background liver when available showed steatosis in 88% cases and non-necrotizing granulomas in 12% cases.

	French Study %	United States %
Lesions		
Solitary	55	54
Multiple	45	46
Gender		
Male	15	9
Female	85	91
Size cm		
Median (range)	5.5 (0.5-29)	7 (0.1-17.5)
Age years		
Median (range)	38 (7-82)	35 (5-74)
HCA Subtypes total		
I-HCA	34	40
B-HCA	10	6
H-HCA	34	22
U-HCA	34	26
I-HCA + B-HCA	7	5
H-HCA + B-HCA	N/A	1
HUMP	7	2
HCC	3	8

Conclusions: This is a large study from United States describing the clinicopathological features of HCAs and the subtype distribution of HCAs. The relative proportion of H-HCA and U-HCA was lower in our study compared to the French study, while distribution of other subtypes was similar.

1640   Hyaline Globules in Kupffer Cells are more Prominent and Easily Identifiable in Cases of Autoimmune Hepatitis-Induced Cirrhosis versus Cirrhosis of Other Causes
Bruce Rottmann[1], Dhanpat Jain[2], Xuchen Zhang[3], Ananta Gurung[4], Romulo Celli[5]
[1]Yale New Haven Hospital, New Haven, CT, [2]Yale University School of Medicine, New Haven, CT, [3]Yale University School of Medicine, Orange, CT, [4]Royal Columbian Hospital, New Westminster, BC, [5]Guilford, CT

Background: Hyaline globules in Kupffer cells (HG) are often seen in liver biopsies of patients with autoimmune hepatitis (AIH), particularly pediatric patients. Our group identified an association between HG and histologic cirrhosis in the setting of AIH. The purpose of this study is to test the specificity of HG as a histologic marker of AIH versus cirrhosis of other etiology.

Design: Biopsies from patients with AIH-induced cirrhosis (Group 1) were identified from our local AIH database. Sequential biopsies from patients with cirrhosis from all other causes (Group 2) were identified from the last 6 months. Cases in Group 2 included the following etiologies: NASH, HCV, alcohol, and cryptogenic. DPAS stained slides were reviewed for the presence or absence of HG and graded (0 = no HG, 1 = small HG, 2 = large HG (apparent at 10-20x, at least 1/5 the area of cytoplasm)). H&E stained slides were reviewed to grade inflammatory activity using the Metavir score. All biopsies were divided into Metavir score 1 (mild) or 2 (moderate). All cases were reviewed by two pathologists independently in a blinded manner. Consensus was reached on all discrepant cases.

Results: A total of 24 Group 1 biopsies and 24 Group 2 biopsies were reviewed. There were significantly more females in Group 1 compared to Group 2 (92% vs. 29%, $p < 0.05$), but there was no difference in mean age (53 vs. 55 years, $p = 0.38$). There was no significant difference in the rate of HG between Groups 1 and 2; however, a trend of higher rate of HG in AIH was noted (71% vs. 42%, $p = 0.08$). Large HG (grade 2) were more common in Group 1 than Group 2 (78% vs. 13%, $p < 0.05$). No significant difference was observed in Metavir inflammation score between Groups 1 and 2 (67% vs. 50%, $p = 0.38$). No significant difference was observed in the rate of HG based on Metavir score; however, there was a trend towards more HG in moderate inflammation (68% vs. 40%, $p = 0.08$). Grade 2 HG were more common in cases of moderate inflammation (78% vs. 13%, $p < 0.05$).

Conclusions: HG were observed both in patients with cirrhosis from AIH and from other causes. However, HG were more prominent, larger, and tended to be more frequent in patients with cirrhosis from AIH. Further studies using objective measuring tools such as digital image analysis may be useful in screening biopsies for HG, which may provide diagnostic assistance in cases of cryptogenic cirrhosis.

1641 Interobserver Variability and Accuracy in the Diagnosis of Focal Nodular Hyperplasia and Effect of Glutamine Synthetase Immunohistochemistry

Daniel Rowan[1], Daniela Allende[2], Andrew Bellizzi[3], Ryan Gill[4], Xiuli Liu[5], Catriona McKenzie[6], Roger Moreira[1], Taofic Mounajjed[1], Samar Said[1], Maria Westerhoff[7], Sarah Jenkins[1], Kenneth Batts[8], Lawrence Burgart[9], Laura Lamps[7], Rondell Graham[1]
[1]Mayo Clinic, Rochester, MN, [2]Cleveland Clinic, Lerner College of Medicine of Case Western University School of Medicine, Avon Lake, OH, [3]University of Iowa Hospitals and Clinics, Iowa City, IA, [4]University of California San Francisco, San Francisco, CA, [5]University of Florida, Gainesville, FL, [6]Royal Prince Alfred Hospital, Camperdown, NSW, Australia, [7]University of Michigan, Ann Arbor, MI, [8]Allina Health Laboratories, Plymouth, MN, [9]Abbott Northwestern Hospital, Saint Paul, MN

Disclosures: Daniel Rowan: None; Daniela Allende: None; Andrew Bellizzi: None; Ryan Gill: None; Xiuli Liu: None; Catriona McKenzie: None; Roger Moreira: None; Taofic Mounajjed: None; Samar Said: None; Maria Westerhoff: None; Sarah Jenkins: None; Kenneth Batts: None; Lawrence Burgart: None; Laura Lamps: None; Rondell Graham: None

Background: Diagnosis (dx) of focal nodular hyperplasia (FNH) on needle biopsy (bx) allows for non-operative management. Glutamine synthetase (GS) is useful in this setting, but the accuracy and reproducibility of bx interpretation has not been specifically studied. By use of virtual biopsy (vbx)-resection pairs, we aimed to assess accuracy and reproducibility of FNH dx and the effect of GS interpretation on dx.

Design: The study included resections of FNH (n=30) and controls: non-lesional liver (n=15), hepatocellular adenoma (HCA) (n=15), and HCC (n=15). GS was performed on all cases. One H&E slide and the corresponding GS slide from each case were scanned and two virtual 18G needle biopsies were randomly taken using software. 7 GI pathologists reviewed and interpreted the vbx in 2 separate rounds with a 7 day washout (round 1 - H&E only; round 2 - H&E and GS stain). 5 reviewers interpreted the H&E vbx again after 10 days (round 3). 3 separate experienced GI pathologists confirmed the "true" dx and adequacy of the vbx.

Results: The diagnostic accuracy was 65.7% in round 1 and 80.4% in round 2 (p=0.04). Interobserver agreement significantly increased from round 1 to round 2 (κ= 0.45, 95% CI: 0.39, 0.51; κ= 0.72, 95% CI: 0.65, 0.79, respectively). Intraobserver agreement was 74.7% (κ= 0.71). Accuracy of FNH dx increased from 71% to 89% with addition of GS (Table 1). Correctly diagnosed FNH cases had ductular reaction, nodularity, abnormal vessels, and central scar in 89%, 89%, 82%, and 69% of cases, respectively. In cases of FNH missed by reviewers, abnormal vessels and central scar were less frequent (32% and 30% of cases). Reviewers unanimously agreed on map-like interpretation of GS in 80% of true FNH cases. In 7% of cases, at least 50% of reviewers interpreted GS staining as not map-like. In these cases, only 64% of reviewers made the correct dx. 10 cases were correctly diagnosed as FNH on H&E alone and then incorrectly diagnosed with GS available because they lacked map-like staining.

TABLE 1

	True Diagnosis			
	Focal nodular hyperplasia (N=210)	**Hepatocellular adenoma (N=105)**	**Hepatocellular carcinoma (N=105)**	**Normal liver (N=105)**
Round 1 Diagnosis				
Focal nodular hyperplasia	150 (71.4%)	3 (2.9%)	4 (3.8%)	0 (0.0%)
Hepatocellular adenoma	5 (2.4%)	64 (61.0%)	19 (18.1%)	0 (0.0%)
Well-differentiated HCC	0 (0.0%)	4 (3.8%)	49 (46.7%)	0 (0.0%)
Descriptive	52 (24.8%)	25 (23.8%)	33 (31.4%)	23 (21.9%)
Normal liver	3 (1.4%)	9 (8.6%)	0 (0.0%)	82 (78.1%)
Round 2 Diagnosis				
Focal nodular hyperplasia	186 (88.6%)	2 (1.9%)	0 (0.0%)	0 (0.0%)
Hepatocellular adenoma	4 (1.9%)	83 (79.0%)	28 (26.7%)	0 (0.0%)
Well-differentiated HCC	0 (0.0%)	3 (2.9%)	49 (46.7%)	0 (0.0%)
Descriptive	20 (9.5%)	12 (11.4%)	28 (26.7%)	1 (1.0%)
Normal liver	0 (0.0%)	5 (4.8%)	0 (0.0%)	104 (99.0%)

Conclusions: Our study shows moderate inter- and intraobserver agreement on vbx interpretation on H&E. The identification of 3 or more features correlated with accurate dx. Agreement and accuracy of FNH dx significantly improved with GS, but lack of map-like staining in

some cases led to misdiagnosis. Our data indicate that correct FNH dx on vbx, and likely actual bx, depends on a combination of H&E features and GS staining.

1642 The Significance of Extramedullary Hematopoiesis in Liver Biopsies

Shahram Saberi[1], Douglas Tremblay[1], John Mascarenhas[1], Thomas Schiano[2], Maria Isabel Fiel[1]
[1]Icahn School of Medicine at Mount Sinai, New York, NY, [2]Mount Sinai Medical Center, New York, NY

Background: Production of blood cell elements outside the bone marrow, extramedullary hematopoiesis (EMH), is a known compensatory response to ineffective or inadequate bone marrow function seen in various chronic hematologic disorders. The most common sites involved by EMH are liver, spleen, and lymph nodes. However, EMH is also found on liver biopsies with non-hematologic disorders.

Aim: We sought to better characterize the presence of EMH that was incidentally found in liver biopsies.

Design: A search of the pathology database covering the period 01/2010-06/2019 was performed to identify liver specimens from adult patients having EMH. EMH was defined as presence of megakaryocytes, nucleated RBCs and myelocyte precursors. Thirty-three cases were identified. All liver biopsy slides were retrieved and/or archival paraffin blocks were sectioned for recuts. Review of the slides to evaluate the background liver disease was performed. Extent of EMH was scored as follows: 1 = 2 or less EMH foci in 10 high power fields (HPF) and score 2 = >2 EMH foci in 10 HPF. Clinical information was gathered from chart review.

Results: There were 12 patients (6 M, 6 F) found to have a hematologic disorder (group 1) while there were 21 patients (7F, 14M) with various other liver diseases (group 2). Demographic data and EMH scores were compared using t-test between the two groups. Score 2 was found in 11 out of 12 in group 1 while only 3 of 21 was found in group 2 (p = 0.0078). No significant difference in age and gender was noted. Table 1 is a summary of the data.

ID	Gender	Age	Background disorder	EMH Score
1	Female	30	Hematologic (Sickle cell anemia)	2
2	Male	27	Hematologic (HIV with decreased CD4)	2
3	Female	53	Hematologic (Hemophagocytic lymphohistiocytosis)	2
4	Female	47	Hematologic (B cell lymphoma)	2
5	Female	68	Hematologic (Myelofibrosis)	2
6	Female	70	Hematologic (Polycythemia vera)	2
7	Male	62	Hematologic (T cell large granular lymphoma)	2
8	Male	50	Hematologic (Protein C deficiency and chronic blood loss)	2
9	Male	18	Hematologic (T cell lymphoblastic lymphoma)	2
10	Female	33	Hematologic (ITP, CVID and atypical lymphoid hyperplasia)	2
11	Male	72	Hematologic (MDS)	1
12	Male	46	Hematologic (HIV with decreased in CD4)	2
13	Male	50	Non-Hematologic (Parenteral Nutrition-related liver injury)	1
14	Male	20	Non-Hematologic (Unknown hepatic necrosis)	1
15	Male	57	Non-hematologic (Chronic venous outflow obstruction)	1
16	Male	51	Non-hematologic (OPV with features of NRH)	1
17	Female	60	Non-hematologic (Primary sclerosing cholangitis)	1
18	Male	49	Non-hematologic (Nonspecific reactive hepatitis)	1
19	Male	67	Non-hematologic (NRH)	2
20	Male	26	Non-hematologic (Acute alcoholic hepatitis)	1
21	Female	71	Non-hematologic (Acute cellular rejection, post-transplant)	1
22	Female	46	Non-hematologic (Hepatocellular adenoma)	2
23	Female	65	Non-hematologic (Hepatocellular adenoma and carcinoma)	1
24	Female	34	Non-hematologic (Drug induced liver injury)	1
25	Male	66	Non-hematologic (Chronic hepatitis C)	1
26	Male	23	Non-hematologic (Nonspecific reactive hepatitis)	1
27	Female	73	Non-hematologic (Chronic venous outflow obstruction)	1
28	Male	43	Non-hematologic (Nonspecific liver changes)	1
29	Male	46	Non-hematologic (Primary sclerosing cholangitis)	1
30	Male	50	Non-hematologic (Chronic venous outflow obstruction)	1
31	Male	29	Non-hematologic (Acute cholestatic hepatitis)	2
32	Female	27	Non-hematologic (Drug induced liver injury)	1
33	Male	23	Non-hematologic (Acute cellular rejection, post-transplant)	1

Conclusions: This is the first study proposing a scoring system for evaluating EMH in liver biopsies. Although EMH is more frequently found in patients with known hematologic disorders it can be seen in patients with non-hematologic disorders. Lesser degrees of EMH may not need to trigger a work-up for a hematologic disorder.

1643 Multispectral Imaging Reveals that Patients with Non-Alcoholic Steatohepatitis (NASH) Harbor Distinctive Intrahepatic Macrophage Phenotypes Depending on Amount of Fibrosis

Omar A. Saldarriaga[1], Jingjing Jiao[2], Laura Beretta[2], Ben Freiberg[3], Santhoshi Krishnan[4], Arvind Rao[5], Adam Booth[1], Heather Stevenson-Lerner[1]
[1]University of Texas Medical Branch, Galveston, TX, [2]The University of Texas MD Anderson Cancer Center, Houston, TX, [3]Visiopharm A/S, Broomfield, CO, DK, [4]Rice University, Houston, TX, [5]University of Michigan, Ann Arbor, MI

Disclosures: Omar A. Saldarriaga: None; Jingjing Jiao: None; Laura Beretta: None; Adam Booth: None

Background: The incidence of non-alcoholic steatohepatitis (NASH) is increasing in the US and approximately 15% of patients will develop fibrosis. Macrophages (macs) from different origins, including resident Kupffer cells (KCs) and monocyte-derived macs distinctly influence the hepatic microenvironment and the development of fibrosis. We hypothesized that the heterogeneity of liver macs determines the variability in the fibrosis progression in patients with NASH.

Design: We used multiplex immunofluorescence and spectral imaging microscopy to evaluate macs from different origins and activation; including, KCs (CD68+), monocyte-derived (Mac387+), pro-fibrogenic (CD163+) macs and their co-expression of pro- (CD14) and anti- (CD16) inflammatory markers. These markers were analyzed in human liver biopsies collected from patients with NASH and either minimal (n=6; stage:0-1) or advanced (n=5; stage:3.5-4/4) fibrosis. NanoString technology was used to evaluate selective gene expression patterns of macs in the same biopsy. The median age was 50 and 57 for the minimal and advanced fibrosis groups, respectively. We used advanced imaging software (Visiopharm) to visualize differences between the two patient groups by comparison of t-distributed stochastic neighbor embedding plots (t-SNE) and phenotype matrices.

Results: Our results suggest that patients have variable macs phenotypes in their liver depending on their propensity to develop hepatic fibrosis. Patients with minimal fibrosis showed a more protective gene expression profiles with increased CD14+ macs. Patients with advanced fibrosis had significantly increased numbers of pathogenic pro-inflammatory and pro-fibrotic macs phenotypes (e.g., Mac387+, CD68+/CD14+/CD163+/Mac387+, CD16+/CD163+/Mac387+, CD163+/Mac387+, CD68+/CD16+/CD163+) and increased expression of genes associated with mixed macs activation (e.g., IL1β, TNFα, PTGS2, CLEC7A, IRF4, PIK3CG, IL4R,IL10R, TGFβ). However, when we analyzed each patient's liver biopsy on an individual basis, subtle variations were observed between the patients in each group. Thus, the phenotype of macs in patients with NASH is complex and is only partially associated with fibrosis stage.

Conclusions: Multispectral imaging analysis is a useful tool to characterize liver macs and to identify pathologic populations in patients with advanced fibrosis when compared to those with minimal fibrosis. However, a more personalized analysis may be necessary in order to accurately predict the risk of developing hepatic fibrosis.

1644 Strong Positive Sonic Hedgehog Immunohistochemistry is Associated with an Increased Requirement of Liver Transplantation in Patients with Alpha-1 Antitrypsin Deficiency

Michael Schild[1], Lani Clinton[2], William Jeck[3], Cynthia Guy[4], Anna Diehl[5], Diana Cardona[1]
[1]Duke University Medical Center, Durham, NC, [2]Duke University Medical Center, Mebane, NC, [3]Boston, MA, [4]Duke University, Chapel Hill, NC, [5]Duke University, Durham, NC

Disclosures: Michael Schild: None; Lani Clinton: None; William Jeck: None; Cynthia Guy: None; Anna Diehl: None; Diana Cardona: None

Background: It is difficult to accurately predict the progression of liver disease in patients with alpha-1 antitrypsin deficiency (A1AT). We have previously shown that hepatocellular expression of Sonic Hedgehog (SHh) is upregulated in various forms of liver injury, including A1AT. In nonalcoholic steatohepatitis, an increased number of positive hepatocytes with SHh immunohistochemistry (IHC) is indicative of severe cellular stress and is associated with multiple negative prognostic factors including fibrosis stage, ballooning severity, and increased inflammation. We hypothesize that positive SHh expression by IHC may be predictive of a worse liver outcome in patients with A1AT.

Design: Following IRB approval, electronic medical records were searched for liver specimens from patients diagnosed with A1AT. For patients with sequential liver specimens, clinical data and hematoxylin and eosin, Masson trichrome, periodic acid-schiff-diastase stained sections were retrospectively reviewed. IHC for SHh was applied and evaluated for the presence of strong positive hepatocellular immunoreactivity.

Results: Nine patients with two specimens each were evaluated. The mean time between specimens was 1,447 days (Range 36 – 5,387 days). The average follow up was 2,814 days (Range 36-6,335 days). Four patients required liver transplantation, and 5 did not. No significant co-existent disease was present in the transplant group. On the first biopsy of patients who required transplantation, four of four

(100%) showed hepatocytes with strong positive immunoreactivity. For the first biopsy of patients who did not require transplantation, only 2 of 5 (40%) showed hepatocytes with strong positive immunoreactivity, and 3 of 5 (60%) were negative (see table). All patients with a negative first biopsy did not require liver transplantation.

Patient	Phenotype	Time between Biopsy (days)	First Biopsy Hh strong positive hepatocytes	Second Biopsy Hh strong positive hepatocytes	Transplant required?	Time to last follow-up (days)
1	MZ	3256	None	Few	N	3774
2	ZZ	5387	Few	None	N	5397
3	Unknown	36	None	Few	N	36
4	MZ	875	None	None	N	1855
5	Unknown	1207	Many	Many	N	1252
6	Unknown	362	Many	Many	Y	3111
7	MZ	810	Few	Few	Y	1460
8	MZ	909	Few	Many	Y	6335
9	MZ	181	Few	Few	Y	2102

Conclusions: While this is a small study, all patients with a first biopsy negative for strong positive hepatocytes with SHh IHC did not require liver transplantation, whereas 67% of patients with strong positive hepatocytes did require transplantation. Our findings suggest that strong positive hepatocellular expression of SHh may be predictive of negative liver outcomes in patients with A1AT. Further investigations with additional patients, including more SZ and ZZ phenotypes, are required to determine if SHh IHC can be used as a predictive factor in A1AT associated liver disease.

1645 Automated Screening of Medical Records for Drug-Induced Liver Injury

Gregory Scott[1], Anne Chen[2], Anna Park[2], John Higgins[3], Brock Martin[4]
[1]Redwood City, CA, [2]Stanford University, Stanford, CA, [3]Stanford University Hospital, Stanford, CA, [4]Stanford University School of Medicine, Stanford, CA

Disclosures: Gregory Scott: None; Anne Chen: None; Anna Park: None; John Higgins: None; John Higgins: None; Brock Martin: None

Background: Drug-induced liver injury (DILI) is a common cause of jaundice (3-5%), acute hepatitis (10%) and the most common cause of acute liver failure and drug market suspension. However, recognizing DILI on liver biopsy is challenging due to the large amount of time required to search medical records and the extensive number of drugs to consider. Reducing these obstacles should help pathologists recognize DILI.

Design: We designed software that compares medical record text spanning the previous year against the DILIrank database, the largest known ranked list of liver-toxic drugs in humans. Identified drugs were annotated with their level of likelihood to cause liver injury (Most, Moderate/Ambiguous, or Less), start and discontinuation dates. As a control, a manual search per routine practice was performed and consisted of 2-5 minutes of reviewing medical records and internet resources (e.g. LiverTox website).

Results: The software evaluated 305 recent adult liver biopsies and identified 191, 248, 265, and 288 "Most concern" drugs and 317, 364, 378, and 402 "Moderate concern" drugs over the previous 1, 3, 6, and 12 months. Many patients had taken more than one liver-toxic drug including 15% with 2+ "Most concern" drugs within 1 month of biopsy (see figure). The most common "Most concern" drugs were acetaminophen (22% of instances), ciprofloxacin (9%), fluconazole (6%), atorvastatin (6%), and cyclosporine (5%), but the remaining 53% consisted of a wide variety of 52 low instance drugs (e.g. valproic acid, terbinafine, gemfibrozil) (see table). The computer software was significantly ($p < 0.05$) faster than a human search (65 vs. 263 seconds per case) and identified more drugs (1.39 vs. 0.48 "Most concern" and 3.68 vs. 0.31 "Moderate concern" drugs per case). Interestingly, half of the DILIrank-implicated drugs were not mentioned in the Gastroenterology/Hepatology clinical consult note.

Drugs most concerning for liver toxicity by NIH LTKB				Drugs moderately concerning for liver toxicity by NIH LTKB			
Drug Name	% total	Drug Name	% total	Drug Name	% total	Drug Name	% total
ACETAMINOPHEN	21.6%	DULOXETINE	1.0 %	METOPROLOL	17.0 %	ENTECAVIR	1.6 %
CIPROFLOXACIN	8.8%	ITRACONAZOLE	1.0 %	FUROSEMIDE	13.4 %	NALTREXONE	1.6 %
FLUCONAZOLE	5.9%	MERCAPTOPURINE	1.0 %	GANCICLOVIR	9.2 %	DEXMEDETOMIDINE	1.6 %
ATORVASTATIN	5.6%	PHENYTOIN	1.0 %	RIFAXIMIN	7.5 %	CHOLESTYRAMINE	1.3 %
CYCLOSPORINE	4.6%	GEMCITABINE	0.7 %	TRAMADOL	7.5 %	TADALAFIL	1.3 %
LEVOFLOXACIN	4.2%	DILTIAZEM	0.7 %	LORAZEPAM	7.2 %	MILRINONE	1.3 %
METHOTREXATE	3.9%	FLUTAMIDE	0.7 %	VALGANCICLOVIR	6.9 %	DIAZEPAM	1.3 %
AZATHIOPRINE	3.6%	ETODOLAC	0.7 %	CASPOFUNGIN	6.2 %	FILGRASTIM	1.3 %

TESTOSTERONE	2.9%	INDOMETHACIN	0.7 %	HYDROMORPHONE	5.9 %	COLCHICINE	1.3 %
AMIODARONE	2.6%	OXALIPLATIN	0.7 %	PIPERACILLIN	5.2 %	RIBAVIRIN	1.0 %
ERYTHROMYCIN	2.3%	TOLVAPTAN	0.7 %	POSACONAZOLE	4.9 %	URSODEOXYCHOLIC	1.0 %
ALLOPURINOL	2.3%	INFLIXIMAB	0.7 %	ATOVAQUONE	4.9 %	ESZOPICLONE	1.0 %
VORICONAZOLE	2.0%	ACETAZOLAMIDE	0.7 %	INTERFERON	4.9 %	LACOSAMIDE	1.0 %
DICLOFENAC	2.0%	BUSULFAN	0.7 %	PROPRANOLOL	3.6 %	TEMAZEPAM	1.0 %
VALPROIC	1.6%	NORTRIPTYLINE	0.7 %	MYCOPHENOLIC	3.3 %	FOSCARNET	1.0 %
TAMOXIFEN	1.6%	TERBINAFINE	0.7 %	DEXAMETHASONE	3.3 %	TIMOLOL	1.0 %
KETOCONAZOLE	1.6%	NIACIN	0.7 %	METHADONE	2.6 %	DECITABINE	0.7 %
RIFAMPIN	1.6%	ASPARAGINASE	0.7 %	ERTAPENEM	2.3 %	SUMATRIPTAN	0.7 %
ISONIAZID	1.3%	SULFASALAZINE	0.7 %	ZOLPIDEM	2.0 %	BUSPIRONE	0.7 %
LABETALOL	1.3%	CLARITHROMYCIN	0.7 %	HALOPERIDOL	2.0 %	BUMETANIDE	0.7 %

Figure 1 - 1645

The proportion of patients taking one or more liver-toxic drugs before biopsy. Bar graphs are color-coded by the level of concern (most, moderate/ambiguous, less) for drug liver toxicity as defined by the NIH Liver Toxicity Knowledge Base.
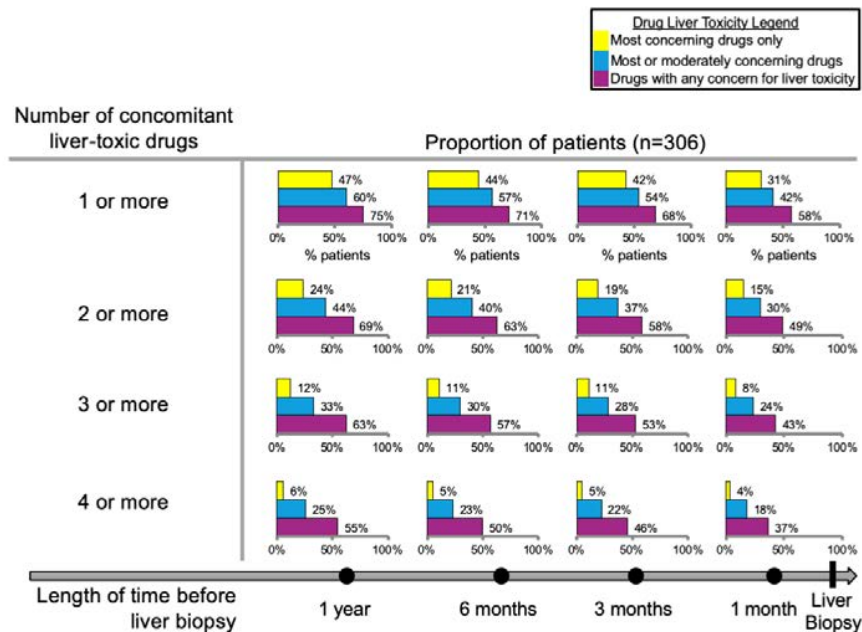
Conclusions: These data suggest retrieval-and-search software can help pathologists assess liver biopsies for DILI with speed and accuracy conducive to routine practice. These data also emphasize the importance of systematically screening every patient for liver-toxic drugs, since many are taking one or multiple of these drugs, including potentially overlooked, low-incidence drugs. Overall, the current study highlights informatics as an aid for practicing pathologists in more accurately assessing DILI in the face of abundant, unstructured medical data.

1646 Identification of Somatic Gene Mutations in Hepatocellular Carcinoma: Clinicopathologic Correlates in a Cohort of 34 Cases

Ahmed Shehabeldin[1], Randall Olsen[2], Jessica Thomas[1], Nicola Dundas[1], Mary Schwartz[1], Constance Mobley[1], Ashish Saharia[1], Maen Abdelrahim[1], Mark Ghobrial[1], Mukul Divatia[1]
[1]Houston Methodist Hospital, Houston, TX, [2]Houston, TX

Disclosures: Ahmed Shehabeldin: None; Randall Olsen: None; Mary Schwartz: None; Mukul Divatia: None

Background: Hepatocellular carcinoma (HCC) is the second most frequent cause of cancer-related mortality worldwide and is associated with specific risk factors. Recent studies have begun seeking to characterize genomic alterations in HCC that may be targets for personalized treatment strategies.

Design: Next-generation sequencing to identify somatic mutations in 50 cancer-associated genes was performed on formalin-fixed paraffin-embedded explanted liver tissue taken from 34 HCC specimens collected during 2016-2018. Clinicopathologic parameters including age, gender, etiology, tumor staging, treatment status, and morphology were reviewed.

Results: In total, somatic mutations were identified in 19/34 cases. Mutated genes included APC, CDKN2A, CTNNB1, IDH1, PTEN, SMAD4, TP53 and VHL. The mutational cohort included 9 females and 10 males; age range: 48-76 years. Tumor size ranged from 0.5 to 6 cm with 8 unifocal and 11 multifocal tumors; tumor stage I-IIIA. 13 patients received prior therapy. Morphologically, tumors with identified mutations were well (5), well to moderately (2), moderately (8), moderately to poorly (2), and poorly differentiated (1) HCCs, with one case of multifocal HCC showing well and poorly differentiated tumors; all with background cirrhosis. HCC etiologies included hepatitis B (1) and C (8), nonalcoholic steatohepatitis (4), autoimmune hepatitis (2), autoimmune hepatitis and primary biliary cholangitis (1), alcoholic hepatitis (2) and cryptogenic hepatitis (1). No statistically significant correlation with sex, age, and histological tumor grading was found.

Figure 1 - 1646
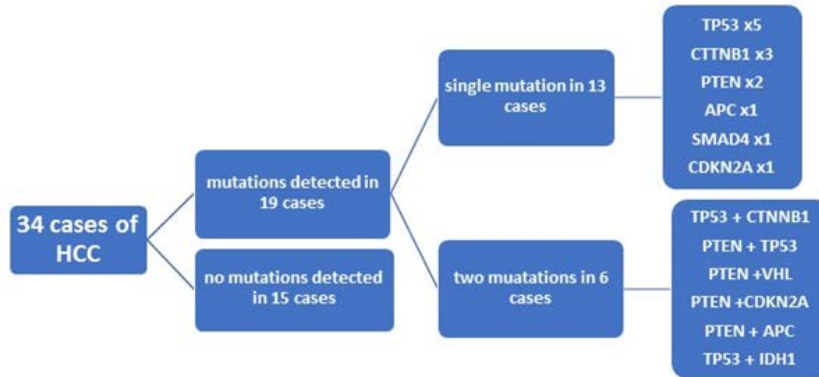
Conclusions: Somatic mutations were detected in more than 50% of the HCCs tested. However, no correlation between the presence of a mutation overall or the specific gene mutated and any clinicopathologic parameter was found. We identified mutations in frequently mutated genes including viral-related HCC genes TP53 (42.1%) and CTNNB1/β-catenin/WNT signaling pathway (21%) along with less prevalent PTEN (31.6%) CDKN2A (10.5%) and SMAD4 (5.3%) mutations. A relatively rare IDH1 mutation (5.3%) reflecting a shift towards a biliary phenotype was also noted. Additional studies are needed to better determine whether stratification of HCC cases by mutational status may be predictive of prognosis or guide personalized treatment strategies

---

1647 Molecular Changes of Hepatocellular Carcinoma(HCC) are Related to Morphological Subtypes, PD-1/PD-L1 Expression and Early Recurrence after Transplantation

Guangyue Shen[1], Jing Han[2], Lingli Chen[3], Yuan Ji[2]
[1]Zhongshan Hospital, Fudan University, Shanghai, China, [2]Zhongshan Hospital of Fudan University, Shanghai, China, [3]Zhongshan Hospital, China

Disclosures: Guangyue Shen: None

Background: To explore the correlation between molecular mutations and morphological subtypes, PD-1/ PD-L1 expression and early recurrence after transplantation of HCC, thereby identifying the role of molecular typing in screening the markers for molecular-targeted therapy while the range of clinical application of sequencing methods represented by second-generation sequencing (NGS) is widened.

Design: A total of 120 HCC cases (2017-2019) were performed NGS with a 508 gene-targeted panel. Morphological composition (any subtype accounted for ≥30% of the lesion was judged to be present, and ≥50% to be the main component), PD-1/ PD-L1 expression in tumor/inflammatory cells(0%: negative, 1-5%: low expression, >5%: high expression) and molecular changes(concluded as five main pathways and other significant mutations such as TSC1/2 mutation) went through correlation tests. As for the liver transplanted cases (83), the contributions of morphology, gene mutations and PD-1/PD-L1(SP142) expression to recurrence within 2 years after transplantation were identified by univariate and multivariate test.

Results: Correlation tests show that TSC1/2 mutation is associated with the presence of macrotrabecular subtype, mutations of histone modification related genes (KMT2C, KMT2D, KDM6A) are correlated with the expression level of PD-1 in tumor infiltrative lymphocytes, and the presence of macrotrabecular subtype is related to the expression level of PD-L1 in inflammatory cells(P=0.01,0.04 and 0.001respectively). Univariate analysis shows that in addition to common risk factors such as male, macrotrabecular subtype and tumor

satellite foci, chromosomal remodeling-related genes (including ARID1A, ARID1B, ARID2, and NCOR1) and RPS6KA3 mutations also show a trend to be correlated with early recurrence (HR= 3.3 and 2.9 respectively; P=0.056 and 0.057 respectively). Further multivariate analysis indicates that chromosomal remodeling-related gene mutations (HR=2.51, P=0.05) and TSC1/2 mutation (HR=4.52, P=0.01) are risk factors for early recurrence.

Figure 1 - 1647
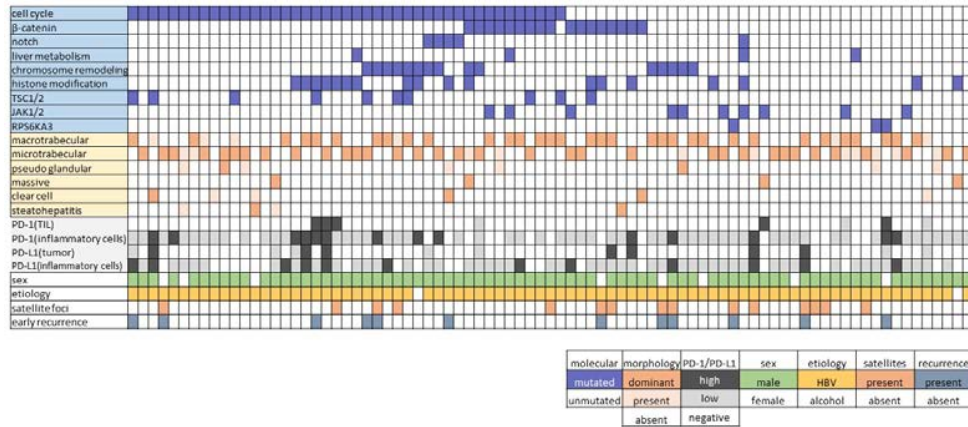
Conclusions: The molecular information obtained by NGS is helpful for screening patients with high risk of early recurrence after liver transplantation, and the relationship between specific molecular changes and PD-1 expression can be a reference for the combination of molecular-targeted therapy and immunotherapy.

1648 CMV Hepatitis in Allograft Liver Biopsies

Angela Shih[1], Ricard Masia[1], Joseph Misdraji[2]
[1]Massachusetts General Hospital, Boston, MA, [2]Harvard Medical School, Boston, MA

Disclosures: Angela Shih: None; Ricard Masia: None; Joseph Misdraji: None

Background: CMV hepatitis is diagnosed in the setting of allograft dysfunction when there is histologic or immunohistochemical evidence of CMV infection on liver biopsy. An association between CMV hepatitis and acute cellular rejection (ACR) has been reported but is not understood or universally accepted. This study describes the clinicopathologic features of CMV hepatitis in liver allografts and explores the relationship with ACR.

Design: Search of the pathology records (2002-2019) identified 10 transplant liver biopsies with CMV hepatitis. H&E and IHC stains for CMV were reviewed for histopathologic characterization. Clinical data were obtained from the medical record.

Results: Ten patients (M:F = 7:3) received liver transplants at a median age of 61 (range: 56 to 73 years). In most cases, CMV status was D+/R- (7 of 9 cases tested). Diagnosis was made at a median time after transplant of 149 days (range: 46-666 days), and patients had a median ALT 180 (range: 37-389 IU/mL); AST 166 (range: 22-379 IU/mL); and AlkP 200 (range: 13.4-351 IU/mL). Median CMV viral load at time of biopsy was 39811 (range: 2290-936000 IU/mL). Prior to diagnosis, 2 patients were treated for presumed ACR without biochemical response. On histology, biopsies showed a wide spectrum of portal and lobular inflammation, interface activity, and lobular activity. Neutrophilic microabscesses were seen in 5 cases and microgranulomas in 3. Bile duct infiltration and injury was seen in 5 cases without duct loss. Equivocal or definite endothelialitis was present in half the cases. CMV viral cytopathic changes were seen in all cases, ranging from rare to abundant (40/section), and IHC highlighted CMV-infected cells in all cases, ranging from rare to abundant (>100/section). Based on histologic features of ACR, 3 cases were diagnosed as CMV and ACR and 2 were diagnosed as CMV and equivocal ACR. All patients were treated with antiviral therapy without treatment for ACR and achieved undetectable serum CMV viral loads with biochemical near normalization.

Conclusions: CMV hepatitis has a wide range of histologic findings but consistently shows viral inclusions if sufficient tissue is provided. Histologic features of ACR are commonly seen in these biopsies, and can cause CMV to be overlooked if inclusions are rare. It is unclear whether there is a relationship between liver allograft rejection and CMV, or whether CMV infection can cause histologic features mimicking rejection in some patients.

1649 Morphology of Tumor and Nontumor Tissue in Resection Specimens for Hepatocellular Carcinoma Following Nivolumab Therapy - A Single Institution Experience

Camila Simoes[1], Swan Thung[2], Maria Isabel Fiel[2], Stephen Ward[2], Myron Schwartz[2]
[1]Mount Sinai Hospital Icahn School of Medicine, New York, NY, [2]Icahn School of Medicine at Mount Sinai, New York, NY

Background: Nivolumab (NIV) is an immune checkpoint inhibitor approved for treatment of many cancers, including hepatocellular carcinoma (HCC). Liver injury is a known complication in patients treated with NIV for non-liver tumors, including reports of fibrin ring granulomas. The morphology of tumor and non-tumor liver in HCC patients treated with NIV is not well characterized.

Design: We identified 14 patients who underwent partial hepatectomy (PH) or liver transplantation (Tx) after receiving NIV for HCC. Tumor slides were evaluated for necrosis and inflammatory infiltrate, non-tumor slides were evaluated for liver injury (including bile duct injury, inflammation and granulomas), and medical records were reviewed.

Results: Our study included 11 males and 3 females, median age of 57 years. Underlying liver disease was HBV in 8, HCV in 5, and unknown in 1. Eight patients had no treatment for HCC prior to NIV while 6 had prior resection and/or embolization. Patients received 2 to 32 doses of NIV (last dose within 2 months prior to surgery). By imaging, 3 patients showed response to NIV, while 7 were stable and 4 progressed. Ten patients underwent PH and 4 underwent Tx following NIV. On review of slides, 2 of 3 cases with radiologic response showed no residual viable tumor while 1 showed 95% necrosis. Tumor infiltrating lymphocytes (TILs) were present in 12/14 cases overall, including all 3 cases with response. Regarding the non-tumor liver, 4/14 cases showed periductal fibrosis, 1/14 cases showed nonnecrotizing granulomas (without fibrin ring features), 1/14 showed prominent bile duct intraepithelial lymphocytes (IELs), and 1/14 showed bile duct loss. Of the 3 cases that showed response to NIV, one case showed both granulomas and bile duct IELs (FIG.), while another showed periductal fibrosis. The case with bile duct loss received 16 months of NIV therapy and showed increase in alkaline phosphatase at initiation of treatment. See table for summary of cases with NIV response.

	Patient 1	Patient 2	Patient 3
Age	67	63	62
Sex	F	M	M
Underlying liver disease	HCV	HCV	HBV
Viral load at time of surgery	Undetectable	Undetectable	Undetectable
Fibrosis stage (Ishak)	5/6	6/6	3/6
Pre-treatment AFP (ng/ml)	86,221	245	4,287
Prior therapy	No	No	No
Tumor necrosis (%)	100	100	95
Tumor infiltrating lymphocytes	Present	Present	Present
Prominent Bile duct IELs	Absent	Present	Absent
Granuloma	Absent	Present	Absent
Periductal fibrosis	Present	Absent	Absent

Table 1: Clinical and pathology findings in 3 patients with response to nivolumab

therapy. AFP = alpha fetoprotein (normal < 9 ng/ml); IELs = intraepithelial lymphocytes.

Figure 1 - 1649
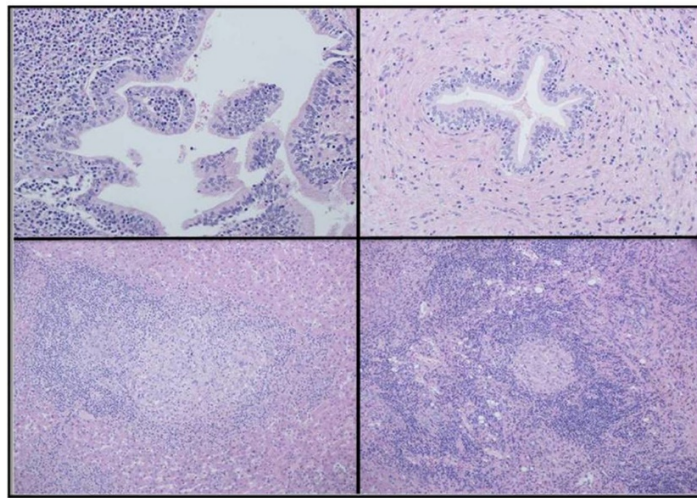
Morphologic changes in nontumor liver parenchyma (table patient #2): biliary intraepithelial lymphocytes and granulomas

Conclusions: We show that NIV resulted in complete or near complete tumor necrosis with associated intratumoral lymphocytes in 3/14 cases, suggesting that NIV is an effective treatment for a subset of HCC patients. Granulomas and bile duct IELs were seen in nontumor liver in one case. Interestingly, this case was 1 of 3 that showed response to NIV and may indicate an activation of the patient's immune system. Future studies evaluating tumor tissue prior to treatment are underway to identify potential markers of response to NIV.

1650   Frequent Loss of BAP1 by Immunohistochemistry can be Seen in Hepatobiliary Carcinomas, Especially Steatohepatitic Variant of Hepatocellular Carcinoma but Not in Tumors of Luminal GI Tract
Aditya Talwar[1], Amy Ziober[1], Kester Haye[1], Rashmi Tondon[1]
[1]Hospital of the University of Pennsylvania, Philadelphia, PA

Disclosures: Aditya Talwar: None; Amy Ziober: None; Kester Haye: None; Rashmi Tondon: None

Background: BAP1 mutation has been widely used as a marker for uveal melanomas and mesotheliomas. However, the frequency of BAP1 mutation has not been extensively studied in carcinomas of luminal GI and hepatobiliary system. We examined frequency of BAP1 loss by IHC in carcinomas of the luminal GI tract and hepatobiliary system to assess its diagnostic value. We also examined the grade and histological subtype in tumor showing loss of BAP1.

Design: Whole-section slides of 100 cases were stained for BAP1; 49 cases were of luminal GI tract (12 esophageal, 13 gastric, 12 small intestinal and 12 colonic adenocarcinomas) and 39 cases of hepatobiliary carcinomas (12 intrahepatic cholangiocarcinomas (IHCC), 15 pancreatic ductal adenocarcinomas, and 12 HCC). Twelve cases were from ampullary adenocarcinomas.

Loss of BAP1 staining by IHC was defined as complete nuclear loss of staining in tumor cells.

Results: BAP1 loss was seen in 23% (9/39) hepatobiliary carcinoma; 58.3% (7/12) cases of HCC and in 16.7% (2/12) cases of IHCC. Of the HCC cases with BAP1 loss, 86% (6/7) were moderately differentiated (MD), of which 67% (4/6) showed steatohepatitic morphology, with the remainder being classic HCC. Only one of the cases of HCC with steatohepatitic features had significant background steatohepatitis, all other cases had minimal steatosis, even in the setting of non-alcoholic steatohepatitis. BAP1 loss in luminal GI adenocarcinomas was seen in 4% (2/49) cases. Of the luminal tumors, both gastric and duodenal adenocarcinomas were poorly differentiated (PD).

Interestingly, one case of esophageal adenocarcinoma showed predominantly MD morphology, with a smaller PD component. This case showed retained staining within the MD component, with abrupt loss of staining in PD area.

Conclusions: To our knowledge, this is one of the first attempts to examine loss of BAP1 by IHC in luminal GI tumors. Our study shows that loss of BAP1 is rare in carcinomas of luminal GI tract (4%) but is frequently seen in HCC (58.3%; p value = 0.0074), especially in

steatohepatitic variant. This is a statistically significant finding, even in our small cohort. Given that BAP1 loss was seen in steatohepatitic variant of HCC and in PD tumors, it may be of use as a potential diagnostic and prognostic marker. Interestingly, loss of BAP1 is seen in 16.7% of IHCC, in contrast to 25-50% as reported in literature. Larger sample size is required to further study the utility of BAP1 IHC in HCC and PD tumors of the hepatobiliary system.

1651 Transcriptomic Analysis of Cirrhosis-like Hepatocellular Carcinoma Reveals Novel and Distinct Molecular Characteristics

Benjamin Van Treeck[1], Roger Moreira[1], Taofic Mounajjed[1], Linda Ferrell[2], Yue Xue[3], Erik Jessen[1], Jaime Davila[4], Rondell Graham[1]
[1]Mayo Clinic, Rochester, MN, [2]University of California San Francisco, San Francisco, CA, [3]Northwestern University Feinberg School of Medicine, Chicago, IL, [4]Mayo Clinic Rochester, Rochester, MN

Disclosures: Benjamin Van Treeck: None; Roger Moreira: None; Taofic Mounajjed: None; Taofic Mounajjed: None; Linda Ferrell: None; Yue Xue: None; Jaime Davila: None; Rondell Graham: None

Background: Cirrhosis-like hepatocellular carcinoma (CL-HCC) forms multiple nodules, displays extensive vascular invasion, mimics cirrhosis grossly and is largely undetectable by imaging studies. The molecular biology of CL-HCC has not been studied.

Design: RNAseq was performed utilizing formalin fixed paraffin embedded tissue from confirmed CL-HCC cases (n=6), along with corresponding non-neoplastic liver (n=4) when available. The transcriptome data were compared between tumor-normal pairs and to publicly curated data from The Cancer Genome Atlas (TCGA).

Results: Histologically, CL-HCC showed minimal intratumoral inflammation, innumerable nodules and extensive vascular permeation.

This morphologic appearance corresponded with several transcriptomic findings. Tumor-normal gene expression analysis revealed consistent overexpression of *FOXM1*, a driver of metastasis, and its downstream cell cycle/proliferation targets (Table 1). Also, genes associated with the presence of tissue and vascular invasion were upregulated including *COL1A1, ASPM, MMP11, MMP16*, and *MMP12*. There was also downregulation of *TIMP2*, an inhibitor of tissue and vascular invasion.

Despite the aggressive morphologic appearance, there was a low tumor mutational burden (average TMB=6.36 SNP per MB).

CL-HCC demonstrated a distinct global differential gene expression profile when compared to fibrolamellar HCC (FL-HCC) (n=6), steatohepatitic HCC (SH-HCC) (n=8), and to other HCC in TCGA (n=424) (Figure 1).

No upregulation of the pathways commonly involved in hepatocellular carcinoma (IL-6, JAK/STAT, WNT/ β-catenin, NF-kB, Hedgehog, mTOR, PI3K/AKT, RAS/RAF, NFE2L2, FGF19) was noted. There were also no mutations in genes (β-*catenin, APC, AXIN1, TP53, JAK1, SALL-4, ARID1A, ARID2*, and MLL family of genes) commonly involved in conventional HCC. No recurring translocations were identified.

CL-HCC did not show significant differential expression in zone 3 marker glutamine synthetase, or zone 1 markers *ASS-1* and *FABP1*.

Figure 1 - 1651

Table 1. Summary of Gene Expression Data			
	Activation Status	**Fold Change**	**P-value**
FOXM1 **and Downstream Proliferation Targets:**			
FOXM1	Activated	2.77	0.000686
KIF4A	Activated	3.43	0.000212
CENPF	Activated	4.11	7.48×10^{-7}
Cyclin B1 *(CCNB1)*	Activated	3.8	1.31×10^{-7}
TOP2A	Activated	3.33	3.04×10^{-6}
KIF20A	Activated	4.71	1.08×10^{-7}
BUB1B	Activated	2.8	0.000265
Vascular Invasion Markers:			
Collagen 1α1 *(COL1A1)*	Activated	2.339	0.0264
Abnormal Spindle-like Microcephaly *(ASPM)*	Activated	5.888	8.16×10^{-11}
Matrix Metallopeptidase 11 *(MMP11)*	Activated	4.145	0.000552
Matrix Metallopeptidase 16 *(MMP16)*	Activated	2.543	0.00797
Matrix Metallopeptidase 12 *(MMP12)*	Activated	9.297	0.0361
Tissue inhibitor of metalloproteinase 2 *(TIMP2)*	Repressed	0.605	0.023
Hepatic Lobule Zonation Markers:			
Glutamine Synthetase *(GLUL)*	Unchanged	1.96	0.0636
Fatty Acid Binding Protein 1 *(FABP1)*	Unchanged	0.727	0.368
Argininosuccinate Synthetase 1 *(ASS-1)*	Unchanged	0.586	0.18952

Figure 2 - 1651
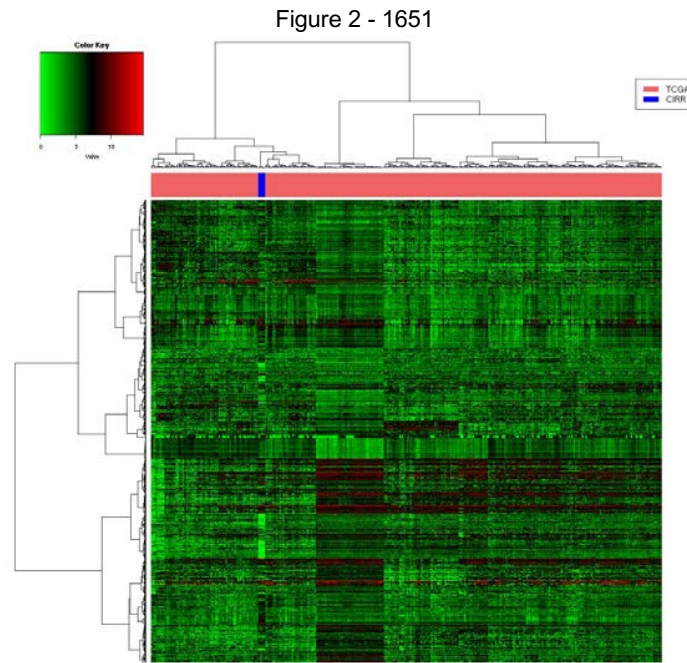
Conclusions: CL-HCC's distinct clinical and morphologic features correspond to a unique gene expression profile when compared to the TCGA and other HCC datasets. CL-HCC shows an expression profile compatible with zone 2 of the lobule and an increased expression of markers of invasiveness and metastasis. CL-HCC should be considered a specific subtype of HCC given its characteristic morphology, distinct gene expression profile and lack of the abnormalities seen in other recognized types of HCC.

1652 The Distinct Genomic Landscapes of Hepatitis C and Alcohol Related Hepatocarcinogenesis Sequences

Alejandro Vargas[1], John Paulsen[2], Varshini Vasudevaraja[3], Stephen Kelly[3], Matija Snuderl[4], George Jour[5], Neil Theise[5]
[1]NYU School of Medicine, New York, NY, [2]Mount Sinai Medical Center, New York, NY, [3]New York University Medical Center, New York, NY, [4]New York University, New York, NY, [5]NYU Langone Health, New York, NY

Disclosures: Alejandro Vargas: None; John Paulsen: None; Varshini Vasudevaraja: None; Stephen Kelly: None; Matija Snuderl: None; George Jour: None; Neil Theise: None

Background: As hepatocellular carcinoma (HCC) develops from premalignant lesions (low and high grade dysplastic nodules; LGDN and HGDN), there is a corresponding accumulation of molecular alterations, some of which have been well described. However, the molecular features of lesions comprising the hepatocellular dysplasia-carcinoma sequence as they relate to different etiologies have not yet been explored. Herein, we characterize the molecular landscape of such lesions in cirrhotic explants with alcohol-related liver disease (ALD) and chronic hepatitis C (CHC).

Design: Tissue was assessed from 27 liver explants (14 CHC, 13 ALD) including 10 LGDNs (5 CHC, 5 ALD), 8 HGDNs (3 CHC, 5 ALD), 10 HCCs arising from HGDNs (5 CHC, 5 ALD), and 10 small HCCs defined as HCC < 2 cm (5 CHC, 5 ALD), as well as non-lesional cirrhotic parenchyma and matched normal non-liver tissue (e.g. porta hepatis structures). DNA was extracted from FFPE tissue for next generation sequencing (NGS) using a customized NGS580 panel targeting all exonic and select intronic areas in 580 cancer related genes. Data was analyzed using customized bioinformatics pipelines with an R package.

Results: TERT promoter HS C228T mutations were identified in 6 of 10 (60%) CHC related HCCs and only 1 of 9 (11%) alcohol related HCC (Figure 1). There was a significant association between *TERT* promoter HS C228T mutations and CHC related HCCs (p<0.02). In contrast, ALD related lesions showed deleterious events affecting tumor suppressor genes (*NF1, BRCA1; CDKN2C*) and histone methylation/chromatin remodeling genes (*KMT2A; KMT2C; ASXL1; RAD21*), which were found in 6 of 13 ALD related lesions (46.2% [3 of 5 small HCCs, 2 of 4 HGDNs, and 1 of 4 HCCs arising in HGDNs]). These events only occurred in 3 of 14 (21.4%) CHC related lesions (Figures 1 and 2). Within the CHC group, 1 HCC arising in HGDN showed copy number gains (CNG) in *MARK4, ERCC2, FGFR4* and *FLT4* and two HGDNs showed CNGs in *NOTCH1* and *TERT*, respectively. No differences in the tumor mutational burden (TMB) were noted between CHC related and ALD related lesions, nor across the DN-HCC sequence. Non-lesional liver and LGDNs did not show recurrent mutations pertaining to a specific pathway.

Figure 1 - 1652
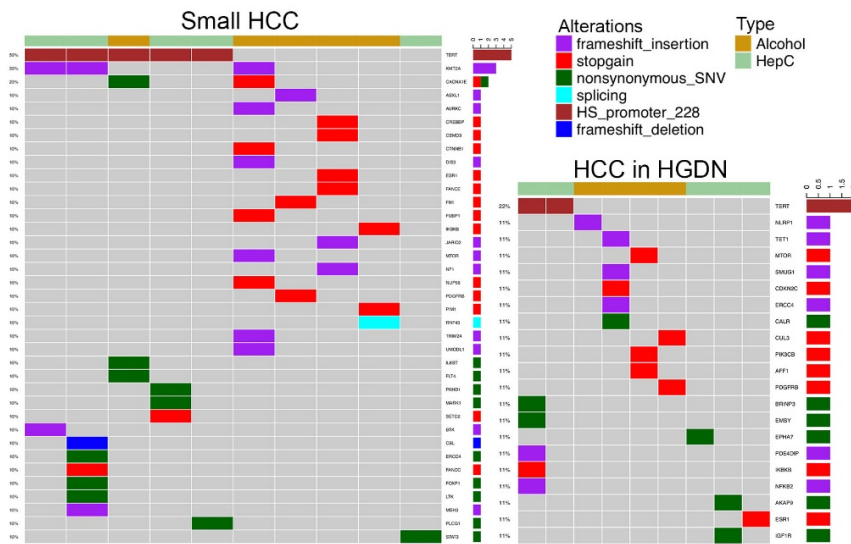
Figure 2 - 1652
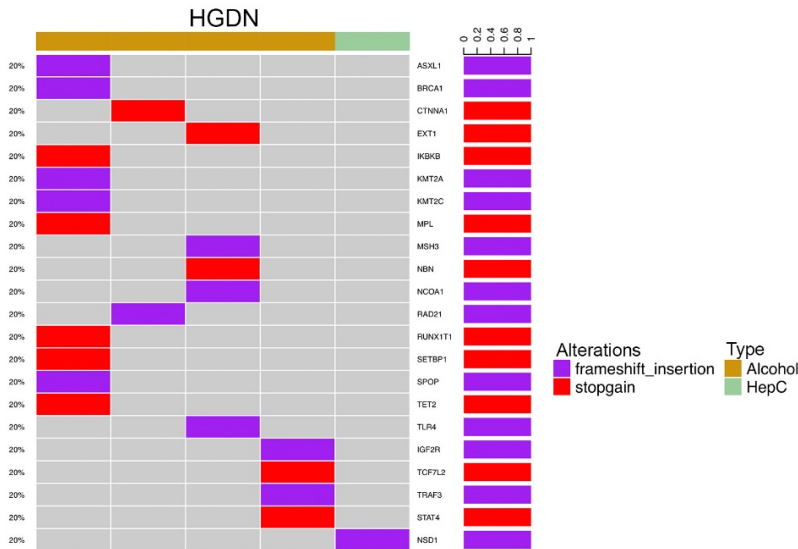
Conclusions: Our findings suggest that the pathways of hepatocarcinogenesis are distinct in ALD and CHC. While upregulation of telomerase activity (TA) and cancer cell immortalization play a pivotal role in CHC related HCC, defective chromatin remodeling appears to contribute to tumorigenesis in ALD related HCC.

1653 Distinctive Histology Features among Liver Biopsies with Biliary-Pattern Injury and Confirmed Clinical Diagnoses

Barbara Vidal[1], Justin Cates[2], Raul Gonzalez[1]
[1]Beth Israel Deaconess Medical Center, Boston, MA, [2]Vanderbilt University Medical Center, Nashville, TN

Disclosures: Barbara Vidal: None; Justin Cates: None; Raul Gonzalez: None

Background: Biliary-pattern injury in the liver (duct injury, ductular reaction, cholestasis), can occur in several conditions, including primary biliary cholangitis (PBC), primary sclerosing cholangitis (PSC), large duct obstruction (LDO), and drug-induced liver injury (DILI). While the histologic changes in these conditions have been well described, distinguishing among them remains often challenging, particularly when

biopsy samples are limited in size, robust clinical information is unavailable, and/or the pathologist does not feel confident in evaluating liver disease. This study assesses histologic findings in biliary-pattern injury to determine whether any suggest particular diagnoses.

Design: We searched for liver biopsies at our institution from 2004-2018 with biliary-pattern injury. Cases were correlated with clinical information, and those with a clinically confirmed diagnosis of PBC, PSC, chronic LDO, or DILI were included. Cases harboring autoimmune hepatitis (AIH), overlap syndrome (AIH/PBC, PBC/PSC, AIH/PSC), or malignancy were excluded. For included cases, we recorded patient age and sex, use of therapy (almost always ursodeoxycholic acid), antimitochondrial antibody [AMA] status, and numerous histologic findings. Findings were compared across diagnoses, with significance set at $P<0.05$.

Results: The cohort comprised 132 cases: 57 PBC (including 5 AMA-negative), 49 PSC (including 6 small-duct), 21 DILI, and 6 chronic LDO. Most cases (77%) were stage 0-2 by METAVIR scoring. Significant histologic differences across diagnoses are summarized in the **Table 1**. Findings similar across diagnoses included lobular acute inflammation, acidophil bodies, portal edema, ductular reaction, duct injury/ductitis, and sinusoidal dilation. The only significant therapy-related changes were decreased portal and lobular chronic inflammation in PBC patients on therapy ($P=0.008$ and $P=0.006$, respectively). There were no significant histologic changes between AMA-positive and AMA-negative PBC patients, or between PSC patients with or without small-duct disease.

	PBC (n=57)	PSC (n=49)	DILI (n=21)	Chronic LDO (n=6)	P-value
Portal chronic inflammation	0/1+: 28% 2+/3+: **72%**	0/1+: 51% 2+/3+: 49%	0/1+: 67% 2+/3+: 33%	0/1+: 17% 2+/3+: **83%**	0.031
Lobular chronic inflammation	Absent: 28% Present: **72%**	Absent: 59% Present: 41%	Absent: 52% Present: 48%	Absent: 0% Present: **100%**	0.001
Neutrophils within ductular reaction	Absent: 65% Present: **35%**	Absent: 37% Present: 63%	Absent: 43% Present: 57%	Absent: 33% Present: 67%	0.016
Cholestasis	Absent: 95% Present: 5%	Absent: 84% Present: 16%	Absent: 52% Present: **48%**	Absent: 17% Present: **83%**	<0.001
Feathery degeneration	Absent: 98% Present: 2%	Absent: 98% Present: 2%	Absent: 86% Present: **14%**	Absent: 83% Present: **17%**	0.013
Onion-skin fibrosis	Absent: 100% Present: 0%	Absent: 86% Present: **14%**	Absent: 95% Present: 5%	Absent: 100% Present: 0%	0.017
Florid duct lesions	Absent: 77% Present: **23%**	Absent: 98% Present: 2%	Absent: 100% Present: 0%	Absent: 100% Present: 0%	0.010
Lobular granulomas	Absent: 56% Present: **44%**	Absent: 94% Present: 6%	Absent: 86% Present: 14%	Absent: 67% Present: 33%	<0.001

Conclusions: In addition to obvious histologic clues (onion-skin fibrosis, florid duct lesions, lobular granulomas), cholestasis and feathery degeneration can help suggest a diagnosis in early-stage liver biopsies, as they are more common in DILI and chronic LDO than in PBC and PSC. Lack of neutrophils in ductular reaction may suggest PBC. These findings are likely most helpful when complicating factors interfere with biopsy interpretation.

1654 DNA Flow Cytometric Analysis of Intrahepatic Cholangiocarcinoma and its Morphologic Mimics

Kwun Wah Wen[1], Peter Rabinovitch[2], Dongliang Wang[3], Aras Mattis[1], Won-Tak Choi[1]
[1]University of California San Francisco, San Francisco, CA, [2]University of Washington, Seattle, WA, [3]SUNY Upstate Medical University, Syracuse, NY

Disclosures: Kwun Wah Wen: None; Peter Rabinovitch: None; Dongliang Wang: None; Aras Mattis: None; Won-Tak Choi: None

Background: The distinction between intrahepatic cholangiocarcinoma (ICC) from its morphologic mimics such as bile duct adenoma (BDA) and hamartoma (BDH) can be challenging, particularly in small biopsies. Although a few cases of BDA and BDH have been reported to undergo malignant transformation into ICC, their neoplastic versus reactive nature remains debated. This study assesses the potential value of DNA content analysis by DNA flow cytometry in the differential diagnosis and/or risk stratification of malignant and benign bile duct lesions using formalin-fixed paraffin-embedded tissue.

Design: DNA flow cytometry was performed on 47 ICC, 15 BDA, and 18 BDH cases. Three to four 60-micron thick sections were cut from each block, and the lesional areas were dissected for analysis.

Results: Aneuploidy was detected in 22 (47%) of ICC, 1 (7%) of BDA, and none of BDH cases. The overall disease recurrence or death rates in all ICC patients (regardless of flow cytometric results) were 17.6%, 55.7%, 71.0%, and 90.3% within 1, 3, 5, and 7 years, respectively. The 1-, 3-, 5-, and 7-year recurrence or death rates in ICC patients with aneuploidy were 27.8%, 66.3%, 66.3%, and 90.3%, respectively, whereas ICC patients in the setting of normal DNA content had 1-, 3-, 5-, and 7-year recurrence or death rates of 6.2%, 44.3%, 71.6%, and 71.6%, respectively. Although the patients with aneuploid tumors appeared to have worse outcomes, especially during the first three years, this difference was not statistically significant (HR = 1.4, p = 0.473) in the present sample size, based on the univariate Cox model with log-rank test. Similarly, none of potential demographic (such as age and presence of primary sclerosing cholangitis) and pathological risk factors (such as multifocality of tumor, size, grade, and stage) was significantly associated with tumor progression in our cohort (p > 0.05).

	ICC (n = 47)	BDA (n = 15)	BDH (n = 18)
Aneuploidy	22 (47%)	1 (7%)	0 (0%)

Conclusions: The presence of aneuploidy was significant higher in ICC (47%) than in BDA (7%) or BDH (0%), suggesting that it can potentially serve as a diagnostic marker of malignancy in challenging situations. Our findings also suggest that a small subset of BDA may represent a precursor lesion to ICC that harbors aneuploidy, whereas BDH is a different process with no malignant potential. Although a larger cohort will be necessary to further determine the prognostic significance of aneuploidy in ICC patients, the patients with aneuploid tumors may have a higher risk for tumor progression, especially during the first three years.

1655 Evaluation of Tumor Mutation Burden (TMB) in Small/Early Hepatocellular Carcinomas (HCCs) and Progressed Hepatocellular Carcinomas: Is There Any Difference?

Mary Wong[1], Eric Vail[2], Jong Kim[3], Stacey Kim[3], Brent Larson[3], Kevin Waters[3], Maha Guindi[4]
[1]Arcadia, CA, [2]Cedars-Sinai Medical Center, West Hollywood, CA, [3]Cedars-Sinai Medical Center, Los Angeles, CA, [4]Cedars-Sinai Medical Center, Beverly Hills, CA

Disclosures: Mary Wong: None; Eric Vail: None; Jong Kim: None; Stacey Kim: None; Brent Larson: None; Kevin Waters: None; Maha Guindi: None

Background: In cirrhotic livers, dysplastic nodules evolve to small/early HCC and then to progressed/advanced HCC. While it is known that TMB is low in HCC, no prior studies have investigated TMB in background cirrhosis compared to early small HCC and progressed HCCs. The purpose of this study is to investigate whether there are differences in TMB between background cirrhosis, early small HCC, small progressed HCC, and large HCC.

Design: 18 cases of HCC were identified from departmental archives: 6 early small well-differentiated (WD) HCCs, 6 small moderately-differentiated (MD) HCCs, 3 large WD HCCs, and 3 large MD HCCs. Criteria: small/early HCC: WD and ≤ 1.5 cm, small progressed HCC: MD and <1.5 cm, large/progressed HCC: WD or MD and ≥ 2.0 cm. None of the patients had extrahepatic disease. Background cirrhosis of early small WD HCC were also included for analysis. Areas with cirrhosis and HCC were microdissected. TMB was reported as number of non-synonymous mutations per megabase and subsequently adjusted for formalin fixation artifact. Statistical analysis was performed via t-test.

Results: Mean adjusted TMB value for cirrhosis, small early WD HCCs, small progressed MD HCCs, large WD HCCs, and large MD HCCs is 0.9, 0.8, 1.7, 1.4, and 2.2, respectively. None of the cases showed high TMB. One case of lymphoepithelioma-like HCC showed low TMB of 1.0, commensurate with reported TMB literature for this subtype. There was no significant difference between early small WD HCCs versus cirrhosis (P=0.98) or versus small MD HCCs (P=0.23). There was also no significant difference between WD and MD small HCCs versus large HCCs (P=0.99). However, there was a significant difference between cirrhosis/early small WD HCCs taken together versus small MD/large HCCs taken together (P=0.045).

Conclusions: There was no significant difference in TMB between the cohorts of HCC when stratified by size, early versus progressed, and differentiation (WD vs. MD). However, there was a significant difference between cirrhosis/early small WD HCCs versus to small MD/large HCCs, suggesting that TMB may be related to at least size or histology. While we did not study high grade dysplastic nodules, the lack of difference in TMB between background cirrhosis and early small non-progressed HCC suggests that TMB is not a useful tool to distinguish between these 2 entities. More studies are needed in the future to address TMB in specific histologic subsets of HCC and in HCC arising in different etiologies of chronic liver disease.

1656 Cirrhotomimetic Hepatocellular Carcinoma: A Single Institution Experience

Meng-Jun Xiong[1], Chirag Patel[1], Upender Manne[1], Sameer Al Diffalha[1]
[1]The University of Alabama at Birmingham, Birmingham, AL

Disclosures: Meng-Jun Xiong: None; Chirag Patel: None; Upender Manne: None; Sameer Al Diffalha: None

Background: Cirrhotomimetic Hepatocellular Carcinoma (CM-HCC) is a recently recognized HCC variant exhibiting diffuse cirrhosis-like micronodular growth, as well as a budding reputation for evading pre-transplant clinical and radiographic detection. A case of CM-HCC prompted review of our single institution's experience of 5 cases of this rare entity.

Design: A case of CM-HCC in native explanted liver prompted a search in our pathology database, which yielded an additional 4 cases, diagnosed from 2015 to 2019. Pre-transplant and clinicopathologic characteristics were collected to include: prior liver disease, radiographically known lesions, serum alpha fetoprotein (sAFP), lobes involved, estimated tumor burden, pathologic grade and stage, and immunohistochemistry (IHC) results. We also collected data on survival and metastasis.

Results: Our cohort comprised 5 male patients, ranging 50 to 66 years-old. Pre-transplant imaging detected dominant nodules with mildly elevated sAFP in 2 patients (4.4 cm with sAFP 232 ng/mL; 1.8 cm with sAFP 93.5 ng/mL). Three patients had clinically occult tumor with normal sAFP and no discreet lesions on imaging. Gross exam showed diffuse, subtly pale, innumerable nodules. On microscopic exam, all 5 cases exhibited bilobar involvement. Predominantly well-to-moderate differentiation was reported. Pseudoglandular and trabecular growth patterns were noted in all cases (Figure 1). IHC showed diffuse Glypican-3 positivity, Mallory-Denk accentuation on ubiquitin, and CD34 "endothelial-wrapping" that confirmed HCC. Interestingly, these tumors were negative for AFP by IHC and exhibited a low MIB-1 index, corroborating the theory that these are well-differentiated tumors (Figure 2). All but one case was staged as T2. One patient with T2 disease developed a solitary metastasis at 1.7 years follow-up. The remaining 3 patients with T2 disease were recurrence-free (follow-up range: 0.6 to 2.4 years). One exceptional patient had prior transarterial chemoembolization and radiation therapy to a dominant nodule and metastasis at time of CM-HCC diagnosis. His tumor exhibited poor histological differentiation and was staged as T3.

|					
Table 1: Clinicopathologic Characteristics of CM-HCC Cases					
Parameters	**Case 1**	**Case 2**	**Case 3**	**Case 4**	**Case 5**
Age (years)	50	58	56	60	66
Sex	Male	Male	Male	Male	Male
Ethnicity	Caucasian	African American	Caucasian	Caucasian	Caucasian
Clinical History	NASH	HCV, HBV, ETOH	HCV	HCV	NASH
Treatment History	None	None	None	Only largest nodule s/p TACE/XRT	None
Pre-operative Serum AFP (ng/mL; result)	10.3; normal	unknown	192; elevated	232; elevated	93.5; elevated
Pre-operative Imaging	No lesions	No lesions	subtle mass-like area	Largest nodules (4.4 cm and 1.2 cm) detected by imaging	multiple indeterminant lesions with dominant nodule (1.8 cm)
Background Liver	Cirrhosis/ESLD	Cirrhosis/ESLD	Cirrhosis/ESLD	Cirrhosis/ESLD	Cirrhosis/ESLD
Lobes involved by CL-HCC	Bilateral	Bilateral	Bilateral	Bilateral	Bilateral
Estimated Volume of Tumor Burden (%)	75	25 to 30	70	Unknown	Unknown
Size Range (cm)	1.0 to 1.7	up to 1.3	0.3 to 1.0	0.2 to 1.3; dominant nodule is 5.2	0.6 to 1.4
Predominant Histologic Pattern	Pseudoglandular & focal steatotic changes	Pseudoglandular	Pseudoglandular & focal steatotic changes	Pseudoglandular	Pseudoglandular
Histologic Grade	G1	G1 to G2	G1 to G2	G3	G2
Pathologic Stage (AJCC 8th Edition)	mpT2 pN0	mpT2 pNX	mpT2 pN0	ypT3a pN1	mpT2 pNX
Recurrence-Free Survival (years)	1.3	0.6	1.7	0.7	0.6
Metastatic disease	No	No	Yes. Solitary metastasis to adrenal	Yes. Metastasis to celiac lymph node & T2 & T4 Bone (later by imaging only)	No
Follow-up period (years)	1.3	0.6	2.4	1.4	0.6
Alive at last follow-up	Yes	Yes	Yes	No	Yes
Abbreviations: s/p=status post; TACE= Transarterial chemoembolization; XRT= radiotherapy; AFP= α-Fetal Protein (abnormal above 14.99ng/mL); ESLD=End Stage Liver Disease; HCV=Hepatitis C; HBV=Hepatitis B; ETOH=alcohol, NASH=Non-Alcoholic Steatohepatitis; AJCC=American Joint Committee on Cancer					

Figure 1 - 1656

Figure 2 - 1656

Glypican-3   Ubiquitin   MIB-1 index (low)
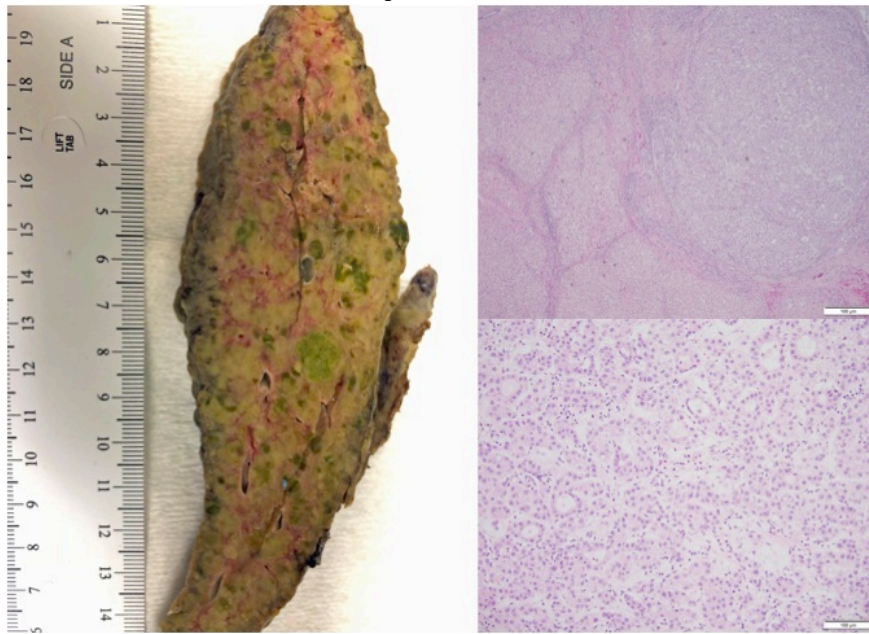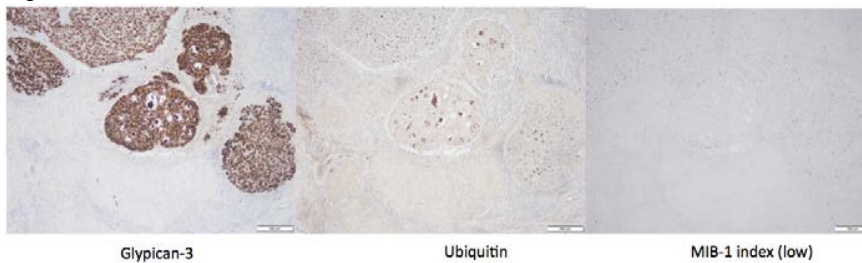
Conclusions: CM-HCC is a rare variant of HCC, whose growth pattern and histology allow adeptness at evading pre-transplant detection. Our CM-HCC cohort had good prognosis at last follow-up upwards to 2.4 years, despite bilobar involvement. Molecular and pathobiology of this tumor remain elusive, and are potential areas for further investigation.

1657 Malignant Transformation of Hepatic Adenomas: Three Distinct Patterns

Saba Yasir[1], Zongming Eric Chen[1], Dhanpat Jain[2], Sanjay Kakar[3], Tsung-Teh Wu[1], Matthew Yeh[4], Michael Torbenson[1]
[1]Mayo Clinic, Rochester, MN, [2]Yale University School of Medicine, New Haven, CT, [3]University of California San Francisco, San Francisco, CA, [4]University of Washington Medical Center, Seattle, WA

Disclosures: Saba Yasir: None; Zongming Eric Chen: None; Dhanpat Jain: None; Sanjay Kakar: None; Tsung-Teh Wu: None; Matthew Yeh: None; Michael Torbenson: None

Background: Hepatic adenomas can develop atypical features and in some cases undergo malignant transformation. Many of the key risk factors remain poorly understood.

Design: Hepatic adenomas were subtyped with LFABP, CRP, SAA, glutamine synthetase and beta-catenin. Atypical adenomas were defined as those with beta catenin activation and/or morphological atypia that did not reach the level of hepatocellular carcinoma (HCC). HCC was identified using morphology, reticulin, glypican-3, and Ki-67.

Results: 163 hepatic adenomas were studied: 50 *HNF1A*- inactivated adenomas (31% of total), 79 inflammatory adenomas (48%), and 33 unclassified adenomas (20%). Of these, 31 (17%) were classified as atypical adenomas and 16 (10%) as having malignant transformation. The 31 atypical adenomas were unclassified (45%), *HNF1A*-inactivated (32%), and inflammatory (18%). Atypical adenomas had beta catenin activation alone (N=16, 52%), morphological atypia alone (N=12, 39%), or both (N=3, 10%). The 16 adenomas with malignant transformation were unclassified (38%), inflammatory (38%), and *HNF1A*-inactivated (25%). Malignant transformation via beta-catenin activation strongly clustered with inflammatory adenomas (6/6 cases) but not *HNF1A*-inactivated adenomas (0/4) (See Table). Finally, a new pattern emerged when examined by age cohort. A first group of adenomas with malignant transformation

occurred in young patients less than 20 (N= 4/11, 36%). In this group, all of the adenomas were inflammatory (N=7) or unclassified (N=4), none were *HNF1A*-inactivated, and most patients had underlying genetic conditions (N=6). The next group of adenomas with malignant transformation occurred in young and middle aged women, aged 20-49, with typical risk factors for adenomas such as estrogen exposure; malignancy (N=6/109) was found exclusively in inflammatory or unclassified adenomas and not in *HNF1A*-inactivated adenomas. A 3rd group was seen in patients over the age of 50 (N=5/42), where malignant transformation was seen only in *HNF1A*-inactivated or unclassified adenomas and not in inflammatory adenomas

Adenoma subtype	Malignant transformation	Beta catenin activation in HCC	No beta catenin activation in HCC
HNF1A-inactivated	4/50	0	4
Inflammatory	6/79	6	0
Unclassified	6/33	3	3

Conclusions: Malignant transformation in hepatic adenomas occurs in 3 distinct clusters: a first group in patients less than 20 with inherited disorders; a second group in young and middle aged women with enrichment for inflammatory adenomas and malignant transformation via beta catenin activation; and a 3rd group in patients >50 with primarily HNF1A inactivated adenomas and malignant transformation without beta catenin activation.

1658   Pathological Features of Immune-Mediated Hepatitis Caused by Immune Checkpoint Inhibitors and Multiple Receptor Tyrosine Kinases

Qiongyan Zhang[1], Yuan Ji[2]
[1]Fudan University Zhongshan Hospital, Shanghai, China, [2]Zhongshan Hospital of Fudan University, Shanghai, China

Disclosures: Qiongyan Zhang: None; Yuan Ji: None

Background: Immune checkpoint inhibitors (ICIs) has shown remarkable effects in many cancers, including Liver Cancer (LC). Meanwhile, immune-mediated hepatitis (IMH) is one of common adverse events since ICIs can cause the imbalance of immune system. Oral small molecule inhibitors of multiple receptor tyrosine kinases (TKIs) such as sorafenib and lenvatinib have been used as first-line treatment in patients with advanced HCC. The rate of IMH has been increased as the combination treatment of ICIs and TKIs are increasing.

Design: Methods. We collected 20 cases of advanced Liver Cancer (LC) patients occurred hepatotoxicity in the treatment of ICIs. 12 cases were treated with monotherapy ICIs, and another 8 cases were treated with ICIs combined with TKIs. The liver biopsy was performed under the direction of ultrasound. We compared the histological features of those biopsy tissues.

Results: Results. Patients treated with monotherapy ICIs presented different levels of lobular hepatitis and portal inflammation. Besides, there also present cholangitis, endothelialitis, activation of Kupffer cell and peliosisihepatitis. 75% cases show mild hepatic injury, while 25% cases show moderate hepatic injury. As for patients in the combination group treated with ICIs and TKIs, the extent of IMH were much more severe, 75% cases occurred moderate-severe portal inflammation, interface hepatitis, confluent or bridging necrosis. Among them, 1 patient developed acute severe hepatitis with massive hepatocyte necrosis, he finally died of liver injury, lung infection and multisystem dysfunction. In addition, many CD 8 positive lymphocytes aggregated in the portal area of those severe liver injury cases. Also there were substantial PD-L1 positive liver cells and kuppfer cells, which indicated the IMH damage.

Figure 1 - 1658
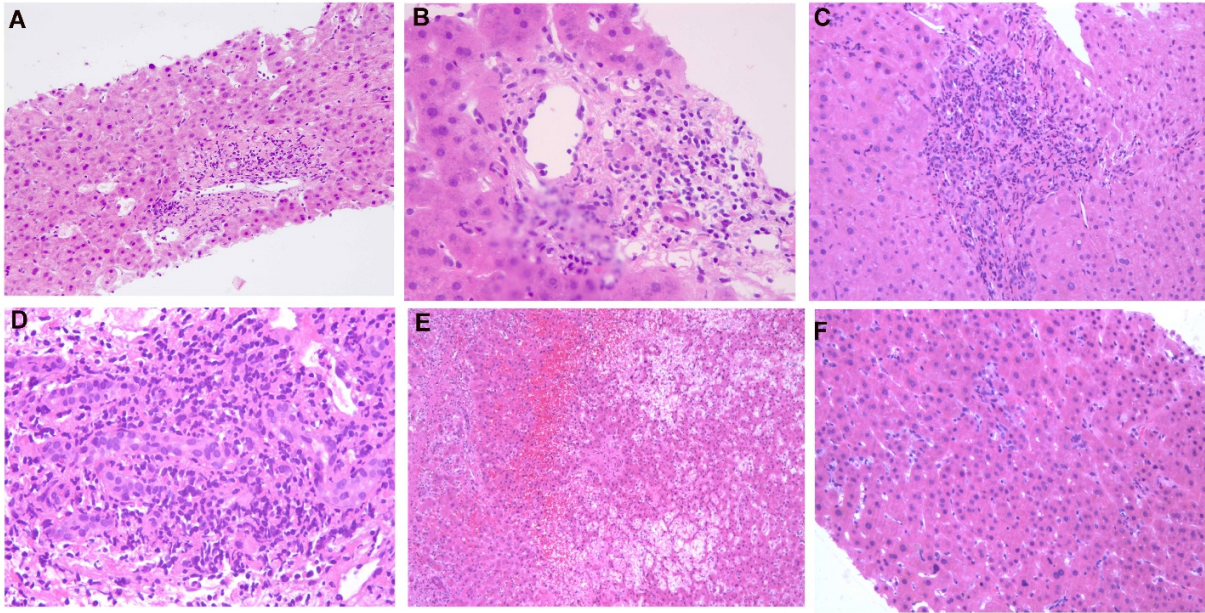
Figure 2 - 1658
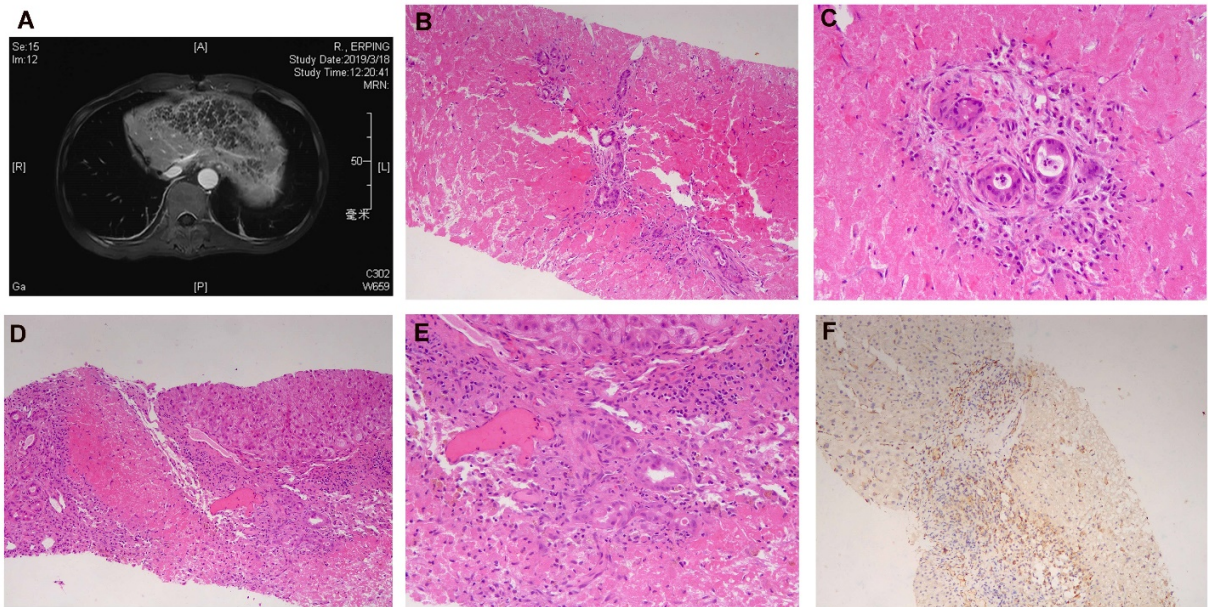
Conclusions: Combination of ICIs and TKIs may cause overlapping hepatocyte injury, which is much worse than the IMH caused by monotherapy ICIs.

1659 TP53 Genetic Alteration is Frequently Seen in High-Grade Intrahepatic Cholangiocarcinoma

Wei Zhang[1], Swan Thung[2], Stephen Ward[2], Maria Isabel Fiel[2]
[1]University of Wisconsin-Madison, Madison, WI, [2]Icahn School of Medicine at Mount Sinai, New York, NY

Disclosures: Wei Zhang: None; Swan Thung: None; Stephen Ward: None; Maria Isabel Fiel: None

Background: Intrahepatic cholangiocarcinoma (IH-CCA) is the second most common primary liver malignancy accounting for 10-20% of primary liver cancers and its incidence has been rising worldwide in the past decade. Although resection is still the first-line approach,

targeted therapy on specific molecular alterations, such as FGFR2 fusion, has emerged in recent years. In the present study, we sought to correlate the genetic alteration with the histopathological findings of IH-CCA.

Design: We retrospectively searched the pathology database for all IH-CCA cases covering the period from January 2014 to March 2019. We subsequently reviewed electronic medical records of cases found and identified the cases that had molecular testing (next-generation sequencing) performed (either by Foundation Medicine or SEMA4 Genomics). Review of slides of both tumor and background liver was performed independently by two liver pathologists.

Results: A total of 25 resection cases were included in the study. The mean age of this cohort is 53 years (range: 40-77) with male to female ratio of 13/12. Seventeen of 25 (68%) had moderately differentiated IH-CCA while 8 of 25 (32%) had poorly-differentiated IH-CCA. The main molecular alterations detected in in this cohort were at TP53 (n=6, 24%), ARID1A (n=5, 20%), FGFR (n=5, 20%), IDH1/2 (n=4, 16%), and BAP1 (n=2, 8%) (Table 1). Interestingly, 3 of the 6 cases with TP53 mutation showed a solid nest growth pattern and high-grade nuclear features. Upon evaluating the background liver, chronic hepatitis B was seen in 2 of the 6 cases, both were grade 1, with 1 case coexisting with steatohepatitis. Steatohepatitis was also identified in 2 other cases in TP53 mutated group. All the TP53 mutations found were missense mutation. Fatty liver as the background liver disease was found in most cases with 10 of 25 (40%) having steatohepatitis while 3 of 25 (12%) had steatosis.

Table 1. Pathologic Features and Molecular Findings of Study Cases

Features	No (%, n=25)
Mean age (SD)	53.0 ± 7.1 (range: 40-77 y)
Male/Female	13/12
Molecular Findings	
TP53	6 (24%)
ARID1A	5 (20%)
FGFR alterations (FGFR2 fusion and FGFR gain)	5 (20%)
IDH1/IDH2	4 (16%)
BAP1	2 (8%)
Chronic Hepatitis	
Chronic Hepatitis B	4 (16%)
Chronic Hepatitis C	1 (4%)
Chronic Hepatitis with Unknown Etiology	1 (4%)
Steatohepatitis/Steatosis	
Steatohepatitis	10 (40%)
Steatosis	3 (12%)

Conclusions: In this cohort of IH-CCA, the most common mutated genes are TP53, ARID1A, FGFR, IDH1/2, and BAP1. Our results suggest that TP53 missense mutation may be associated with high-grade tumor morphology, which possibly leads to a poor prognosis. Survival analysis is ongoing. In addition, the underlying chronic liver disease, particularly steatohepatitis, might play an important role in the pathogenesis of IH-CCA tumor.

1660   Immunophenotypical Signatures of Hepatic Macrophages Differ in Chronic Liver Disease Compared to Normal and Cluster with Disease Etiology

Xiaoming Zhang[1], Alexandra Thompkins-Johns[2], Amy Ziober[1], Paul Zhang[3], Emma Furth[4]
[1]Hospital of the University of Pennsylvania, Philadelphia, PA, [2]The Hospital of the University of Pennsylvania, Philadelphia, PA, [3]Hospital of the University of Pennsylvania, Media, PA, [4]University of Pennsylvania, Philadelphia, PA

Disclosures: Xiaoming Zhang: None; Alexandra Thompkins-Johns: None; Amy Ziober: None; Paul Zhang: None; Emma Furth: None

Background: Varying etiologies of liver disease induce an inflammatory response which plays a central role in initiating fibrogenesis. Macrophages (Mφ) are phenotypically heterogeneous and part of this cellular immune response. Specifically, those expressing CD163 produce proinflammatory cytokines while Mφ expressing IBA1, a calcium-binding protein, play a role in chemotaxis, and CD68+ Mφ play a role in phagocytosis. We hypothesized that differing etiologies of chronic liver disease (CLD) incite early in fibrogenesis differing immune responses with distinct Mφ phenotypic and zonal geographic signatures.

Design: Our cohort was composed of liver biopsies from normal (n=19) and CLD (n=29) with mild to moderate fibrosis [5 NASH, 5 Hep C, 4 alcoholic liver disease (ALD), 5 PSC, 5 PBC, and 5 AIH]. IHC was done for 3 Mφ markers (CD163, CD68, and IBA1; Fig 1) and glutamine synthetase was utilized to demarcate the hepatic zone 3 (Z3). Digital image analysis and automated cell count (QuPath software) were used to calculate the densities of immunostained cells in zone 1 (Z1) and Z3, respectively. Statistical analysis was performed with SPSS software.

Results: In all cases including normal, the density of both CD163+ and IBA1+ cells were far greater than CD68+ cells in both Z1 and Z3 (Fig 2). The absolute and relative densities of the phenotypes with relationship to zones and etiologies of liver disease showed distinct patterns. Hierarchical cluster analysis showed four groups: 1) significant increase in selected Mφ densities in both Z1 and Z3 – Hep C; 2) significant increase in Mφ densities only in Z1 – ALD, PSC, and PBC; 3) significant increase in densities of all types of Mφ in both Z1 and Z3 – AIH; and 4) no significant increase in Mφ densities in either Z1 or Z3 – NASH. NASH was distinct in having a shift in CD163/IBA1 ratio without change in density (table); interestingly, a similar shift in ratio was also found in Hep C but with increased total density.

Table. Ratio of macrophage marker expression in liver biopsies.							
	N	**CD68/CD163 (mean±SD)**		**CD68/IBA1 (mean±SD)**		**CD163/IBA1 (mean±SD)**	
		Zone 1	Zone 3	Zone 1	Zone 3	Zone 1	Zone 3
Normal	19	0.44±0.80	0.47±0.39	0.24±0.20	0.47±0.20	0.79±0.38	1.12±0.26
CLD	29						
NASH	5	0.28±0.08	0.42±0.22	0.25±0.08	0.60±0.38	0.89±0.09	1.41±0.20
p-value*		0.663	0.774	0.894	0.267	0.578	*0.031*
Hep C	5	0.22±0.15	0.28±0.18	0.21±0.12	0.38±0.18	1.04±0.26	1.43±0.26
p-value*		0.550	0.307	0.814	0.394	0.181	*0.030*
ALD	4	0.23±0.12	0.38±0.16	0.18±0.12	0.39±0.12	0.76±0.11	1.11±0.32
p-value*		0.608	0.661	0.604	0.485	0.878	0.948
PSC	5	0.26±0.12	0.43±0.22	0.21±0.11	0.49±0.21	0.81±0.10	1.19±0.16
p-value*		0.618	0.799	0.789	0.806	0.904	0.606
PBC	5	0.33±0.13	0.45±0.07	0.29±0.11	0.48±0.07	0.88±0.20	1.08±0.10
p-value*		0.766	0.874	0.581	0.871	0.593	0.774
AIH	5	0.35±0.16	0.49±0.13	0.32±0.17	0.48±0.13	0.89±0.10	0.99±0.12
p-value*		0.797	0.913	0.441	0.855	0.572	0.297
p*-value for comparison of ratio: corresponding chronic liver disease vs normal; Statistical analysis was performed using IBM SPSS (Chicago, IL), version 23.0; Abbreviations: CLD, chronic liver disease; NASH, nonalcoholic steatohepatitis; Hep C, hepatitis C; ALD, alcoholic liver disease; PSC, primary sclerosing cholangitis; PBC, primary biliary cholangitis; AIH, autoimmune hepatitis.							

Figure 1 - 1660

Figure 2 - 1660
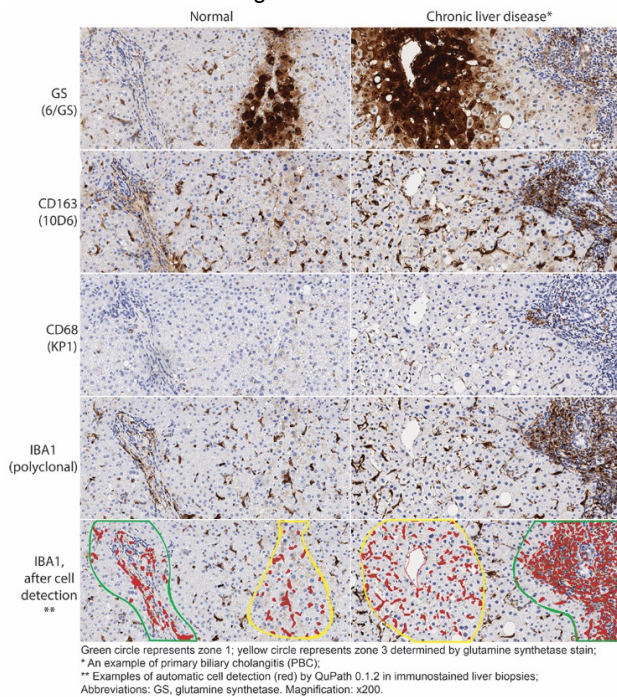
Green circle represents zone 1; yellow circle represents zone 3 determined by glutamine synthetase stain;
* An example of primary biliary cholangitis (PBC);
** Examples of automatic cell detection (red) by QuPath 0.1.2 in immunostained liver biopsies;
Abbreviations: GS, glutamine synthetase. Magnification: x200.
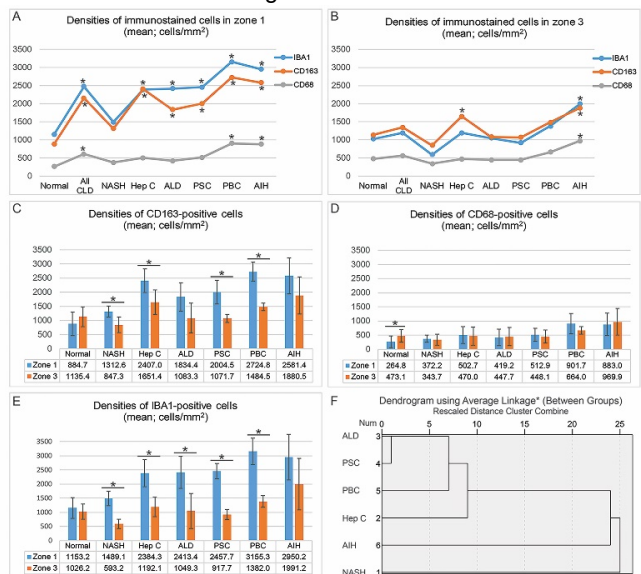
* in Fig. 2A and 2B: significantly increased compared with normal liver (*p*<0.05);
* in Fig. 2C, 2D, and 2E: significantly different between zone 1 and zone 3 (*p*<0.05);
* in Fig. 2F: obtained by hierarchical cluser analysis. Num: order of variable input;
Statistical analysis was performed using IBM SPSS (Chicago, IL), version 23.0;
Abbreviations: CLD, chronic liver disease; NASH, nonalcoholic steatohepatitis; Hep C, hepatitis C; ALD, alcoholic liver disease; PSC, primary sclerosing cholangitis; PBC, primary biliary cholangitis; AIH, autoimmune hepatitis.

Conclusions: There are distinct Mφ phenotype signatures correlating with etiologies of CLD in early stages of fibrosis. In particular, NASH has a very distinctive phenotype differing from ALD which interestingly clustered with the cholestatic diseases PBC and PSC. While both hepatic injury patterns, Hep C and AIH each fell into differing and distinct cluster groups illustrating differing immune responses in these diseases. By understanding the immune response in liver disease, we may be able to devise treatment interventions to mitigate fibrosis.

1661   Vascular Mass Lesions of the Liver: A Contemporary Clinicopathologic Analysis of 167 Cases

Wei Zheng[1], Alyssa Krasinskas[2]
[1]University of Emory, Atlanta, GA, [2]Emory University, Atlanta, GA

Disclosures: Wei Zheng: None; Alyssa Krasinskas: None

Background: Hepatic vascular mass lesions (HVML) are a heterogeneous group of relatively uncommon entities that may pose diagnostic challenges radiologically and pathologically. However, there is little published literature regarding the clinicopathologic features of these lesions.

Design: A search was made through our institutional Hepatic Pathology and Soft Tissue Pathology files between 2010 and 2018 for cases of HVML.

Results: 167 cases of HVML were identified with 133 (79%) cases of hemangiomas (HA), 17 (10%) cases of angiosarcomas(AS), 9 (5%) cases of epithelioid hemangioendotheliomas(EHE), 5 (3%) cases of angiomyolipomas (AML), and 3 (2%) cases of tumor-like vascular malformation (VM). The patients often presented with abdominal discomfort or hepatomegaly, and some had distinct palpable mass. Among HA (77% females, mean age 51 years), lesions measured 7.1 cm in average and were solitary or multifocal, solid and/or cystic. Intratumoral hemorrhage, calcification, and infarction were common. 21% HA had coexisting primary or metastatic tumors. Cavernous and capillary HA were most common while anastomosing variant was most diagnostically challenging. Among EHE (89% females, mean age 50 years), 67% cases were multifocal and measured 2-6 cm. 3 cases had CAMTA1 fusion and 1 case had YAP fusion. Among AS (72% males, mean age 60 years), 18% were hepatic primary with all cases having epitheliod morphology and 82% were metastatic AS from scalp, spleen or retroperitoneum. Focal cytokeratin positivity in a subset of EHE and AS led to diagnostic confusion. Among AML (80% females, mean age 54 years), 60% lesions were located in the right lobe and measured 4-7 cm. Most cases were disease-free 3 years after surgical resection. Among VM, 2 cases were venous abnormalities and 1 case was lymphatic malformation.

Conclusions: This is one of the largest studies of HMVL to date. These lesions, in general, have a slight female and right-lobe predominance. Benign tumors accounted for the majority of the cases. Large size with intratumoral heterogeneity is common in HA, which mimics malignancy and highlights a potential clinical/radiological diagnostic pitfall. A subset of HA may have coexisting primary or metastatic tumors, requiring sufficient specimen sampling and thorough microscopic examination. Hepatic EHE and AS often have multiple lesions, making their distinction from a metastatic tumor challenging by liver imaging. Focal cytokeratin expression in a subset of EHE and AS may also lead to confusion with carcinoma.